STATISTICAL ANALYSIS OF LO-LOCAT TURBULENCE DATA FOR USE IN THE DEVELOPMENT OF REVISED GUST CRITERIA

JOHN W. McCLOSKEY

JAMES K. LUERS

JOHN P. RYAN
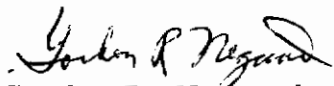
NICHOLAS A. ENGLER

FOREWORD

This report is a summary of the results of statistical analyses performed on the low-level critical atmospheric turbulence (LO-LOCAT) data conducted from March 1, 1969 through March 1, 1971. This report was prepared by the University of Dayton Research Institute (UDRI). The work accomplished was administered by the Air Force Flight Dynamics Laboratory under Contract F33615-69-C-1477 with Mr. Paul Hasty as Project Engineer.

The research was conducted at the University of Dayton under the management of Mr. Nicholas Engler, Project Director of the Applied Systems Analysis Section of UDRI. The technical effort was performed by Dr. McCloskey, Mr. Luers, Mr. Ryan, and Mr. Engler.

This technical report has been reviewed and is approved.

Gordon R. Negaard, Major, USAF
Chief, Design Criteria Branch
Structures Division

ii

ABSTRACT

LO-LOCAT is an extensive low level turbulence program utilizing statistically representative samples of turbulence data obtained over a wide range of meteorological, topographical, seasonal, and time of day conditions. UDRI has attempted to identify which of the various meteorological and environmental conditions affect the turbulence as reflected through a number of turbulence parameters. The turbulence parameters considered were: σ, the standard deviation of the gust velocity; b, the turbulence intensity; L, the scale of turbulence; and N_o, the characteristic frequency.

The basic method of mathematical analysis was a stepwise regression scheme which related the environmental conditions to the various turbulence parameters based upon statistical priority. It is felt that the regression scheme provides a detailed outline of statistical relationships which can be used as a guide for further investigation.

TABLE OF CONTENTS

iv

TABLE OF CONTENTS

v

TABLE OF CONTENTS

LIST OF FIGURES

LIST OF FIGURES

LIST OF TABLES

LIST OF TABLES

LIST OF TABLES

LIST OF SYMBOLS

A, B, C	Coefficients of the least squares quadratic fit relating gust velocity x to ln F(x).
$\bar{A}$	Structural response quantity relating gust velocity to the response parameters.
b	The least squares fit to the slope of ln N(x) versus x for each flight leg and each component of gust velocity x(t).
b_1, b_2	Constants in the analytical expressions of the peak count probability distributions.
f(x)	Probability density function of the variable x.
F(x)	Cumulative probability distribution function of the variable x.
$H_y(w)$	Frequency response function for variable y.
L	Von Karman scale of turbulence (feet).
L_u, L_v, L_w	Von Karman scale of turbulence for the longitudinal, lateral, and vertical components, respectively (feet).
m_1, m_2, m_3	The first, second, and third moments of a probability distribution.
n	Number of legs used in the given analysis.
N_o	Characteristic response frequency (zero crossings per foot).
N_{ou}, N_{ov}, N_{ow}	Characteristic response frequency for the longitudinal, lateral, and vertical components, respectively (zero crossings per foot).
N(x)	Number of gust velocity peaks exceeding the gust velocity x.
PSD	Power Spectral Density.
P_1, P_2	Intercepts of the exponential curves for the analytical expressions of the peak count probability distributions.
u, v, w	The longitudinal, lateral, and vertical gust velocities (feet/sec).

LIST OF SYMBOLS

$u_{max}, v_{max}, w_{max}$	The maximum longitudinal, lateral, and vertical gust velocities encountered for each leg (feet/sec).
$u_{min}, v_{min}, w_{min}$	The minimum longitudinal, lateral, and vertical gust velocities encountered for each leg (feet/sec).
WA	Wind angle with the aircraft.
WD	Wind direction.
WG	Vertical wind gradient.
WS	Wind speed.
x_q	One-half x_m.
x_m	The largest gust velocity encountered in a group of data when fitting $\ln F(x)$ to a quadratic equation.
α, β	Parameters in the log-normal fit of the distribution of extremes.
σ	Standard deviation of the filtered gust velocity time history.
$\sigma_u, \sigma_v, \sigma_w$	Standard deviation of the longitudinal, lateral, and vertical component gust velocity time histories.
$\phi_x(\ )$	Power spectral density function of a random disturbance x.
ω	Circular frequency (radians/sec).
Ω	Spatial frequency.

SECTION I

INTRODUCTION

Military bombers and logistic aircraft, as well as commercial transports, are designed to carry large payloads for long range at high speed and altitude, and as a consequence, are characterized by a high degree of structural flexibility. This structural flexibility gives rise to substantial amplification to the gust-response characteristics (such as stress, bending moment, center of gravity acceleration). The gust velocity inputs are due to the atmospheric turbulence environment which appears to be consistently more severe at the lower altitudes. In recent years, a military operational requirement has been added which entails high speed low level terrain following in order to avoid radar detection. At least two catastrophic incidents have been attributed to clear air turbulence environment; and other aircraft have sustained significant structural damage in this low level terrain following mode. These results make it imperative that a better definition of the atmospheric turbulence environment be determined.

Some of the pioneering efforts in applying results from the theory of generalized harmonic analysis (or Power Spectral Analysis) to the analysis of gust loads on airplanes in continuous rough air are shown in References 4 and 5. In these references, and in others where Power Spectral Analysis methods have been fruitfully applied to experimental data, the following limitations were typical:

(1)   Many of the parametric identification signatures were not recorded or were lost due to compositing of data prior to acquisition.

(2)   Vertical accelerometers were used as the primary source of experimental data, thus limiting the data to one direction.

(3)   Transformation of acceleration data to true gust velocity was accomplished using assumptions of single degree of freedom, Dryden or wind tunnel spectrum model, and scale length of 1000 feet.

These programs were invaluable, but the data were limited in quantity and relied on indirect methods to determine the probability density distribution of the standard deviation of the filtered gust velocity time history (σ). Advances in instrument technology and calibration techniques following these programs made the calculation of three dimensional turbulence in the lower frequency range possible. Improved computers using large quantities of data made the accomplishment of a turbulence research program on a statistical basis feasible.

1

A contract called Low Altitude Critical Air Turbulence (LO-LOCAT) was awarded to the Boeing Company in April 1966. This LO-LOCAT program is a part of an overall effort known as ALLCAT. ALLCAT is designed to investigate atmospheric turbulence outside clouds from the earth's surface to an altitude of 200,000 feet. The Boeing Company LO-LOCAT contract involved collection of turbulence data for terrain clearance altitudes below 1000 feet grouped into statistically representative samples obtained over a wide range of meteorological, topographical, seasonal, and time of day conditions.

The University of Dayton initiated a study on 1 March 1969 for the Development of Low Altitude Gust Criteria for Aircraft Design. The primary source of data for this study has come from the Boeing Company LO-LOCAT study. The calculated data from the Boeing Company study were recorded on magnetic tapes which will be referred to as the "Air Force Combined Tapes". There are two different tape formats available. One tape format called "Time History Tapes" gives the three components of the gust velocity time history, peak count, amplitude count, power spectra, and, for the Phase III study, the level crossing count. The other tape format, referred to as "Master" tapes, gives minimum and maximum values, standard deviations, scale lengths, meteorological data and various other data.

The purpose of this program is to "Determine a probabilistic mathematical model, which agrees with the experimental turbulence environment in the 0-1000 feet terrain altitude region, to predict gust criteria for use in advanced vehicle systems".

The participation of the University of Dayton in the fulfillment of this goal is as follows:

(1)   To develop a mathematical model for turbulence which conforms with current acceptable procedures in the spectral approach to gust response and design requirements.

(2)   To develop a procedure and to calculate values for certain basic design criteria parameters (such as P's, b's, L's, etc.) using data extracted from the "Air Force Combined Tapes".

(3)   To determine the effect that the available environmental conditions have on the turbulence environment as reflected through a number of recorded turbulence parameters.

SECTION II

DISCUSSION OF THE LO-LOCAT PROGRAM

The Boeing Company at Witchita, Kansas was awarded a contract by The Air Force Flight Dynamics Laboratory to conduct a (data gathering) program (LO-LOCAT) to investigate the characteristics of atmospheric turbulence below 1000 feet terrain altitude. The (LO-LOCAT) program consisted of three phases of testing. The data collection for Phases I and II utilized four C-131B aircraft as instrumentation platforms and measured turbulence wavelengths up to 7000 feet in length. The purpose of Phase III was to extend the statistical definition of the turbulence environment and to define wavelengths up to 14,000 feet by using a higher speed (T-33A) airplane as the instrumentation platform. Figure 2.1 is a schematic of the LO-LOCAT Program presenting the position of the University of Dayton Research Institute with respect to the total endeavor of the program.

The Phase I and II LO-LOCAT atmospheric turbulence data were obtained over a 15-month period. Each C-131B aircraft was located at a different base (Edwards - California, Peterson - Colorado, McConnell-Kansas, Griffiss - New York) and was flown specified routes to give a wide range of topographical and climatological conditions. Each route consisted of eight straight legs, each of which was approximately 20 nautical miles in length. The legs were traversed in the same direction on each flight at approximately 180 knots. Five and one-half minutes of time history constituted a turbulence leg sample.

The LO-LOCAT Phase III data were obtained during a 10-1/2 month flight period. A T-33A was instrumented and flown at approximately 360 knots over essentially the same routes as established for Phases I and II. All legs were extended to a length of 30 nautical miles to obtain a data recording time interval of four and one-half minutes. Some legs were relocated due to this extension in length.

Normally, three missions were scheduled every other day during all three phases of testing; one at dawn, one at mid-morning and one in the afternoon. This schedule was varied as necessary when weather conditions, aircraft maintenance problems, or other factors interfered. All flight legs (with the exception of the high mountain legs of the Peterson routes) were contour flown; that is, the pilot followed the terrain contour as close as safety allowed at either 250 feet altitude or 750 feet altitude. On any one flight date, only one contour altitude was flown, with the test altitude being alternated on successive flight dates. For example, all legs from a given base would be flown at 250 feet altitude for the three time periods and two days later only 750 feet altitudes would be flown. The terrain of the Peterson legs, Phases I and II, was so severe that constant terrain altitude could not be safely maintained; thus altitude definitions assigned for these legs were low altitude and high altitude.

BOEING

Lo-Locat Data Collection
Gust & PSD Calculations
Environmental Conds.
Analytic Procedures

| Phase I & II C-131 Data | | Phase III T-33 Data | | Air Force FDTE Project Monitor |

ETAC

Data Extraction

| Master Tapes | Reports Mid-Term Final | Reports Monthly Mid-Term Final | TAPES Time History Peak-Ampl.- Level Cross. PSD Data - - - - - - Master Tape & Environment |

UDRI

Calculate and/or collect PSD parameters and their
  associated environmental signatures.
Perform regression analysis on parameters in terms
  of environmental signatures.
Relate most important environmental parameters to
  statistical design application.
Formulate gust design requirements in table and/or
  equation form.
Perform extreme value analysis and apply to design
  requirements.

Air Force
FDTR Project
Monitor

Figure 2.1: Schematic of LO-LOCAT Program

4

2.1 Flight Test Procedure

    2.1.1 Pre-Flight

        (a) Instrumentation checks

        (b) Pilot is briefed by meteorologist concerning weather

        (c) Pilot decides whether to fly mission and/or exclude certain legs

        Note: Plane is not flown in clouds or rain to preclude moisture accumulation in gust probe.

    2.1.2 Pre-Leg

        (a) Pilot stabilizes aircraft at 1000 feet terrain altitude and flies over the leg starting point. Ten seconds of atmospheric survey data are recorded at this altitude.

        (b) An instrumentation standardization cycle is initiated automatically. During this cycle the pilot initiates a descending turn to 100 feet terrain altitude on a course to pass over the leg starting point.

        (c) At completion of the standardization cycle and/or the combined descent turn maneuver, the aircraft is stabilized and ten seconds of atmospheric survey data are recorded at 100 feet altitude as near as possible to the first survey location.

        (d) The pilot makes a climbing turn to the designated terrain altitude for the day so as to pass over the leg starting point on the preassigned course heading.

    2.1.3 Flight Leg

        As the aircraft approaches the leg starting point, the pilot actuates the sequencing switch to record leg gust data. Throughout the leg the pilot attempts to maintain the assigned speed and terrain altitude. The pilot switches off the recorder on completion of the leg and flies to the starting point of the next leg to repeat the cycle.

2.2 Data Processing and Categorization

    The detailed steps taken by Boeing to reduce the raw data to time histories of the longitudinal, lateral, and vertical true gust velocities, the

power spectral density of these quantities, and the calculation of associated parameters are well documented in References 1 and 2.

2.2.1 Phase I and II Data

The resultant data compilation for the Phase I and II study consisted of 669 reels of magnetic tape which were delivered to USAF ETAC, Asheville, North Carolina. Three of these tapes, which have been termed by UDRI as "Master Tapes", were duplicated by ETAC and delivered to the University of Dayton in May, 1969. The remaining 666 "Time History Tapes" contain the gust velocity time histories, peak and amplitude count data, and power spectral densities for the longitudinal (u), lateral (v), and vertical (w) components.

The University of Dayton had intended to use only the "Master Tapes" to perform the required study on Phases I and II data. It was found that the probability density distribution of the root mean square gust velocity, σ, from the data of Phases I and II did not conform to the assumptions and methodology of such classical developments as NACA 1272, NACA 4332, (Ref. 3 and 4) etc. and that to utilize the methods outlined in the above reports, empirical peak count or level crossing data would be necessary. The logistics involved by having ETAC duplicate 666 tapes, ship them to the UDRI, and then have UDRI extract the required peak count data from these tapes, seemed horrendous. It was estimated that the time history data (u, v, w) usurped more than 98% of the tape space. Thus, if all data (other than time history data) were extracted by ETAC from these tapes, less than a dozen tapes would be involved. A formal request was made to ETAC in September, 1969, to perform this extraction, and the resultant tapes (three in number) were received during March of 1970.

Appendix A gives the details of data contained in the Phases I and II master tapes. The parameters are grouped into simulated card type images and each parameter is described with dimensional units, method of determination (description or by equation) and reference.

2.2.2 Phase III Data

The calculated data for the LO-LOCAT Program, Phase III, were recorded on 117 magnetic tapes. These tapes are referred to as the "Air Force combined tapes" and were received by UDRI in late January, 1970. Tape T117 can be considered the master tape for the Phase III data. This master tape contains additional parameters to those shown in the three master tapes of Phases I and II. The changes and/or additions to the master tape format of Appendix A are shown in Appendix B.

The remaining 116 tapes contain the gust velocity time histories, primary peak, amplitude, and level crossing count data, and power spectral densities for the longitudinal (u), lateral (v) and vertical (w) components. All data, with the exception of the gust velocity time history data, was extracted

6

from the 116 Phase III tapes and collected on a single tape. The format of this tape matches the format of the three tapes generated by ETAC containing the same information for the Phases I and II data.

The Two Master Tapes from the Phases I and II, and Phase III Programs along with the four (three from Phases I and II, 1 from Phase III) tapes containing peak, amplitude, level crossing, and PSD data, served as the input turbulence data for the UDRI analysis of Clear Air Turbulence for Low Level Design Criteria.

SECTION III

DETERMINATION OF PARAMETERS OF GUST EXCEEDANCE EQUATION

The present model set forth by military specification for the determination of gust induced response exceedances for aircraft design is given as

$$\frac{N(y)}{N_o} = P_1 \, \exp\left(\frac{-y/\bar{A}}{b_1}\right) + P_2 \, \exp\left(\frac{-y/\bar{A}}{b_2}\right) \tag{3.1}$$

where

$N(y)$ = average number of response peaks per mile exceeding the value y

N_o = average number of response peaks per mile in continuous turbulence

y = response quantity (acceleration, bending moment or stress)

$\bar{A}$ = gust response factor relating gust velocity to the response parameter y.

P_1, P_2, b_1, b_2 are parameters of the turbulence environment which will be discussed in greater detail in the following pages. The historical developments in the evolution of the load exceedances (Equation 3.1) are basically contained in References 3, 4, and 8. In all of these developments, use is made of Rice's equation which relates frequency of exceedance at amplitude level x of a random time history x(t).

$$N(x) = \frac{1}{2\pi} \left[\frac{\int_0^\infty \omega^2 \, \phi(\omega) \, d\omega}{\int_0^\infty \phi(\omega) \, d\omega} \right]^{1/2} e^{-x^2/2\sigma^2} \tag{3.2}$$

This equation was derived (Ref. 5) under the assumption the time history is stationary and Gaussian. The equation is exact for the number of level crossings per second with positive slope at a given value x, but is an approximate expression for the number of peak exceedance above a given value of x. For large values $(x > 2\sigma)$ the number of level crossings at amplitude x approximates the number of peaks exceeding x.

Examination of Equation 3.2 indicates that the number of peaks per second above a given value depends upon σ^2, which is the area under the spectrum, $\phi(\omega)$, and upon the radius of gyration of the spectrum about the origin.

8

Ref. 3 provides one of the original developments for converting gust and acceleration peak data into a form appropriate for use in spectral calculations. In this report the application of Rice's equation to turbulence patches resulted in the following assumptions and conclusions:

(a) The spectral shape of a gust turbulence patch for a given altitude appeared to be invariant with weather conditions and varied only in intensity (root mean square gust velocity). Based on these assumptions, Equation 3.2 relating to gust exceedance can be rewritten as

$$N(x) = N_o \ e^{-x^2/2\sigma^2} \tag{3.3}$$

where the constant N_o represents the expected rate of zero crossings of the gust velocity with positive slope and can be considered the characteristic frequency of the random disturbance $x(t)$.

(b) By assuming linearity in the input (gust) - output (response) relationship, a transformation was made in the frequency plane, relating the output spectra of the response variable y to input spectra of the gust velocity x through the frequency response function H_y.

$$\varphi_y(\omega) = H_y(\omega)^2 \ \varphi_x(\omega) \tag{3.4}$$

For a given altitude, gross weight, speed, etc., the frequency response function was also considered invariant and the substitution of $\varphi_y(\omega)$ into Equation (3.2) will give

$$N(y) = N_o e^{-y^2/2\sigma_y^2} \tag{3.5}$$

where the constant N_o represents the expected rate of zero crossings of the response (accelerometer) with positive slope and is the characteristic frequency of the response y.

In Ref. 3, application to Rice's equation was through the use of the response Equation (3.5). This was due to the fact that the primary source of data was from VGH recordings. Equations (3.3) and/or (3.5) apply to individual sample flight records which approximate a Gaussian disturbance. A grouping of operational data would be expected to cover a continuous variation in intensity, therefore, three different exponential probability density distributions of the root mean square acceleration were assumed in Ref. 3. One of these assumed distributions had a form which, when transformed to $f(\sigma)$, gave

$$f(\sigma) = \frac{1}{b} \sqrt{\frac{2}{\pi}} \ e^{-\sigma^2/2b^2} \tag{3.6}$$

9

The expected number of gust exceedances for the limiting case of a continuous variation in σ was specified as

$$N(x) = N_o \int_0^\infty f(\sigma) \, e^{-x^2/2\sigma^2} \, d\sigma \quad . \tag{3.7}$$

Substitute Equation (3.6) into Equation (3.7) and integrating gives

$$\frac{N(x)}{N_o} = P \, e^{-x/b} \quad . \tag{3.8}$$

Early NACA studies using limited operational data encountered two general types of turbulence, 1) severe, which was generally associated with storm conditions and 2) moderate or less severe, which was usually associated with moderately rough clear air.

Ref. 4 developed expressions in terms of Ud_e for two different types of probability distributions which were called storm and non-storm. Through the use of relations between Ud_e and $\bar{A}$, and the application of collected operational data, values were determined for P_1, P_2, b_1, and b_2 using a two-component probability density distribution of the form

$$f(\sigma) = P_1 \, \frac{1}{b_1} \sqrt{\frac{2}{\pi}} \, \exp\left(-\frac{\sigma^2}{2b_1^2}\right) + P_2 \, \frac{1}{b_2} \sqrt{\frac{2}{\pi}} \, \exp\left(-\frac{\sigma^2}{2b_2^2}\right) \quad . \tag{3.6a}$$

The substitution of Equation (3.6a) into Equation (3.7) and integrating gives the cumulative probability of exceeding the gust velocity x,

$$F(x) = \frac{N(x)}{N_o} = P_1 \, e^{-x/b_1} + P_2 \, e^{-x/b_2} \quad . \tag{3.8a}$$

It can be shown in like manner (Ref. 3 and 4) that with appropriate substitution and transformation and by using the assumed probability density distribution of Equation (3.6a), the response relationship can be specified by Equation (3.1).

$$\frac{N(y)}{N_o} = P_1 \, e^{-y/\bar{A}b_1} + P_2 \, e^{-y/\bar{A}b_2}$$

3.1 Application to LO-LOCAT Data Using Master Tape Data

Past experience has shown that Equation (3.8a) provides a good fit to empirical peak count gust velocity data.   UDRI did not initially pursue this approach for two reasons.   First, a direct calculation of F(x) from gust velocity peak count data requires peak count distributions which were not contained in the Master Tapes.   Second, the Master Tapes did provide the standard deviation (σ) and other related data for each flight leg; therefore, since the data was obtained from non-storm conditions, and since the probability density distribution $f(\sigma)$ was heretofore an assumed expression, an effort was made to apply the results of this data to previously developed continuous turbulence theory.   If, for example, the empirical distribution of $f(\sigma)$ could be duplicated by a simple mathematical expression and when substituted into Equation (3.7) providing a closed form solution and good correlation with F(x) from empirical peak count data, methods could be devised whereby peak counts would no longer be needed. The following paragraphs point out some of the problems encountered in applying LO-LOCAT data to classical continuous turbulence theoretical developments.

3.1.1   Application to Rice's Equation

The application of Rice's Equation (3.2) to a stationary Gaussian patch of gust turbulence results in Equation (3.3).   The Master Tapes for Phases I and II provided N_0 values for 16% of the flight legs based on calculations from the truncated spectrum (See Appendix A).   Also the maximum and minimum recorded peaks were provided on the Master Tapes.

A representative value of N_0 for the Phases I and II data is $N_0 = 1.5$ crossings/second.   A five and a half minute flight leg would yield approximately $330\ N_0 = 495$ peak counts.   The cumulative probability of meeting or exceeding the largest peak count, x_{max}, in a five and one-half minute flight leg is on the overall, $1/495$.   The probability of exceeding the maximum peak count can also be estimated from the exceedance distribution given by Equation (3.3).   For LO-LOCAT flight legs, x_{max}/σ has consistently been found to be greater than five for each flight leg.   Substituting this value into Equation (3.3) yields the probability of exceeding as;

$$\frac{N(5\sigma)}{N_o} = 3.7 \times 10^{-6} \quad ,$$

a value immensely different from $1/495$.   The consistent occurences of unusually large ratios of x_{max}/σ makes the stationary Gaussian assumption highly suspect.

Although the UDRI did not feel that this test convincingly proved the nonapplicability of Rice's theory to LO-LOCAT data, it did provide strong indications that the assumptions made in Rice's development (Stationary, Gaussian) are not satisfied by the individual flight legs from LO-LOCAT data.

11

3.1.2 Application to a Continuous Variation in σ

In the preceeding discussion, it was pointed out that under the assumption that the aircraft encounters turbulence of all intensities (continuous variations in root mean square gust velocity) having the same spectral shape (fixed value of L for the von Karman model), that Equation (3.7) can be used to determine $F(x)$ the cumulative probability of a level crossing exceeding the value x. The verification of Equation (3.7) using LO-LOCAT empirical data requires the determination of $F(x) = N(x)/N_0$ in terms of peak count exceedances. The assumed probability density distribution of σ Equation (3.6a) has gained wide acceptance for use in Equation (3.7) because it allows an analytic integration that results in a cumulative probability function of exceedances, Equation (3.8a) that fits empirical data quite well. Section 5.3 contains numerous examples to substantiate this fact. However, the goodness of fit of the frequency distribution (Equation 3.6a) to empirical data had not been checked until recently since suitable data was not available. The first such data was derived during the B-66 Low Level Gust Study. Although the σ values from the B-66 study cannot be considered as a random sample of all σ values, they were fit by a modified chi-square distribution (Ref. 3.3) and this density function was used in Equation (3.7) and numerically integrated to obtain $F(x)$. The resulting $F(x)$ did not agree with the observed distribution of peak counts as it was concave downward instead of the characteristic concave upwards shape, and, hence drastically underestimated the probability of high values of x.

The observed values of σ from the LO-LOCAT program do provide a random sample for the 0-1000 feet altitude band. A brief look at the histogram of the σ values from the LO-LOCAT program indicates that the density function is different from that of Equation (3.6a). That is, a sketch of Equation (3.6a) would appear as in Figure 3.1,
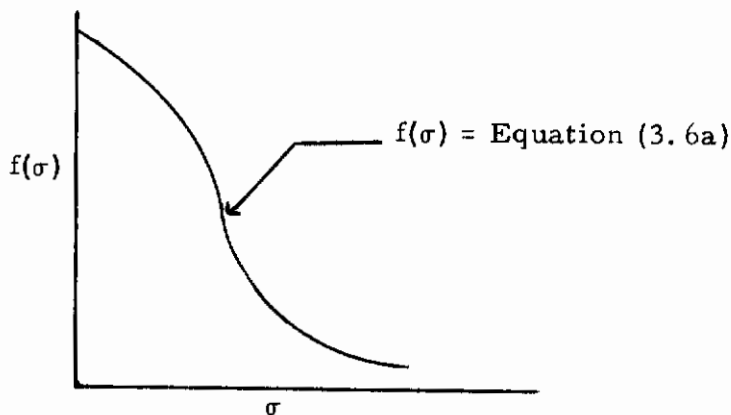
Figure 3.1: Sketch of Analytic Expression for $f(\sigma)$.

while the histogram of $f(\sigma)$ for the LO-LOCAT data appeared as in Figure 3.2.

12
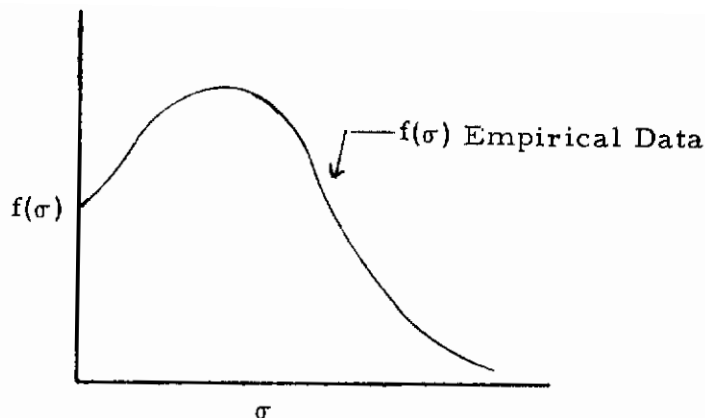
Figure 3.2 Sketch of Empirical $f(\sigma)$ from LO-LOCAT Data

Figures 3.1 and 3.2 show that the density function $f(\sigma)$ provided by Equation (3.6a) cannot be used to fit empirical $f(\sigma)$ data yet the resulting cumulative distribution obtained from Equation(3.7) does provide a good fit to the empirical peak count data.

To further test the validity of using the model of Equation (3.7) a function was found that did provide a good fit to the data. The density function used

$$f(\sigma) = \frac{1}{1 - F(a)} \left[\frac{1}{\sqrt{2 \pi} \, b} \, e^{\frac{-(\sigma - \mu)^2}{2b^2}} \right] \qquad (3.9)$$

is a normal distribution truncated at $\sigma = a$. The truncation was necessary due to the unknown effects of noise at the small values of σ. A comparison of Equation (3.9) to LO-LOCAT Data is contained in Ref. 1, p.123, for $\mu = 2.75$, $b=1.31$, and $a=1$. A substitution of Equation (3.9) into (3.7) yields

$$F(x) = \frac{1}{1 - F(a)} \frac{1}{\sqrt{2 \pi} b} \int_a^\infty e^{\frac{-x^2}{2\sigma^2} - \frac{(\sigma-u)^2}{2 b^2}} d\sigma \qquad (3.10)$$

Since a closed form solution to the integral could not be found, $F(x)$ was determined by numerical integration. Figure 3.3 shows the results of $F(x)$ calculated by Equation (3.10) versus the empirical LO-LOCAT Data. Again, the results are unacceptable.

Thus, using an $F(\sigma)$ that fits the observed data, an unacceptable $F(x)$ results, and using an $f(\sigma)$ that does not fit the data an acceptable $F(x)$ results. From this contradiction, it would appear that the necessary assumptions regarding the model of Equation (3.7) are not met and that it is impossible to determine an acceptable distribution of $F(x)$ through the exclusive use of data contained on the Master Tapes (See Figure 3.4).

13

F(x) From Truncated Normal Distribution

Compared to Empirical Observations
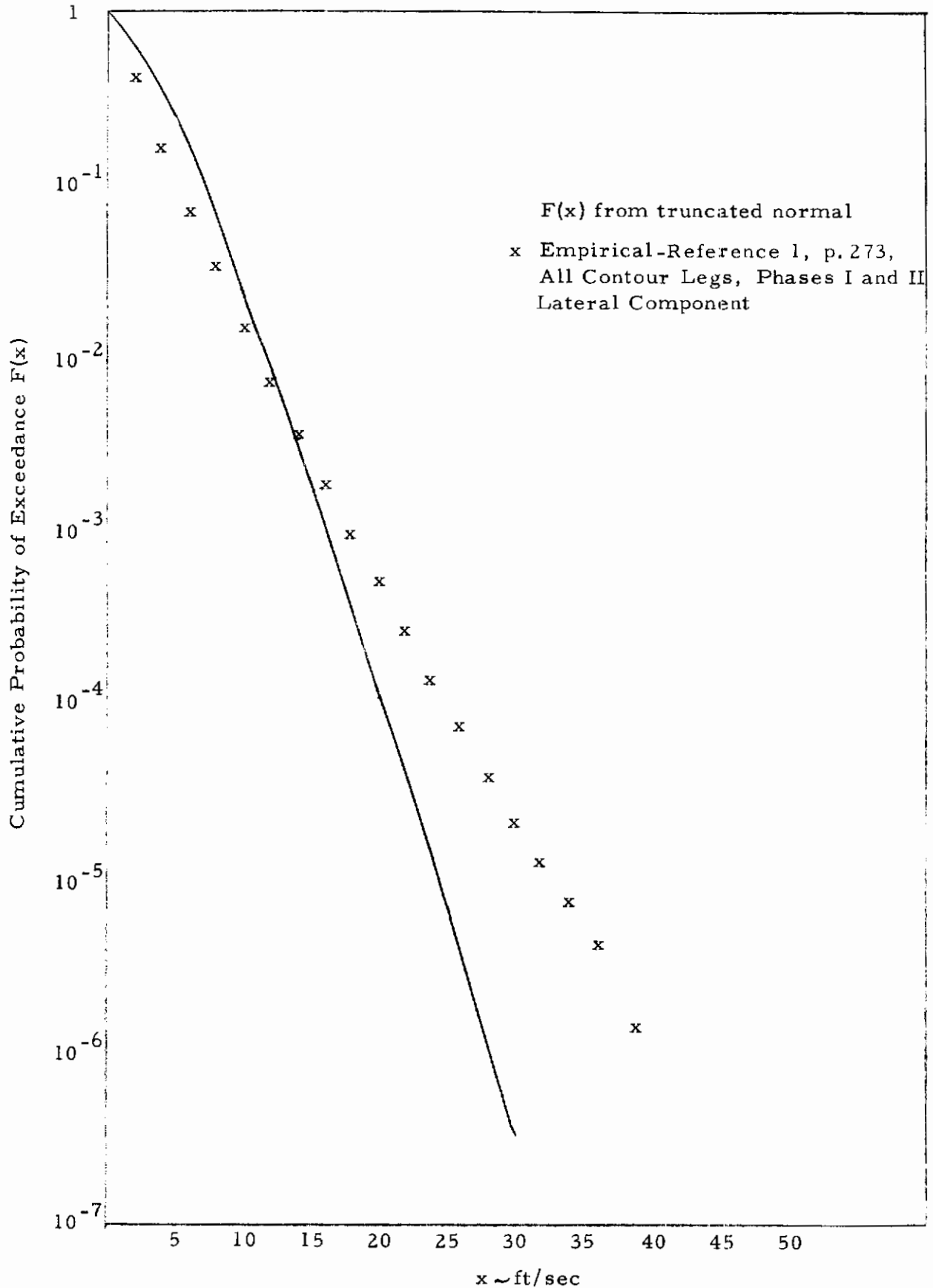
Figure 3. 3 Comparison of Empirical to Analytic Expressions for
Cumulative Probability of Exceedance

14

ATTEMPTED APPLICATIONS

Master Tapes

Determination of Gust Load Exceedance Equation

σ_u, σ_v, and σ_w from master tapes

Fit σ to

$$f(\sigma) = \frac{P_1}{b_1\sqrt{2\pi}}e^{-\frac{\sigma^2}{2b_1{}^2}} + \frac{P_2}{b_2\sqrt{2\pi}}e^{-\frac{\sigma^2}{2b_2{}^2}}$$

(1)

Apply Rice's Eq.

$$N(x) = N_0\,e^{-\frac{x^2}{2\sigma^2}}$$

$$F(x) = \int_0^\infty f(\sigma)e^{-\frac{x^2}{2\sigma^2}}\,d\sigma$$

$$F(x) = P_1 e^{-\frac{x}{b_1}} + P_2 e^{-x/b_2}$$

(2)

Assumptions

1) Each Patch S.G.

2) N(x) Level Crossings

Assuming Shape of Spectra Same for all Turbulence

Eq. 3.6 — Emp.

f(σ)   σ

Apply Equation 3.7

Emp.   Eq. 3.7   F(x)   x

Emp. good fit   Eq. 3.9

f(σ)   σ

Apply Equation 3.7

Eq. 3.7   Emp.   F(x)   x

Rice's Equation for Maximum Peak

$$F(x\,max) = e^{-\frac{x^2\,max}{2\sigma^2}}$$

Calculate F(x max) by the above equation

Does not agree with calculation of $F(x\,max) = 1/TN_0$ by flight leg data

Figure 3.4 Summary Schematic of Applications of Rice's Equations to LO-LOCAT Data.

15

Conclusions

The technique of obtaining the cumulative probability of exceedance $F(x)$ by employing the theory of Stationary Gaussian Processes has been shown to be non-applicable to LO-LOCAT turbulence samples. Extreme gust velocities are encountered on a much more frequent basis than would occur probabilistically if turbulence were truly stationary and gaussian. The introduction of the empirical $f(\sigma)$ into Equation (3.7) also resulted in poor correlation with empirical peak count observations (Figure 3.3). The fruitless attempts at using Master Tape data for determining the parameters of the gust exceedance equations are schematically shown in Figure 3.4. As a result the UDRI was unable to determine $F(x)$ merely from the σ values for individual flight legs. A detailed study was made of three classical reports. Ref. 3, 4, and 6 were reviewed with the perspective of determining whether the techniques used in these reports to determine $F(x)$ were applicable to the LO-LOCAT data.

The approach pursued in the above reports relied upon peak count accelerometer response data and appropriate transformation to determine cumulative exceedance curves. In each of these reports an assumed probability density distribution of turbulence intensity was used either directly or indirectly. The most commonly used expression for $f(\sigma)$ is shown in Equation (3.6a).

As a result of these findings, and from discussions with AFFDL personnel, it was decided to obtain $F(x)$ directly from the peak counts of all the flight legs. Since peak counts were not available on the Master Tapes of Phases I, II or III, a request was made through AFFDL to the National Records Center (Asheville, North Carolina) to extract the peak count data from the 666 time history tapes of Phases I and II data. These tapes were received at UDRI in March of 1970. The Phase III time history tapes (117) were sent directly to UDRI from the Boeing Company for extraction of peak counts. These tapes were received in late January 1970.

3.2 Calculation of F(x) from Peak Count Data

To determine the cumulative probability distribution $F(x)$ from the peak counts three techniques were considered: (1) A graphical fit to the cumulative distribution of the peak counts, (2) an analytic fit to the frequency distribution of the peak counts and (3) an analytic fit to the cumulative distribution of the peak counts (See Figure 3.5).

3.2.1 Graphical Method

The usual method of estimating the parameters P_1, P_2, b_1, and b_2 is a graphical technique derived from a plot of $F(x)$ versus x on semi-log paper. From such a plot, the cumulative probability is piece-wise fit by two line segments. Although this procedure does provide a satisfactory fit to the data the determination of values for the parameters P_1, P_2, b_1 and b_2 depend

16
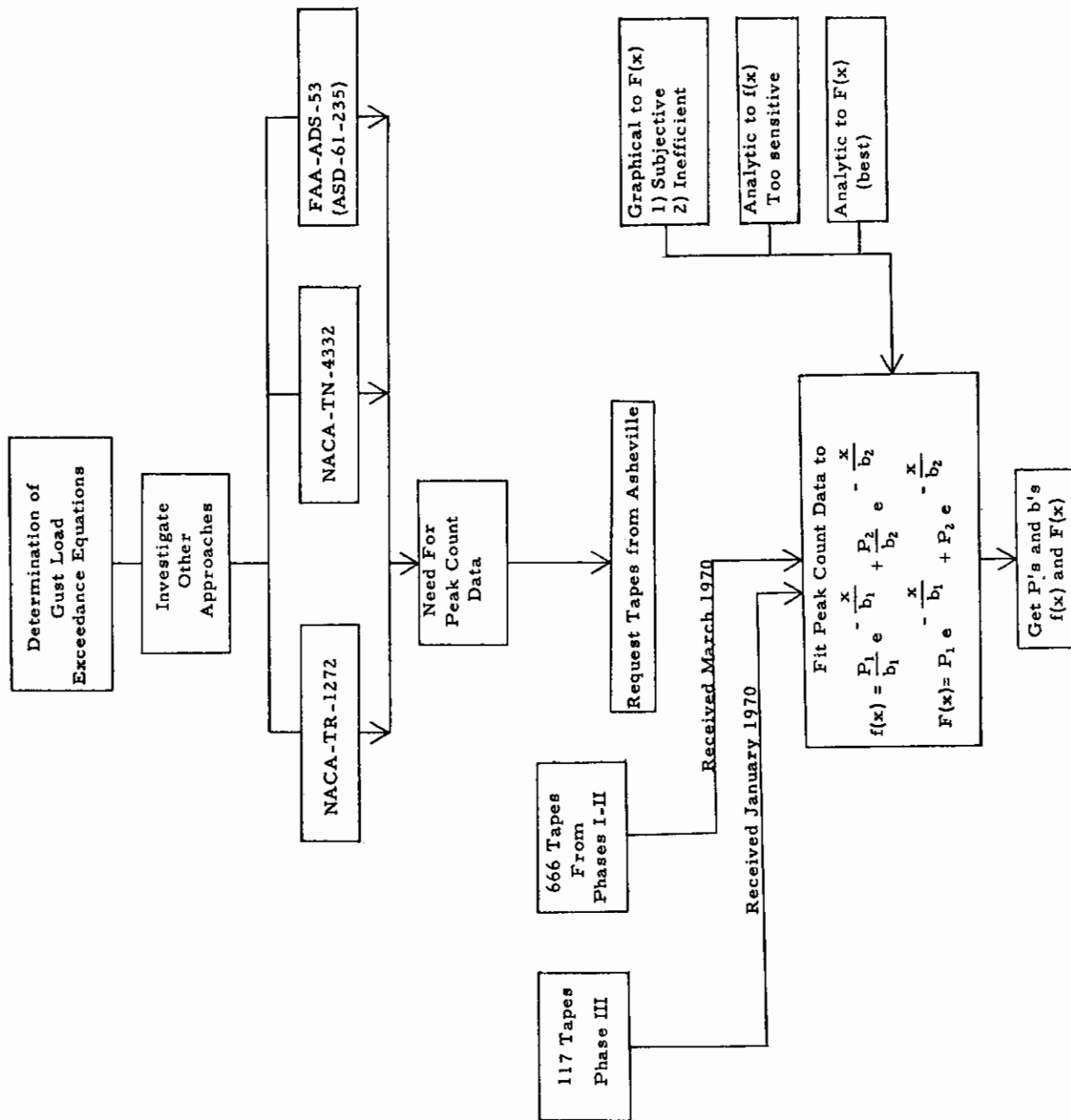
Figure 3.5 Schematic of Approaches for Obtaining Cumulative Probability of Exceedance Curves.

to a large extent upon the subjective decisions made in (1) fitting the curve to the data points, and (2) determining the slope of the fitted curve. Another undesirable feature is that the graph of the data must be drawn before any fit can be made. Hence, any large scale operation of the graphical method is time-wise prohibitive.

3.2.2 Analytic Fit to Frequency Distribution $f(x)$

The approach taken is that the cumulative distribution of peak count exceedance is $F(x)$ and that a reasonably good fit of the observed distribution of peaks is:

$$F(x) = P_1 \, e^{-x/b_1} + P_2 \, e^{-x/b_2} \qquad (3.11)$$

thus the density function of (3.11) is expressed as

$$f(x) = \frac{P_1}{b_1} \, e^{-x/b_1} + \frac{P_2}{b_2} \, e^{-x/b_2} \qquad (3.12)$$

For this density the first three moments are given by

$$m_1 = \int_0^\infty x f(x) \, dx = P_1 \, b_1 + P_2 \, b_2 \qquad (3.13)$$

$$m_2 = \int_0^\infty x^2 \, f(x) \, dx + 2P_1 \, b_1{}^2 + 2P_2 \, b_2{}^2 \qquad (3.14)$$

$$m_3 = \int_0^\infty x^3 \, f(x) \, dx = 6P_1 \, b_1{}^3 + 6P_2 \, b_2{}^3 \qquad (3.15)$$

Defining $P_1 + P_2 = 1$, there are four equations in four unknowns if the sample moments are substituted for m_1, m_2, and m_3. Thus, the solution is given by

$$b_2 = \frac{-2(m_3 - 3m_1 \, m_2) \pm \left[4(m_3 - 3m_1 \, m_2)^2 - 24(2m_1{}^2 - m_2)(3m_2{}^2 - 2m_3 m_1) \right]^{1/2}}{12(2m_1{}^2 - m_2)} \qquad (3.16)$$

$$b_1 = \frac{m_2 - 2m_1 \, b_2}{2(m_1 - b_2)} \qquad (3.17)$$

$$P_1 = \frac{m_1 - b_2}{b_1 - b_2} \qquad (3.18)$$

$$P_2 = 1 - P_1 \qquad (3.19)$$

18

Careful examination of these equations indicates the difficulty of using this approach for the problem. Typically, P_1 is much larger than P_2, and hence, the first term of Equation (3.12) will dominate. Thus, it would be expected that $2m_1{}^2 - m_2$ would be close to zero, and, since this term appears in the denominator of Equation (3.16) the estimator for b_2 would be highly sensitive to the sample moments. A similar comment can be made for every term in the expression for b_2. That is, if $P_2 = 0$, and theoretical moments are substituted in Equation (3.16), the expression for b_2 is indeterminate.

As a sample problem, Phases I and II data were taken from Ref. 1, page 273 item 10. Three different methods were used for estimating the moments for this particular distribution.

Method (a) considered the discrete moments of the rectangular density histogram with centroid at the mid-value of the rectangle.

Method (b) assumed that the first five data blocks could be sufficiently described by the density distribution.

$$f(x) = \frac{1}{m_1} e^{-x/m_1} \tag{3.20}$$

m_1 was estimated initially by using Method (a). The moment contribution from the first five data blocks was then calculated by using m_1 in Equation (3.20) to analytically estimate $f(x)$ over the first five data blocks. The contribution from the remaining blocks was calculated by Method (a).

Method (c) assumed the probability density distribution could be expressed by a series of trapezoids (i.e., linear segments when plotted on semi-log paper). The moments m_1 and m_2 were calculated by integrating Equations (3.13) and (3.14) over the trapezoids.

Table 3.1 is shown to compare the three methods of estimating the moments.

TABLE 3.1

COMPARISON OF THREE METHODS OF CALCULATING MOMENTS

Method	m_1	m_2	m_3
a	2.38223846	10.7427613	80.070224
b	2.38306104	11.4915558	86.1175969
c	2.306803581	10.69103930	80.44875562

Though the moments are in general agreement, a substitution of these values into Equations (3.16), (3.17), (3.18), and (3.19) shows the extreme sensitivity that exists.

19

Table 3.2 presents these results.

TABLE 3.2

P's AND b's FROM THREE METHODS OF CALCULATING MOMENTS

Method	P_1	P_2	b_1	b_2
a	1.00718	-.00782	2.3357	-4.14395
b	.9975	.0025	2.3701	7.5166
c	.99998	.00002	2.3062	42.2445

Methods (a) and (b) were applied to other models of cumulative peak count probability, and the extreme sensitivity provided equally disastrous results. Since the methods of moments approach has not provided generally acceptable answers using three different integration schemes, this approach was abandoned.

3.2.3 Analytic Fit to Cumulative Probability Distribution F(x)

In an attempt to find various analytical fits to the cumulative distribution of peak counts, it was observed that in several instances test data plotted on Weibull probability paper provided a straight line over the majority of the amplitude range. The only regions where linearity dropped off was in the extreme ends of the amplitude range. Although the Weibull function did not lend itself to a determination of the parameters of F(x) as given in Equation (3.8a), it was still felt that the best approach was to use Equation (3.8a) since from this equation the load exceedance Equation (3.1) could be easily evaluated. Hence, it was decided to automate the Graphical procedure described in Section 3.2.1, that is, the determination of the P's and b's from empirical peak count data using the model Equation (3.8a). If a computerized method is not used, the task of determining P's and b's for the LO-LOCAT data becomes insurmountable. If the method is not objective, a statistical interpretation of the data is impossible. The following paragraphs describe this computerized program.

In order to develop an objective method it was first necessary to find a function that would fit the cumulative empirical peak count data. Equation (3.8a) could not be fitted directly to the data to find a function because the very small probabilities of large gust velocity are not given sufficient weight by this fit. It was found, however, that the $\log_e F(x)$ could be represented by a quadratic of the form

$$\text{Ln } F(x) = A + Bx + Cx^2 \tag{3.21}$$

20

and provide sufficient accuracy in the fit for large values of x.

The cumulative probability of exceedance is determined at gust velocity bands of 2 ft/sec by cumulatively summing the peak counts obtained from the time history tapes. After taking the logarithm of the cumulative probability at each band, Equation (3.21) is fit to the data by least squares.

To eliminate the effect of instrumentation noise which produces ficticious gust velocity in the low amplitude bands, the cumulative probability for the 0-2 ft/sec band is not used in the least square fit. The constant A in Equation (3.21) reflects the percentage of data in the 0-2 ft/sec band that is considered noise. Transformation from Equation (3.21) to the function:

$$F(x) = P_1 \ e^{-x/b_1} + P_2 \ e^{-x/b_2} \tag{3.22}$$

requires a representation of P_1, P_2, b_1, and b_2 in terms of A, B and C.

If C, the coefficient of x^2 is negative in Equation (3.21), this indicates that the cumulative probability function is concave down. The best fit that can be made with Equation (3.22) to such data is to define $P_1 = 1$ and $P_2 = 0$. Thus, the natural logarithm of Equation (3.22) reduces to:

$$Ln \ F(x) = -x/b_1.$$

b_1 is evaluated by a least squares linear fit of the form

$$Ln \ F(x) = A - m \ x$$

where $m = \dfrac{1}{b_1}$. For the case when C is positive P_1, P_2, b_1, and b_2 are determined from the coefficients of Equation (3.21) as follows. b_1 is defined as the negative reciprocal of the slope of Ln F(x) at x = 0.

Thus
$$b_1 = -1/B$$

To determine b_2, the point of transition between the influences of the first and second terms of Equation (3.22) is chosen as $x_c = \dfrac{x_m}{2}$ where x_m is the maximum gust velocity encountered. b_2 is defined as the negative recriprocal of the Ln F(x) half way between x_c and x_m. Thus

$$-1/b_2 = B + \frac{3 \ Cx_m}{2}$$

P_1 and P_2 are calculated by solving the system of equations

21

$$P_1 + P_2 = 1 \tag{3.23}$$

$$P_1 \exp(-x_c/b_1) + P_2 \exp(-x_c/b_2) = \exp(Bx_c + Cx_c^2) \tag{3.24}$$

Equation (3.24) imposes the condition that Equation (3.21), after a logarithmic translation by A units to compensate for instrument noise, and Equation (3.22) coincide at the mid-gust velocity (x_c).

A computer program has been written to implement this technique of obtaining P's and b's. The program has been used on approximately 120 cumulative distributions for various categories. Section 5.3 shows plots of the distributions and resulting P's and b's. In all but 16 of the 120 cases the technique produced P's and b's that provided an excellent fit to the empirical data. The remaining cases were characterized by the occurrence of large gust velocities, generally in excess of 30 ft/sec. The technique was modified for these cases by defining b_1 as the negative reciprocal of the slope of Equation (3.21) at $\frac{x_c}{2}$, instead of at $x = 0$. The calculation of b_2 and the P's remained the same as previously. Plots of the empirical distributions and the analytical function (Equation (3.21) for the 16 cases showed the modified technique provided a good representation for the empirical data.

SECTION IV

SENSITIVITY ANALYSIS

A sensitivity analysis was performed on the LO-LOCAT data to determine which flight and environmental conditions had an influence upon the turbulence encountered by the aircraft as reflected through a number of turbulence parameters obtained from the gust velocity time histories. The turbulence parameters considered for each low level leg were:

1) σ_u, σ_v, σ_w--the standard deviation of the longitudinal, lateral, and vertical component gust velocity time histories.

2) u_{max}, v_{max}, and w_{max}--the maximum component gust velocities encountered for the leg.

3) u_{min}, v_{min}, and w_{min}--the minimum component gust velocities encountered for the leg.

4) N_{ou}, N_{ov}, and N_{ow}--the characteristic frequency of the turbulence components.

5) L_u, L_v, and L_w--the scale of turbulence for the Von Karman model of turbulence.

Turbulence parameters (1)-(3) are obtained from the filtered gust velocity time histories and are available for each low level leg. Turbulence parameters (4)-(5), however, are obtained from a power spectral density (PSD) analysis of the gust velocity time histories and are available for only a fraction of the low level legs--roughly 20% of the legs for Phases I and II and 40% of the legs for Phase III.

The flight and environmental conditions investigated as possibly relating to the turbulence parameters (1)-(5) were initially (1) location, (2) altitude, (3) atmospheric stability, (4) time of day, (5) season, and (6) terrain. A subsequent investigation extended the analysis to (7) wind speed, (8) wind direction, (9) Richardson's number, (10) vertical wind gradient, and (11) wind angle with the aircraft.

4.1 Regression Analysis

The principal analytical procedure used in the sensitivity analysis was the stepwise regression procedure BMDO2R. In this program the flight and environmental conditions were used as the independent variables with the various turbulence parameters used as the dependent variable. The use

23

of this procedure eliminated any subjective bias or preconceived notions about the data in that the resulting regression equations are developed in a stepwise fashion, with each environmental condition being considered according to its statistical significance to the turbulence parameters. The regression analysis on Phases I and II was conducted in three basic steps. First a regression was performed on each turbulence parameter for the u, v, and w components at each location (Edwards, Griffiss, Peterson, and McConnell) using environmental conditions (2)-(6) as the independent variables. Second, the analysis was extended to include the meteorological conditions (7)-(11) for each component location combination in an effort to improve on the relationships established in the initial regression procedure. And, finally, the data from all three turbulence components was analyzed together, using environmental conditions (1)-(11) as the independent variables.

4.1.1 Analytical Procedure

The eleven environmental conditions were initially broken down into categories as given in Table 4.1. The categories for conditions (1)-(6) were established by the Boeing Company and are coded into the record for each low level leg on the "Master Tape" received from Boeing. The categories for conditions (7)-(11) were established from meteorological considerations by UDRI. Each category was then represented by a dichotomous variable which took a value one if the condition was present for the given leg and took a value zero if the condition were not present for the leg given. For example, the dichotomous variable representing the category "Dawn" would take a value one for those legs flown at dawn and take a value zero for those legs not flown at dawn. These dichotomous variables were then used as the independent variables in the stepwise regression procedure BMDO2R with the various turbulence parameters used as the dependent variable.

Since the dichotomous variables take only values of zero and one, this regression procedure reduces to a decomposition of low level legs into categories represented by the dichotomies of the independent variables with the regression coefficients indicating a measure of the effect produced in the turbulence parameter by the flight conditions of the dichotomies. In addition, the order of entrance of the dichotomous variables into the regression equation ranks environmental conditions on their order of influence to the dependent turbulence parameter.

After several test runs it was evident that the regression coefficients must be referred to a common environmental condition in order to compare results from different runs. The dichotomous variables representing the underlined categories in Table 4.1 were therefore eliminated from the analysis in the first two regression phases. The elimination of these variables does not suppress the effect of any of these categories but merely references the effects in the analysis to these conditions.

TABLE 4.1

DECOMPOSITION OF ENVIRONMENTAL CONDITIONS

Environmental Condition	Condition Categories
1) Location	Edwards, Griffiss, Peterson, McConnell
2) Altitude	<u>250 Ft.</u>, 750 Ft.
3) Season	Spring, <u>Summer</u>, Fall, Winter
4) Time of Day	Dawn, <u>Mid-Morning</u>, Mid-Afternoon
5) Atmospheric Stability	Very Stable, Stable, <u>Neutral</u>, Unstable
6) Terrain	High Mountains, Low Mountains, <u>Plains</u>, Desert
7) Wind Speed	$WS < 15$ Ft/Sec, $\underline{15\ \text{Ft/Sec} < WS < 30\ \text{Ft/Sec}}$, 30 Ft/Sec $< WS < 45$ Ft/Sec, $WS > 45$ Ft/Sec, $0^\circ < WD \leq 90^\circ$, $\underline{90^\circ < WD \leq 180^\circ}$, $180^\circ < WD \leq 270^\circ$, $270^\circ < WD \leq 360^\circ$
9) Richardson's Number	$R < .25$, $\underline{.25 \leq R < 1.0}$, $R \geq .10$
10) Vertical Wind Gradient	$WG < .02$, $\underline{.02 \leq WG \leq .06}$, $WG > .06$
11) Wind Angle with the Aircraft	$\begin{pmatrix} 45^\circ < WA \leq 90^\circ \\ 270^\circ < WA \leq 315^\circ \end{pmatrix}$ $\begin{pmatrix} 0^\circ < WA \leq 45^\circ \\ 315^\circ < WA \leq 360^\circ \end{pmatrix}$ $\begin{pmatrix} 90^\circ < WA \leq 135^\circ \\ 225^\circ < WA \leq 270^\circ \end{pmatrix}$ $\underline{135^\circ < WA \leq 225^\circ}$

4. 1. 2 Results on Phase I and II Gust Velocity Standard Deviations

The results of the stepwise regression analysis for 1265 low level legs
at Edwards Air Force Base during Phases I and II with the standard deviation
of the lateral component of the gust velocity as the dependent variable and
environmental conditions (2)-(6) as the independent variables are given in
Table 4. 2. At step 0 the mean lateral standard deviation for the 1265 legs
is given as 2. 77 ft/sec. At step 1, the legs are decomposed into two groups,
those flown in very stable air having a fitted mean σ_v of 3. 24 - 1. 31 = 1. 93 ft/sec,
while those not flown in very stable air have a fitted mean 3. 24 ft/sec. The
category "very stable air" was considered first because the dichotomous
variable representing this category was most strongly correlated to the
dependent variable in the regression procedure. Additional categories are
considered in their order of influence upon the residual of the dependent
variable after the effects of the dichotomous variables already considered
have been removed. In this case, the category "desert" produced the next
strongest effect upon the lateral standard deviations of the 1265 legs. At
this stage the legs have been decomposed into four groups with, for example,
the predicted mean lateral standard deviation for legs flown in very stable
air over the desert given as 3. 47 - 1. 31 - . 79 = 1. 37 ft/sec. and for legs
flown over the desert not in very stable air as 3. 47 - . 79=2. 68 ft/sec. The
decomposition continues for nine steps with the coefficients being referenced
to the eliminated categories under each environmental condition. No
coefficients for categories Fall and Winter are given because no discernible
difference in the dependent variable was detected for these categories.
The final correlation coefficient of 0. 658 indicates that the decomposition
presented explains $100(. 658)^2$ = 43. 3% of the total variation in the lateral
standard deviation of the 1265 Edwards legs. Additional information can
be obtained from Table 4. 2 by noting some of the interlocking relationships
between the coefficients. Note, for example, at step 5, that the entrance of
the category dawn into the regression procedure alters the value of the
coefficient for very stable air from the previous step. This phenomenon
occurs because the categories dawn and very stable air are highly correlated
and part of the effect of the category dawn is carried by the category very
stable air until dawn is entered into the regression equation. The correlation
between these two categories is illustrated in Table 4. 3 where the frequency
of occurrence of each time of day stability condition is given for the Edwards
legs.

Even though stability and time of day categories are strongly correlated,
the analysis in Table 4. 2 illustrates that atmospheric stability has the stronger
influence upon the dependent variable. This result is verified by the results
in Table 4. 4 where the mean lateral standard deviation of the gust velocity
is computed for each stability time of day category for the Edwards legs.
While this table illustrates many of the relationships established in Table
4. 2 there is considerable distortion present in the means of Table 4. 4 due
to the fact that all categories are not uniformly distributed among the 12
stability time of day categories. For example, no leg flown over the desert at

26

TABLE 4.2

SIGMA REGRESSION, PHASES I AND II, EDWARDS, LATERAL

Phases I and II
Edwards σ_v Regression
Lateral Component
n = 1265

Step	Constant	Altitude 750 ft.	Stability			Time of Day		Season			Terrain		Correl. Coeff.	Standard Deviation
			Very Stable	Stable	Unstable	Dawn	Altern.	Spring	Fall	Winter	High Mount.	Desert		
0	2.77													1.243
1	3.24		-1.31										.508	1.071
2	3.47		-1.31									-.79	.586	1.007
3	3.75	-.30	-1.57	-.71								-.83	.626	0.970
4	3.90	-.31	-1.55	-.68								-.84	.638	0.959
5	3.92	-.30	-1.30	-.58		-.34						-.84	.645	0.951
6	3.78	-.30	-1.17	-.45	+.35	-.34						-.81	.651	0.946
7	3.89	-.30	-1.18	-.45	+.34	-.44	-.22					-.81	.655	0.942
8	3.83	-.30	-1.17	-.44	+.31	-.45	-.22				+.15	-.74	.657	0.940
9	3.80	-.30	-1.14	-.43	+.28	-.48	-.23	+.12			+.16	-.75	.658	0.939

27

TABLE 4.3

NUMBER OF FLIGHT LEGS AT EDWARDS BY STABILITY AND TIME OF DAY

ATMOSPHERIC STABILITY

		Very Stable	Stable	Neutral	Unstable
Time of Day	Dawn	421	114	15	4
	Mid-Morning	63	131	211	150
	Mid-Afternoon	60	130	204	118

TABLE 4.4

MEAN SIGMA FOR EDWARDS LEGS BY STABILITY AND TIME OF DAY

ATMOSPHERIC STABILITY

		Very Stable	Stable	Neutral	Unstable
Time of Day	Dawn	1.76	2.42	3.67	4.25
	Mid-Morning	1.84	2.84	3.41	3.92
	Mid-Afternoon	1.89	2.79	3.05	3.68

28

dawn at 750 ft. altitude encountered neutral or unstable atmospheric conditions. The results of the extension of the regression analysis to the longitudinal and vertical components of the standard deviation of the gust velocity at Edwards are given in Tables 4.5 and 4.6. These tables indicate consistent relationships for all three components with generally smaller standard deviations occurring in very stable air and over the desert. A comparison of these results with the Peterson data in Tables 4.7 - 4.9 shows that there is a stronger seasonal effect and a stronger time of day effect at Peterson with a corresponding decrease in the influence of atmospheric stability. The final decomposition in Tables 4.2, 4.5 - 4.9 together with similar results for McConnell and Griffiss have been recorded in Table 4.10. This table basically summarizes the relationship of the component standard deviation σ_u, σ_v, and σ_w to the environmental conditions (2) - (6). Important characteristics are as follows:

1)   Altitude -- A negative coefficient indicates that generally smaller standard deviations were obtained during the 750 ft. legs. The magnitude of the coefficient is consistently smaller for the vertical components indicating a weaker dependence upon altitude in this case.

2)   Atmospheric Stability-- Stability is the most influential of the environmental conditions considered, with generally less turbulence being encountered with increased stability of air.

3)   Time of Day -- Generally smaller standard deviations were observed at dawn with the strongest influence occurring in the vertical component. There was very little detectable difference between the mid-morning and the afternoon standard deviations except at Peterson where considerably larger values were observed during the afternoon.

4)   Season -- There were few consistent trends for season except that generally higher standard deviations were observed during spring. In general, the seasonal effect is smaller at Edwards than at the other bases with practically no seasonal effect observed in the lateral and longitudinal components.

5)   Terrain -- There are no strong terrain effects except at Edwards where generally smaller standard deviations were observed over the desert.

6)   Correlation Coefficient -- While the correlations are not excessively high, it seems worth noting that the correlations are consistently higher for the vertical component at all four bases. This shows a stronger influence of the vertical standard deviation upon the environmental conditions.

An extension of the regression procedure to include the meteorological environmental conditions (7)-(11) for the Phases I and II data indicated that wind velocity was the most important of these conditions relating to the component gust velocity standard deviations. The results of the regression procedure for the Edwards lateral standard deviations are given in Table 4.11. A comparison with Table 4.2 indicates that the environmental conditions

29

Phases I and II
Edwards σ_u Regression
Longitudinal Component
n = 1596

TABLE 4.5

SIGMA REGRESSION - PHASES I AND II, EDWARDS, LONGIDUTINAL

Step	Constant	Altitude 750 ft.	Stability			Time of Day		Season			Terrain		Correl. Coeff.	Standard Deviation
			Very Stable	Stable	Unstable	Dawn	Aftern.	Spring	Fall	Winter	High Mount.	Desert		
0	2.58													1.124
1	2.99		-1.24										.519	0.961
2	3.20		-1.23									-.68	.589	0.903
3	3.42		-1.45	-.63								-.69	.628	0.875
4	3.62	-.40	-1.42	-.60								-.70	.653	0.852
5	3.64	-.42	-1.11	-.49		-.42						-.70	.666	0.840
6	3.51	-.41	-1.00	-.38	+.29	-.41						-.67	.671	0.835
7	3.45	-.41	-1.00	-.37	+.25	-.43					+.18	-.60	.674	0.832
8	3.48	-.41	-.99	-.35	+.23	-.43			-.12		+.18	-.60	.675	0.831
9	3.52	-.40	-.97	-.35	+.20	-.45			-.16	-.19	+.18	-.60	.677	0.829
10	3.57	-.40	-.97	-.35	+.20	-.49	-.09		-.16	-.19	+.18	-.61	.678	0.829
11	3.54	-.40	-.96	-.35	+.19	-.50	-.09	+.07	-.13	-.17	+.18	-.61	.678	0.829

TABLE 4.6

SIGMA REGRESSION, PHASES I AND II, EDWARDS, VERTICAL

Phases I and II
Edwards σ_w Regression
Vertical Component
n = 1579

Step	Constant	Altitude 750 ft.	Stability			Time of Day		Season			Terrain		Correl. Coeff.	Standard Deviation
			Very Stable	Stable	Unstable	Dawn	Aftern.	Spring	Fall	Winter	High Mount.	Desert		
0	2.93													1.265
1	3.51		-1.74										.637	0.992
2	3.63		-1.08			-1.00							.695	0.925
3	3.80		-1.08			-1.00						-.58	.725	0.836
4	4.02		-1.47	-.70		-.78						-.58	.753	0.847
5	4.10		-1.42	-.64		-.79			-.35			-.59	.763	0.832
6	4.19		-1.32	-.59		-.84			-.47	-.61		-.59	.779	0.808
7	4.34		-1.31	-.53		-.99	-.29		-.48	-.63		-.60	.784	0.799
8	4.45	-.21	-1.29	-.57		-1.00	-.29		-.47	-.62		-.60	.789	0.792
9	4.34	-.21	-1.27	-.54		-1.02	-.29		-.47	-.62	+.22	-.50	.792	0.788
10	4.25	-.21	-1.20	-.46	+.21	-1.00	-.28		-.45	-.59	+.20	-.49	.794	0.785

31

TABLE 4.7

SIGMA REGRESSION, PHASES I AND II, PETERSON, LATERAL

Phases I and II
Peterson σ_v Regression
Lateral Component
n = 978

Step	Constant	Altitude 750 ft.	Stability			Time of Day		Season			Correl. Coeff.	Standard Deviation
			Very Stable	Stable	Unstable	Dawn	Aftern.	Spring	Fall	Winter		
0	2.48											1.099
1	2.84					-1.18					.492	0.957
2	2.49					-.83	+.78				.574	0.901
3	2.36		-.39			-.82	+.80	+.60			.614	0.869
4	2.47		-.43			-.69	+.73	+.56			.631	0.854
5	2.57	-.30	-.41			-.66	+.76	+.59			.644	0.843
6	2.75	-.34	-.54			-.66	+.75	+.44	-.31		.656	0.832
7	2.86	-.32	-.55	-.18		-.64	+.72	+.44	-.30		.659	0.830
8	2.80	-.31	-.68	-.21		-.64	+.71	+.51	-.24	+.28	.662	0.827
9	2.92	-.31		-.32	-.27	-.64	+.71	+.50	-.23	+.28	.665	0.824

32

TABLE 4.8

SIGMA REGRESSION, PHASES I AND II, PETERSON, LONGITUDINAL

Phases I and II
Peterson σ_u Regression
Longitudinal Component
n = 1082

| Step | Constant | Altitude 750 ft. | Stability | | | Time of Day | | Season | | | Correl. Coeff. | Standard Deviation |
			Very Stable	Stable	Unstable	Dawn	Aftern.	Spring	Fall	Winter		
0	2.13											0.964
1	2.46					-1.01					.494	0.839
2	2.16					-.71	+.68				.571	0.792
3	2.07	-.36				-.71	+.70	+.46			.602	0.771
4	2.18	-.41				-.70	+.73	+.50			.628	0.752
5	2.36	-.43				-.70	+.72	+.34	-.31		.644	0.740
6	2.44	-.43	-.23			-.62	+.68	+.32	-.31		.651	0.734
7	2.37	-.41	-.23			-.63	+.67	+.39	-.24	+.28	.656	0.730
8	2.48	-.40	-.36	-.19		-.61	+.64	+.40	-.22	+.30	.660	0.727
9	2.59		-.48	-.30	-.26	-.60	+.64	+.39	-.22	+.30	.664	0.724

33

TABLE 4.9

SIGMA REGRESSION, PHASES I AND II, PETERSON, VERTICAL

Phases I and II
Peterson σ_w
Vertical Component
n = 1082

Step	Constant	Altitude 750 ft.	Stability			Time of Day		Season			Correl. Coeff.	Standard Deviation
			Very Stable	Stable	Unstable	Dawn	Aftern.	Spring	Fall	Winter		
0	2.22											1.149
1	2.73					-1.51					.622	0.901
2	2.37					-1.15	+.82				.635	0.838
3	2.63					-1.14	+.79		-.59		.730	0.787
4	2.74		-.50			-.98	+.69		-.55		.753	0.758
5	2.60		-.48			-.99	+.71	+.38	-.42		.762	0.746
6	2.72		-.61	-.18		-.98	+.69	+.39	-.42		.764	0.743
7	2.80		-.69	-.26	-.18	-.97	+.69	+.38	-.41		.766	0.741

34

TABLE 4.10

SUMMARY OF SIGMA REGRESSION, PHASES I AND II

Phases I and II
Gust Velocity Standard Deviation
Summary Table

Base	Component	n	Constant	Altitude 750 ft.	Stability			Time of Day		Season			Terrain			Correl. Coeff.	Standard Deviation
					Very Stable	Stable	Unstable	Dawn	Aftern.	Spring	Fall	Winter	High Mount.	Low Mount.	Desert		
Edwards	Lateral	1265	3.80	-.30	-1.14	-.43	+.28	-.48	-.23	+.12			+.16		-.75	.658	0.939
Edwards	Long.	1596	3.54	-.40	-.96	-.35	+.19	-.50	-.09	+.07	-.13	-.17	+.18		-.61	.678	0.829
Edwards	Vertical	1579	4.25	-.21	-1.20	-.46	+.21	-1.00	-.28		-.45	-.59	+.20		-.49	.794	0.785
Peterson	Lateral	978	2.92	-.31	-.68	-.32	-.27	-.64	+.71	+.50	-.23	+.28	*	*	*	.665	0.824
Peterson	Long.	1082	2.59	-.40	-.48	-.30	-.26	-.60	+.64	+.39	-.22	+.30	*	*	*	.664	0.724
Peterson	Vertical	1082	2.80		-.69	-.26	-.18	-.97	+.69	+.38	-.41		*	*	*	.766	0.741
Griffiss	Lateral	1248	3.90	-.57	-1.86	-.56		-.26	-.09	+1.05	+.28	+.72	*	+.16	*	.599	1.200
Griffiss	Long.	1463	3.80	-.65	-1.66	-.48		-.33	-.09	+.87	+.22	+.46	*	+.08	*	.617	1.045
Griffiss	Vertical	1420	3.62	-.20	-1.47	-.46	+.15	-.67	-.17	+.71		+.21	*	+.27	*	.703	0.842
McConnell	Lateral	1944	3.04	-.42	-1.44	-.11	+.22	-.30	-.10	+.64	+.29	+.53	*	*	*	.724	0.798
McConnell	Long.	2303	2.79	-.53	-1.22	-.11	+.27	-.26		+.66	+.32	+.52	*	*	*	.712	0.749
McConnell	Vertical	2307	2.75	-.04	-1.29	-.19	+.23	-.55		+.51	+.15	+.21	*	*	*	.801	0.596

TABLE 4.11

SIGMA REGRESSION WITH METEOROLOGICAL PARAMETERS
PHASES I AND II, EDWARDS LATERAL

n = 1070

Step	Constant	Alt. 750 ft.	Very Stable	Stable	Unstable	Dawn	Aft.	Spring	Fall	Winter	High Mount.	Desert	<15	30-45	≥45	<.25	>1	0-45 315-360	45-90 270-315	90-135 225-270	Correl. Coeff.	Standard Deviation
0	2.78																					1.235
1	3.23		-1.28																		.49	1.074
2	3.54		-1.11										-.75								.58	1.010
3	3.70		-1.12									-.68	-.66								.63	0.962
4	3.94		-1.39	-.69								-.73	-.60								.66	0.925
5	4.31		-1.42	-.71								-.81	-.63					-.52			.69	0.890
6	4.48	-.32	-1.39	-.68								-.83	-.62					-.53			.71	0.876
7	4.52	-.33	-1.11	-.57		-.39						-.83	-.62					-.56			.72	0.865
8	4.71	-.34	-1.10	-.55		-.56	-.38					-.83	-.64					-.56			.73	0.852
9	4.60	-.35	-1.06	-.53		-.59	-.40					-.84	-.55	+.44				-.55			.73	0.842
10	4.54	-.35	-1.03	-.51		-.60	-.39					-.86	-.50	+.49	+.70			-.53			.74	0.836
11	4.44	-.35	-1.02	-.50		-.61	-.39				+.22	-.76	-.50	+.50	+.71			-.54			.74	0.831
12	4.20	-.34	-.82	-.41		-.61	-.39				+.23	-.76	-.48	+.48	+.71	+.25		-.55			.75	0.827
13	4.12	-.34	-.82	-.41		-.60	-.38				+.21	-.78	-.48	+.48	+.72	+.25		-.47		+.25	.75	0.824
14	4.04	-.33	-.76	-.33	+.23	-.59	-.37				+.19	-.77	-.47	+.47	+.68	+.25		-.47		+.25	.75	0.821
15	4.09	-.33	-.75	-.34	+.22	-.62	-.37			-.19	+.19	-.78	-.46	+.47	+.71	+.23		-.49		+.25	.75	0.819

36

(2)-(6) enter the regression procedure in roughly the same manner with wind velocity exerting an additional strong effect when added to the list of independent variables. In this procedure, strong winds indicate more turbulence with light winds indicating less turbulence as reflected through the component gust velocity standard deviations. Wind Angle also seems to have some effect with less turbulence being experienced when the aircraft is flying into the wind.

The differences in Tables 4.2 and 4.11 at steps 0 and 1 are caused by the fact that a few legs had to be deleted from the extended regression because all of the environmental conditions were not available for some legs. The improvement in the regression procedure with the addition of the meteorological conditions can be observed by noting the increase in the correlation coefficient in Table 4.11 over that obtained in Table 4.2. These results obtained at Edwards are typical of those obtained at the other bases when the meteorological conditions are added to the list of independent variables.

As a final analysis on the gust velocity standard deviations, all the data from the four bases and the three components were used in a regression analysis with environmental conditions (1)-(6) as the independent variables and introducing dichotomous variables to represent the three components. Wind speed was also added to the list of independent variables since a relationship to this meteorological condition was observed in Table 4.11. In addition, no dichotomous variables for the categories of conditions (1)-(6) were eliminated since there was no need for comparison between runs. The results of this regression analysis are given in Table 4.12. The results of this analysis are similar to those found earlier except that the base Griffiss enters into the regression very early. This result indicates that generally more turbulence was encountered at Griffiss than under similar environmental conditions at other bases. This statement is verified by Table 4.13 which contains a listing of the average gust velocity standard deviations by base and terrain type. The fact that Griffiss does enter into the regression equation indicates that the effect produced is unique to Griffiss and cannot be explained by any of the environmental conditions considered.

4.1.3 Results on Other Turbulence Parameters

The regression analysis described for the gust velocity standard deviation was also performed on several other turbulence parameters to determine if the various parameters contained similar information about the turbulence.

4.1.3.1 Maximum and Minimum Gust Velocity Regression

Using the maximum component gust velocities for each leg as the dependent variable, the stepwise regression procedure was performed for each location and component with environmental conditions (2)-(6) as the independent variables. The results with u_{max} at Edwards are given in

37

TABLE 4.12

SIGMA REGRESSION, PHASES I AND II, ALL FLIGHT LEGS
ALL COMPONENTS

Step	Constant	Alt. 250 750	Very Stable	Stable	Neut.	Unst.	Dawn	Mid Morn.	Mid Aft.	Spr.	Su.	F.	W.	Hi Mt.	Low Mt.	Pl.	Des.	0-15	15-30	30-45	>45	Ed.	Pct.	Mc.	Gr.	Long.	Lat.	Ver.	Correl. Coeff.	Std. Dev.
0	2.69																													1.218
1	3.08		-1.38																										.51	1.047
2	2.92		-1.34																						+.73				.56	1.006
3	3.19		-1.62	-.60																					+.81				.60	0.974
4	3.30		-1.57	-.58														-.40							+.78				.62	0.956
5	3.17		-1.57	-.54			-.55											-.47						+.47	+.92				.64	0.937
6	3.20		-1.19	-.46			-.60											-.49						+.49	+.90				.66	0.916
7	3.45		-1.14	-.44			-.60											-.77	-.46					+.55	+.93				.68	0.897
8	3.63	-.36	-1.15	-.41			-.60											-.81	-.49					+.59	+.92				.69	0.879
9	3.64	-.37	-1.15	-.42			-.64											-.79	-.51					+.78	+.93				.70	0.865
10	3.54	-.38	-1.08	-.38			-.64			+.38						-.67		-.76	-.49					+.77	+.88				.71	0.853
11	3.48	-.38	-1.08	-.38			-.66			+.37						-.67		-.76	-.49					+.77	+.87			+.22	.72	0.846
12	3.38	-.39	-1.08	-.37			-.66			+.36						-.67		-.66	-.39	+.37				+.78	+.88			+.22	.72	0.842
13	3.34	-.39	-1.07	-.37			-.66			+.40			+.15			-.67		-.66	-.39	+.37				+.78	+.87			+.22	.72	0.840
14	3.34	-.39	-1.07	-.36			-.66			+.40			+.16	+.23		-.57		-.66	-.39	+.37				+.68	+.87			+.22	.73	0.838

TABLE 4.13

PHASES I AND II

MEAN SIGMA BY BASE, TERRAIN, AND COMPONENT

	σ_u Longitudinal	σ_v Lateral	σ_w Vertical
Edwards High Mountains	2.94	3.16	3.26
Edwards Low Mountains	2.66	2.91	2.93
Edwards Desert	2.07	2.21	2.45
Griffiss Low Mountains	3.33	3.63	3.29
Griffiss Plains	3.24	3.46	2.99
Peterson Plains	2.09	2.44	2.23
McConnell Plains	2.48	2.66	2.38

TABLE 4.14

REGRESSION ON MAXIMUM GUST VELOCITY

PHASES I AND II

EDWARDS

LONGITUDINAL

Phases I and II
Edwards Longitudinal Maximum Gust u_{max} n = 1596

Step	Constant	Altitude 750 ft.	Stability Very Stable	Stable	Unstable	Time of Day Dawn	Aftern.	Season Spring	Fall	Winter	Terrain High Mount.	Desert	Correl. Coeff.	Standard Deviation
0	11.95													5.290
1	13.46		-4.52										.403	4.844
2	14.75		-4.47									-4.26	.548	4.430
3	15.51		-5.23	-2.18								-4.29	.570	4.349
4	16.28	-1.51	-5.14	-2.07								-4.34	.588	4.242
5	16.35	-1.56	-3.79	-1.58		-1.79						-4.33	.599	4.242
6	15.76	-1.56	-3.66	-1.41		-1.89					+1.20	-3.79	.606	4.215
7	15.47	-1.53	-3.38	-1.12	+.79	-1.86					+1.10	-3.75	.608	4.209
8	15.36	-1.53	-3.28	-1.09	+.71	-1.93		+.50			+1.10	-3.75	.609	4.206

TABLE 4.15

REGRESSION ON MAXIMUM GUST VELOCITY, PHASES I AND II, PETERSON, LONGITUDINAL

Phases I and II
Peterson Longitudinal Maximum Gust u_{max}
n = 1083

Step	Constant	Altitude 750 ft.	Stability Very Stable	Stability Stable	Stability Unstable	Time of Day Dawn	Time of Day Aftern.	Season Spring	Season Fall	Season Winter	Correl. Coeff.	Standard Deviation
0	9.71											4.13
1	8.82						+3.08				.339	3.891
2	9.69					-1.84	+2.21				.387	3.815
3	9.33	-1.49				-1.84	+2.26	+1.73			.421	3.754
4	9.80	-1.70				-1.82	+2.41	+1.90			.456	3.686
5	10.56	-1.70				-1.80	+2.34	+1.25	-1.29		.476	3.645
6	10.26	-1.75				-1.81	+2.32	+1.56	-.97	+1.21	.482	3.631
7	10.47		-.72			-1.58	+2.19	+1.50	-.94	+1.22	.487	3.621
8	10.79		-1.11	-.56		-1.54	+2.11	+1.54	-.91	+1.31	.490	3.616
9	11.11		-1.45	-.90	-.76	-1.51	+2.10	+1.51	-.89	+1.31	.492	3.613

TABLE 4.16

SUMMARY OF REGRESSION ON MAXIMUM GUST VELOCITY
PHASES I AND II

Phases I and II
Maximum Gust Regression
Summary Table

Base	Component	n	Constant	Altitude 750 ft.	Stability Very Stable	Stability Stable	Stability Unstable	Time of Day Dawn	Time of Day Aftern.	Season Spring	Season Fall	Season Winter	Terrain High Mount.	Terrain Low Mount.	Terrain Desert	Correl. Coeff.	Standard Deviation
Edwards	Lateral	1565	18.11	-1.59	-4.62	-1.34	+1.10	-1.40		+.57					-4.81	.593	4.988
Edwards	Long.	1596	15.36	-1.53	-3.28	-1.09	+.71	-1.93		+.50			+1.10		-3.75	.609	4.206
Edwards	Vertical	1578	19.78	-.85	-5.30	-2.13		-3.40	-1.19	+.56	-1.04	-1.32	+1.20		-3.35	.653	4.736
Peterson	Lateral	994	12.81	-1.87	-2.11	-1.16	-1.62	-1.98	+3.35	+2.07	-.97	+1.85	*	*	*	.549	4.344
Peterson	Long.	1083	11.11	-1.68	-1.45	-.90	-.76	-1.51	+2.10	+1.51	-.89	+1.31	*	*	*	.492	3.613
Peterson	Vertical	1082	12.75	-.50	-2.47	-1.04	-.66	-3.60	+2.83	+1.93	-1.31	+1.05	*	*	*	.660	3.831
Griffiss	Lateral	1332	16.33	-2.28	-7.99	-2.27			-.43	+4.49	+1.18	+2.90	*	+.88	*	.566	5.188
Griffiss	Long.	1463	14.97	-2.13	-5.81	-1.49		-.96	-.43	+3.62	+.88	+1.92	*	+.57	*	.529	4.672
Griffiss	Vertical	1420	16.81	-.63	-6.72	-2.14		-2.41	-.50	+3.54		+1.12	*	+.91	*	.633	4.414
McConnell	Lateral	2255	12.50	-1.61	-4.99	-.65	+1.24	-.87	+.34	+2.85	+1.03	+1.88	*	*	*	.645	3.563
McConnell	Long.	2302	10.94	-1.91	-4.05	-.24	+1.25	-.94	+.26	+2.86	+1.47	+2.28	*	*	*	.623	3.439
McConnell	Vertical	2306	13.11	-.48	-5.63	-.98	+1.00	-2.31	+.22	+2.41	+.86	+1.01	*	*	*	.752	3.076

42

Table 4.14. These results are typical and a comparison with the results on σ_u in Table 4.5 indicates general consistency in that the independent variables enter into the regression equation in roughly the same order to produce the same pattern of dependence upon the environmental conditions. The relative magnitude of the regression coefficients is similar, indicating the two turbulence parameters σ_u and u_{max} contain much the same information about turbulence. Table 4.15 contains the results of a similar run for u_{max} at Peterson and Table 4.16 is the summary table for the maximum gust regression at all bases. A comparison with Table 4.10 shows good consistency with the earlier results. One notable difference in the results is that the correlation coefficients for the maximum gust regressions are consistently lower than the corresponding coefficients for the σ_u, σ_v, and σ_w regressions. This implies that the parameters σ_u, σ_v, and σ_w relate more strongly to the environmental conditions than do the corresponding parameters u_{max}, v_{max}, and w_{max}.

The regression procedure was also performed using the minimum gust velocity as the dependent variable. The results were very similar to those for the maximum gust velocity. A typical example is given for u_{min} at Edwards in Table 4.17.

4.1.3.2 N_o Regression

For approximately 20% of the low level legs, a PSD was performed and for these legs the turbulence parameter N_o was used as the dependent variable in the regression analysis. The results for the three components at Edwards are given in Tables 4.18 - 4.20 and the summary for all bases is given in Table 4.21. General trends of the N_o regression are as follows:

1) Generally smaller values of N_o were observed at 750 ft. altitude with the weakest dependence upon altitude occurring in the longitudinal component.

2) Larger values of N_o were observed in very stable air with little dependence occurring in the other stability levels.

3) Generally larger values of N_o occur at dawn, with the strongest dependence occurring in the vertical component.

4) No strong trends with season, except for generally larger values of N_o occurring in the fall and winter in the vertical component.

5) Little dependence upon terrain, except for larger values of N_o occurring over the desert.

6) The correlation coefficient for the vertical component is consistently larger than the correlation for the lateral and longitudinal components.

43

TABLE 4.17

REGRESSION ON MINIMUM GUST VELOCITY, PHASES I AND II, EDWARDS, LONGITUDINAL

Phases I and II
Edwards Longitudinal Minimum Gust u_{min}
n = 1595

Step	Constant	Altitude 750 ft.	Stability			Time of Day		Season			Terrain		Correl. Coeff.	Standard Deviation
			Very Stable	Stable	Unstable	Dawn	Aftern.	Spring	Fall	Winter	High Mount.	Desert		
0	-12.14													5.933
1	-13.67		+4.61										.366	5.523
2	-14.96		+4.56									+4.26	.493	5.163
3	-16.10	+2.12	+4.48									+4.33	.525	5.055
4	-15.47	+2.04	+3.98		-2.03							+4.11	.538	5.007
5	-15.06	+2.04	+4.03		-1.77						-1.07	+3.66	.543	4.989
6	-15.25	+2.07	+3.27		-1.57	+1.23					-1.13	+3.65	.548	4.972
7	-15.62	+2.04	+3.79	+0.82	-1.23	+1.01					-1.10	+3.71	.550	4.965
8	-15.48	+2.04	+3.66	+0.77	-1.13	+1.10		-.63			-1.11	+3.72	.552	4.961

TABLE 4.18

REGRESSION ON N_o, PHASES I AND II, EDWARDS, LATERAL

Phases I and II
Edwards Lateral N_o
n = 273
All Coefficients x 10^{-3}

Step	Constant	Altitude 750 ft.	Stability			Time of Day		Season			Terrain		Correl. Coeff.	Standard Deviation
			Very Stable	Stable	Unstable	Dawn	Aftern.	Spring	Fall	Winter	High Mount.	Desert		
0	5.36													0.870
1	5.61	-.51											.291	0.836
2	5.47	-.50										+.56	.403	0.803
3	5.36	-.50	+.38									+.60	.445	0.787
4	5.24	-.53	+.52	+.35								+.60	.476	0.774
5	5.27	-.56	+.68	+.43		-.28						+.58	.490	0.769
6	5.40	-.57	+.68	+.45		-.41	-.31					+.60	.513	0.758
7	5.36	-.56	+.71	+.47		-.44	-.32	+.14				+.59	.518	0.757
8	5.25	-.56	+.71	+.46		-.46	-.33	+.25	+.22			+.58	.529	0.753

TABLE 4.19

REGRESSION ON N_o, PHASES I AND II, EDWARDS, LONGITUDINAL

Phases I and II
Edwards Longitudinal N_o
n = 362
All Coefficients x 10^{-3}

Step	Constant	Altitude 750 ft.	Stability Very Stable	Stability Stable	Stability Unstable	Time of Day Dawn	Time of Day Aftern.	Season Spring	Season Fall	Season Winter	Terrain High Mount.	Terrain Desert	Correl. Coeff.	Standard Deviation
0	4.44													0.670
1	4.34											+.37	.242	0.656
2	4.25		+.38									+.42	.338	0.637
3	4.20		+.37						+.16			+.42	.357	0.633
4	4.27		+.38						+.17		-.15	+.34	.370	0.631
5	4.24		+.42		+.14				+.18		-.18	+.36	.376	0.630
6	4.15		+.51	+.17	+.22				+.17		-.18	+.37	.390	0.627

TABLE 4.20

REGRESSION ON N_o, PHASES I AND II, EDWARDS, VERTICAL

Phases I and II
Edwards Vertical N_o
n = 357
All Coefficients x 10^{-3}

Step	Constant	Altitude 750 ft.	Stability			Time of Day		Season			Terrain		Correl. Coeff.	Standard Deviation
			Very Stable	Stable	Unstable	Dawn	Aftern.	Spring	Fall	Winter	High Mount.	Desert		
0	5.09												.432	1.000
1	4.85					+1.02							.498	0.905
2	4.70					+.95			+.55				.562	0.872
3	4.56					+.97			+.68	+.83			.592	0.833
4	4.74	-.38				+.94			+.72	+.88			.612	0.813
5	4.56	-.37				+.90		+.48	+.89	+1.05			.627	0.795
6	4.66	-.38				+.93		+.46	+.88	+1.05	-.24		.637	0.788
7	4.62	-.38	+.32			+.78		+.49	+.88	+1.01	-.26		.647	0.780
8	4.54	-.39	+.47	+.28		+.69		+.51	+.85	+.98	-.22		.651	0.773
9	4.47	-.40	+.54	+.35	+.22	+.69		+.50	+.87	+1.01	-.27			0.771

TABLE 4.21

SUMMARY OF N_o, REGRESSION, PHASES I AND II

Phases I and II
No Regression
Zero Crossings/foot x 10^{-3}
Summary Table

Base	Component	n	Constant	Altitude 750 ft.	Stability			Time of Day		Season			Terrain			Correl. Coeff.	Standard Deviation
					Very Stable	Stable	Unstable	Dawn	Aftern.	Spring	Fall	Winter	High Mount.	Low Mount.	Desert		
Edwards	Lateral	273	5.25	-.56	+.71	+.46		-.46	-.33	+.25	+.22				+.58	.529	0.753
Edwards	Long.	362	4.15	-.40	+.51	+.17	+.22				+.17		-.18		+.37	.390	0.627
Edwards	Vertical	357	4.47	-.57	+.54	+.35	+.22	+.69		+.50	+.87	+1.0	-.27			.651	0.771
Peterson	Lateral	174	5.28	-.24	+.98	+.35			-.40	-.57		+.32	*	*	*	.675	0.669
Peterson	Long.	184	4.53	-.58	+.56	+.28		+.26	-.23	-.43			*	*	*	.515	0.625
Peterson	Vertical	182	5.24	-.35	+1.02		-.46	+.85	-.46		+.79	+.64	*	*	*	.743	0.871
Griffiss	Lateral	261	5.45	-.16	+.40			+.54		-.17			*	-.21	*	.497	0.666
Griffiss	Long.	303	4.69	-.81	+.34			+.41		-.16			*	-.13	*	.383	0.648
Griffiss	Vertical	294	5.75	-.45		+.17		+1.36			+.62	+.63	*	-.39	*	.695	0.762
McConnell	Lateral	342	5.47	-.32	+.98		+.27	+.30			+.28	+.40	*	*	*	.460	0.960
McConnell	Long.	411	4.71		+.55		+.14	+.23	-.35			+.17	*	*	*	.561	0.565
McConnell	Vertical	412	6.86	-1.15	+1.17	+.20		+1.37	-.22	+.31	+.32	+.34	*	*	*	.729	0.926

TABLE 4.22

Phases I and II   SUMMARY OF VON KARMAN L REGRESSION, PHASES I AND II

Scale of Turbulence Regression

Von Karman Model

Summary Table

Base	Component	n	Constant	Altitude 750 ft.	Stability			Time of Day		Season			Terrain			Correl. Coeff.	Standard Deviation
					Very Stable	Stable	Unstable	Dawn	Aftern.	Spring	Fall	Winter	High Mount.	Low Mount.	Desert		
Edwards	Lateral	274	364.5	+73.1	-39.7	-45.9		+106.6	+47.6			+33.3			-67.7	.459	118.47
Edwards	Long.	363	376.7					+55.3	+29.5				+21.7		-27.0	.230	131.0
Edwards	Vertical	358	386.3	+98.4		-39.0	-35.6	+50.8	+59.2		-78.2	-120.8	+38.7		-28.6	.469	140.99
Peterson	Lateral	173	410.6	+118.7	-169.2	-96.5		+78.8		+197.1		-54.4	*	*	*	.701	136.51
Peterson	Long.	181	356.2	+43.8	-52.7	-47.8	+48.4	-52.2	+58.4	+115.9			*	*	*	.507	132.00
Peterson	Vertical	181	301.2	+173.9	-56.4		+55.1	+56.7		+96.6	-69.2	-72.3	*	*	*	.730	117.78
Griffiss	Lateral	262	309.8	+108.3		+23.3		-81.8		+79.4		+103.5	*	+33.7	*	.472	149.41
Griffiss	Long.	304	336.6	+55.6	-28.9			-60.2		+36.6			*	+46.6	*	.370	122.12
Griffiss	Vertical	295	268.9	+122.0	+68.4	-35.7		-68.9		+51.4			*	+60.1	*	.474	139.89
McConnell	Lateral	336	298.3	+143.5	-79.3	-33.7		-60.9		+55.7	+32.7	+90.7	*	*	*	.605	111.72
McConnell	Long.	407	305.5	+62.4	-73.3			-39.1	+81.4	+43.4	+29.7		*	*	*	.546	107.92
McConnell	Vertical	408	245.5	+211.4	-35.7	-18.6		-81.4	+40.3				*	*	*	.728	109.76

49

4.1.3.3 Scale of Turbulence Regression

The scale of turbulence L for the Von Karman model was also used as the dependent variable in the regression procedure. The summary table of results for this regression is given in Table 4.22. General trends present in the data are as follows:

1) Generally longer scale lengths occurred at 750 ft. altitude with the weakest dependence occurring in the longitudinal component.

2) The dependence upon stability is inconclusive with no overall trends occurring. However, there is a tendency to slightly smaller scale lengths with increased stability.

3) Generally shorter scale lengths occur at dawn at all bases except Edwards where just the opposite is true.

4) Longer scale lengths generally occur in spring, but the dependence upon the other seasons is inconclusive.

5) Terrain seems to have little effect upon the scale of turbulence, but there does seem to be a negative influence over the desert at Edwards.

6) The correlation coefficients at Edwards and Griffiss are considerably smaller than those at Peterson and McConnell. In all cases, however, the longitudinal correlation is the smallest of the three components.

4.1.4 Results of Regression on Phase III Data

There was considerably less data available in Phase III than in Phases I and II with considerable imbalance in the number of legs flown under the various environmental conditions. For example, no data was obtained in fall and winter at Griffiss and none at 750 ft. altitude at McConnell in Phase III. This imbalance has a tendency to confound the effects of the environmental conditions making comparisons with results for Phases I and II less meaningful. However, the Phase III data at Edwards is reasonably balanced among all environmental conditions except season which had a minimal effect at Edwards during Phases I and II. The Edwards data was therefore, used in the regression analysis with σ, N_0, and L as the dependent variables and the environmental conditions (2)-(6) as the independent variables. The summary table for these regression analyses at Edwards is given in Table 4.23. A comparison of these results with those obtained from Phases I and II leads to the following observations on the turbulence and its relation to the environmental conditions:

σ -- Regression

1) Terrain has a stronger effect on σ in Phase III

2) The stability of the air has a weaker influence on σ in Phase III

50

TABLE 4.23

SUMMARY OF σ, N₀, AND L REGRESSION - PHASE III

Phase III Edwards Regression

σ Regression

Component	n	Constant	Altitude 750 ft.	Stability			Time of Day		Season			Terrain			Correlation Coefficient	Standard Deviation
				Very Stable	Stable	Unstable	Dawn	Afternoon	Spring	Fall	Winter	High Mount.	Low Mount.	Desert		
		ft/sec	ft/sec	ft/sec	ft/sec	ft/sec	ft/sec	ft/sec	ft/sec	ft/sec	ft/sec	ft/sec	ft/sec	ft/sec		ft/sec
Lateral	521	2.93	-.33	-.64	-.26			+.15	*	+.42	*	+.65		-.97	.633	0.871
Longitudinal	521	2.99	-.45	-.54					*	+.42	*	+.34		-1.14	.562	0.974
Vertical	521	3.25	-.45	-.84	-.19		-.36	+.20	*	*	*	+.80		-.82	.640	1.010

N₀ REGRESSION
All coefficients x 10⁻³ crossings/foot

Component	n	Constant	Altitude 750 ft.	Stability			Time of Day		Season			Terrain			Correlation Coefficient	Standard Deviation
				Very Stable	Stable	Unstable	Dawn	Afternoon	Spring	Fall	Winter	High Mount.	Low Mount.	Desert		
Lateral	150	3.19	-.16	-.13			-.28		*	*	*	-.21			.565	0.302
Longitudinal	180	2.50	-.05				-.23		*	*	*		+.08		.372	0.270
Vertical	152	3.50	-.12			-.11			*	*	*	-.46		-.16	.522	0.365

SCALE OF TURBULENCE REGRESSION
Von Karman Model

Component	n	Constant	Altitude 750 ft.	Stability			Time of Day		Season			Terrain			Correlation Coefficient	Standard Deviation
				Very Stable	Stable	Unstable	Dawn	Afternoon	Spring	Fall	Winter	High Mount.	Low Mount.	Desert		
		ft.	ft.	ft.	ft.	ft.	ft.	ft.	ft.	ft.	ft.	ft.	ft.	ft.		ft.
Lateral	150	520.9		+189.0			+540.3		*	*	*	+265.7			.554	434.9
Longitudinal	180	669.1		+100.1			+452.6		*	*	*	+85.2			.478	352.7
Vertical	152	527.2					+375.8	-155.6	*	*	*	+381.1			.524	420.5

* indicates that no data was available for this category

A blank indicates that no correction to the constant term is necessary in the presence of the given condition

3)   The time of day has a weaker influence on σ in Phase III

4)   The correlation coefficient is consideraly smaller in Phase III for both the longitudinal and vertical component σ regressions

N_o -- Regression

Generally smaller N_o's were observed in Phase III with less influence upon all the regression parameters.

Scale of Turbulence Regression

1)   Generally longer scale lengths were observed in Phase III with a much stronger relationship to time of day. That is, scale lengths were generally 500 ft. longer at dawn in Phase III, while earlier phases indicated an increase in scale length of less than 100 ft. at dawn.

2)   Terrain had a stronger influence upon scale length in Phase III with generally longer scale lengths occurring over high mountains.

3)   While somewhat longer scale lengths were observed at 750 ft. altitude in Phases I and II, no dependence upon altitude was detected in Phase III.

A comparison of the means of the dependent variables for the various phases is given in Table 4.24. While the σ values are roughly the same in all phases, it was found that N_o was considerably smaller in Phase III and the scale of turbulence L was considerably larger in Phase III.

4.2 Extreme Value Analysis for Phases I and II Data

The regression analysis on the extreme gust velocities encountered for each leg in Phases I and II revealed several dependencies of the extreme values upon the environmental conditions. A further analysis of the extreme values has been conducted to determine the distribution of the extreme values for the purposes of extrapolation to the probability of occurrence of extremes not encountered in the study and for comparison of distribution parameters under various environmental conditions.

A computer program has been written to compile the available maximum and minimum values into frequency distributions. Since the maximum gust velocity and the minimum gust velocity showed similar distributions, the two components were combined by taking their absolute value for the purposes of the extreme analysis.

Plots revealed that the cumulative distributions of extreme values could be represented quite well by a log-normal distribution with parameters

TABLE 4.24

COMPARISON OF MEAN σ, N_o, AND L BETWEEN PHASES I AND II AND PHASE III

EDWARDS DATA

	Lateral Component		Longitudinal Component		Vertical Component	
	Phases I, II	Phase III	Phases I, II	Phase III	Phases I, II	Phase III
Mean σ ~ft/sec	2.77	2.79	2.58	2.71	2.93	2.63
Mean N_0 ~crossings/ ft $\times 10^{-3}$	5.36	2.95	4.44	2.43	5.09	3.20
Mean scale of turbulence ~ft.	409.9	772.5	400.8	803.1	417.1	652.3

α and β. That is, the $\log_e$ of the extreme values followed a normal distribu-
tion with mean α and standard deviation β. The cumulative distribution of
extreme values will, therefore, plot as a straight line on log-normal paper.
That is, normal probability scale on the ordinate and a log scale along the
abscissa. Such a plot of the cumulative distribution of extreme values has
been made for the various terrain conditions for the longitudinal, lateral,
and vertical components in very stable air in Figures 4.1-4.3. In addition,
the distribution parameters α and β for the three components under the
various stability conditions have been tabulated in Tables 4.25 - 4.27. The
median extreme gust, the 1% extreme gust, and the 0.1% extreme gust have
also been tabulated for the various flight conditions in these tables. Since
both the minimum and maximum extreme gusts were used in this analysis,
the 1% extreme gust for a given category refers to the extreme, either
positive or negative, that would be expected to occur once in 50 flight legs
of 5.5 minutes each under the given condition, or equivalently the extreme
gust velocity that would be expected once in 275 minutes of flying under the
given condition. The 0.1% extreme gust represents the extreme that would
be expected to occur once in 2750 minutes or 45.83 hours under the condition.

The extremes presented are only examples of the values that can be
calculated. Actually, the expected extreme gust velocity for any given
number of flight hours can be calculated from the log-normal parameters α
and β as shown in Table 4.28.

The log-normal distributions on the extreme values presented in Tables
4.25 - 4.27 show similar trends to those exhibited in earlier regression runs
on the turbulence parameters. In particular, there is a difference in the
distributions of extremes with respect to atmospheric stability in that the
α and β values vary considerably under the various stability classes. There
were also large differences in the parameters under the various terrain
categories but this effect is confounded with the location effect in that most
of the data under certain terrain categories was obtained at a single location.
In particular, all of the desert data was obtained at Edwards and most of the
plains data was obtained at McConnell. The fact that location does exert an
effect on the turbulence encountered was illustrated previously in the results
obtained in Table 4.12.

A comparison of Tables 4.25 - 4.27 shows that there are differences in
the distribution of extremes for the three components, but that these differences
are small when compared to the effects produced by stability and terrain.
This result was also obtained in examining other turbulence parameters as
shown in Table 4.12.

An examination of the parameters of the extreme distributions reveals
that the parameter β increases with increased stability of the air. This
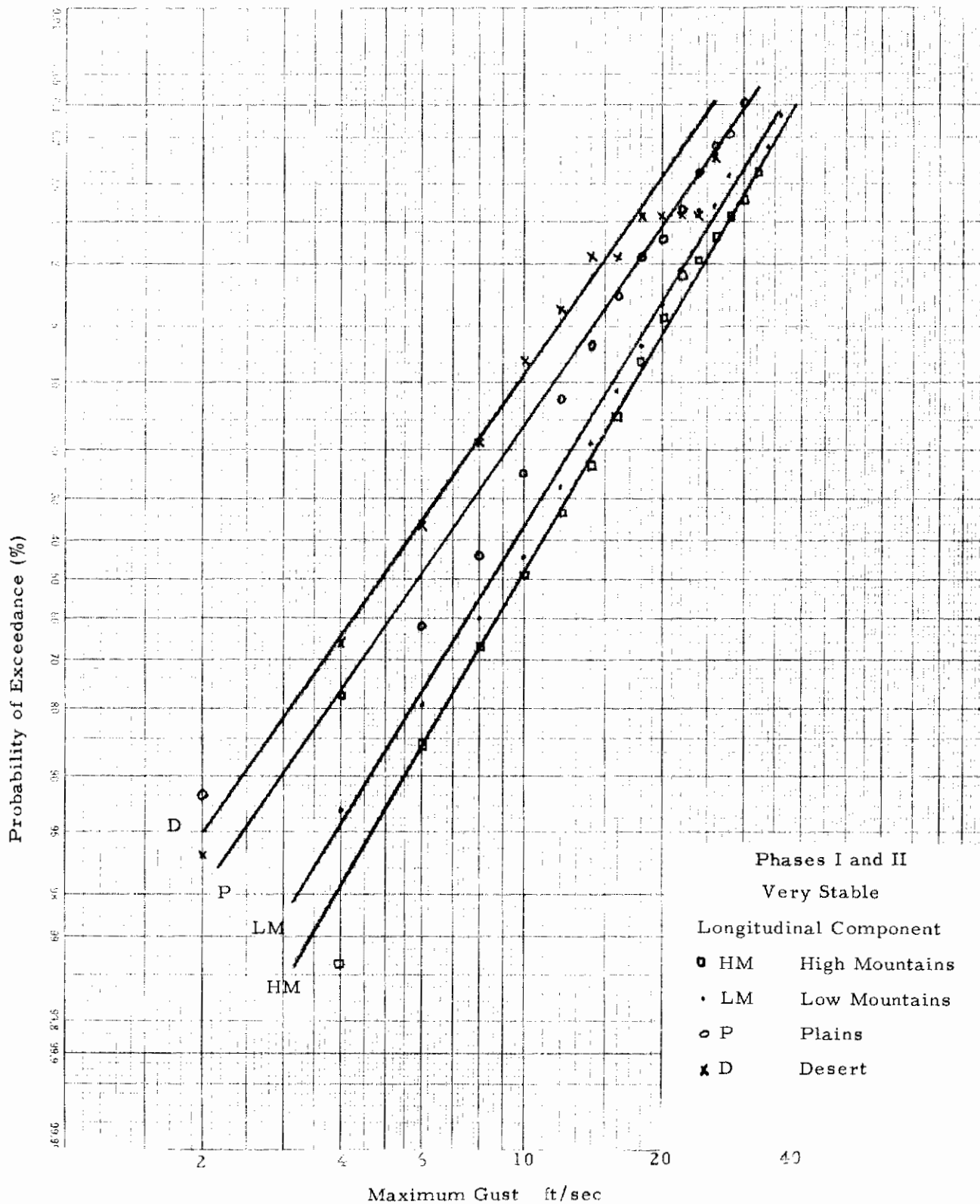
Figure 4. 1 - Cumulative Distribution of Extreme Values
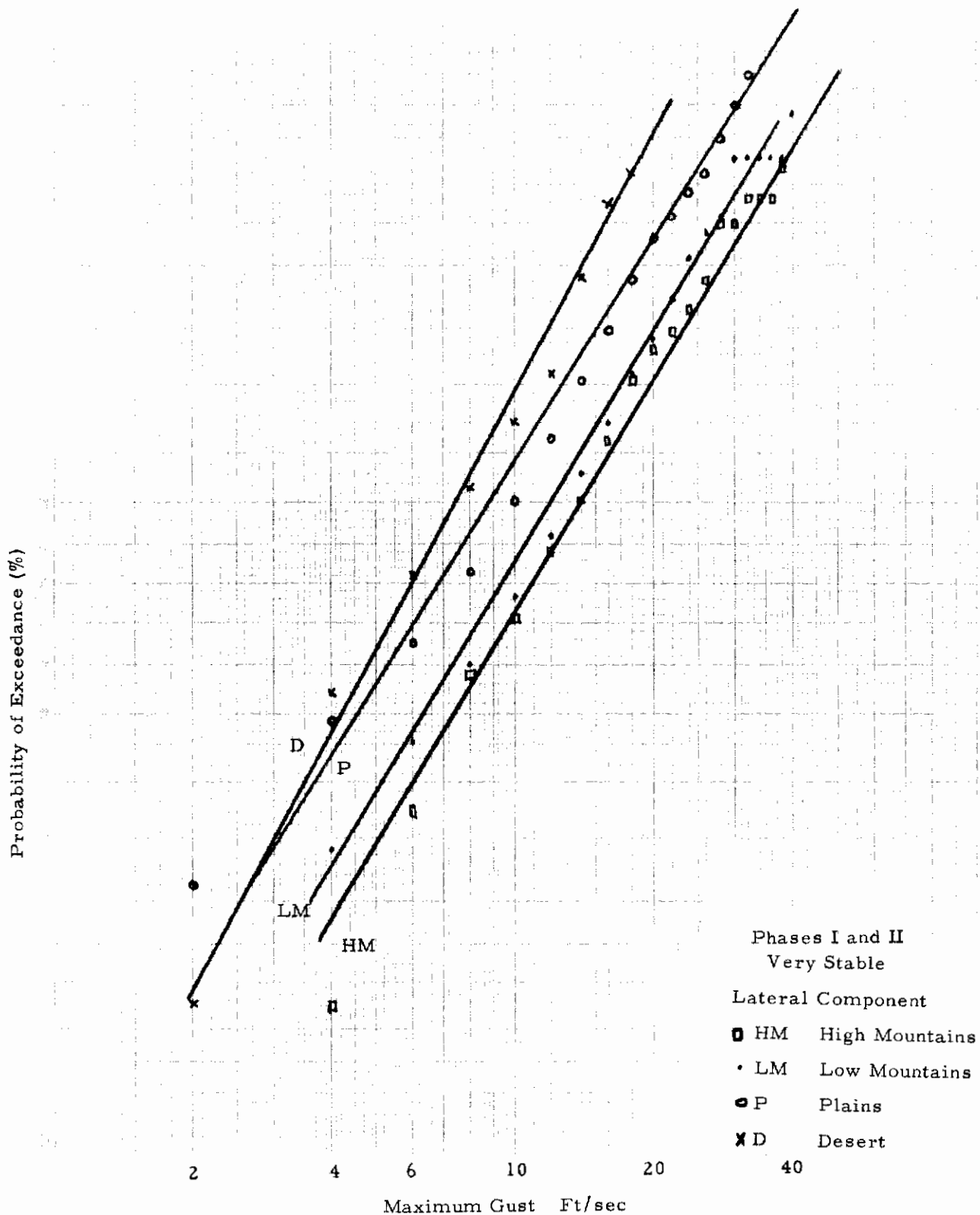Longitudinal Component in Very Stable Air

55

Figure 4. 2 - Cumulative Distribution of Extreme Values
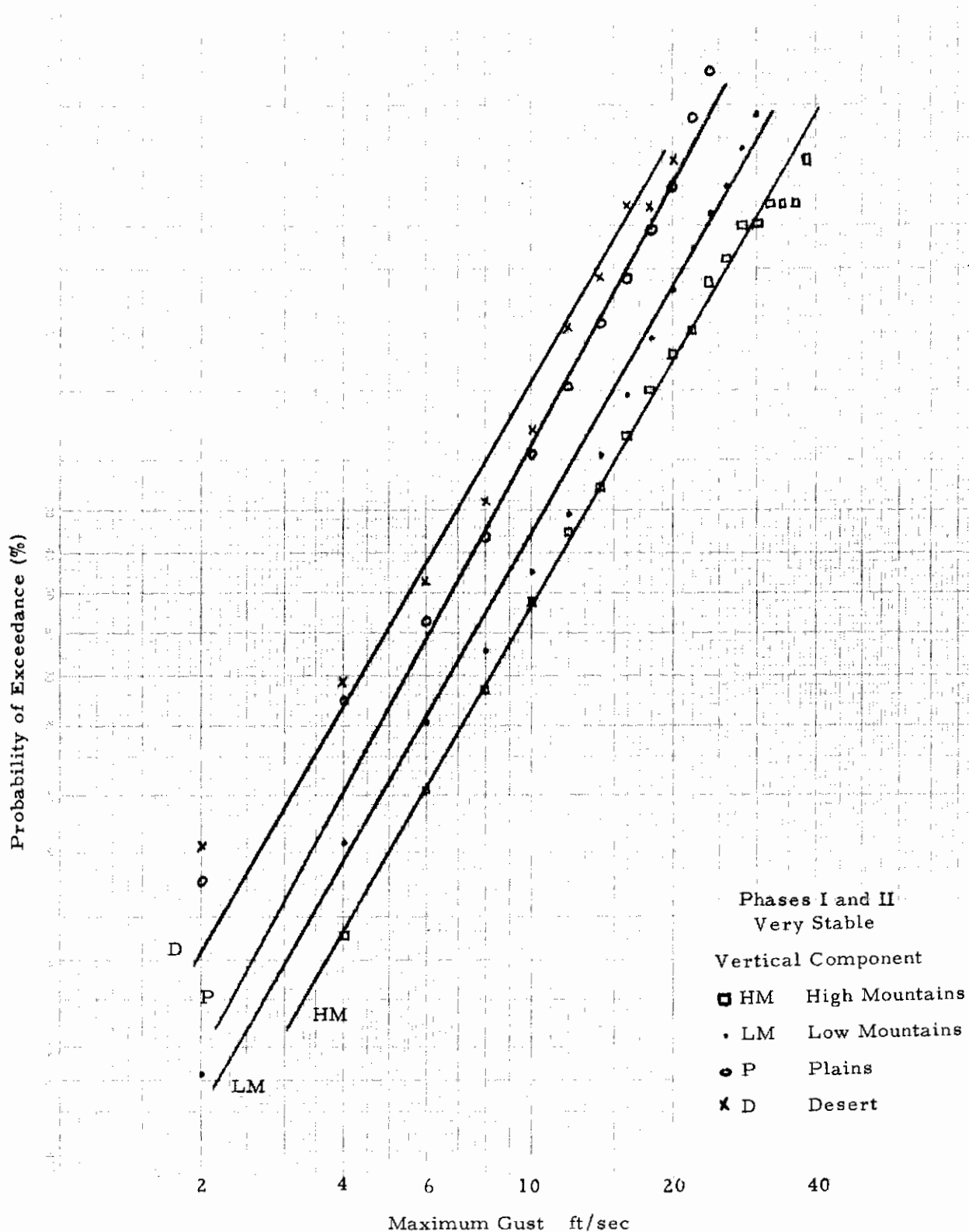Lateral Component in Very Stable Air

56

Figure 4.3 - Cumulative Distribution of Extreme Values
Vertical Component in Very Stable Air

57

TABLE 4.25

LOG-NORMAL DISTRIBUTION OF EXTREME VALUES, LONGITUDINAL COMPONENT

PHASES I AND II

Stability	Terrain	Mean α	Standard Deviation β	Median Extreme ft/sec e^{α}	1% Extreme Gust ft/sec $e^{\alpha+2.33\beta}$	0.1% Extreme Gust ft/sec $e^{\alpha+3.09\beta}$
Very Stable	Desert	1.58	0.59	4.9	19.2	30.1
Very Stable	Plains	1.77	0.55	5.9	21.1	32.1
Very Stable	Low Mount.	2.14	0.48	8.5	26.0	37.5
Very Stable	High Mount.	2.28	0.46	9.8	28.6	40.5
Stable	Desert	2.10	0.46	8.2	23.9	33.8
Stable	Plains	2.26	0.41	9.6	24.9	34.0
Stable	Low Mount.	2.53	0.37	12.6	29.7	39.4
Stable	High Mount.	2.60	0.44	13.4	37.5	52.4
Neutral	Desert	2.29	0.34	9.9	21.8	28.2
Neutral	Plains	2.48	0.32	11.9	25.2	32.1
Neutral	Low Mount.	2.66	0.35	14.3	32.3	42.2
Neutral	High Mount.	2.64	0.39	14.0	34.8	46.8
Unstable	Desert	2.62	0.26	13.7	25.2	30.7
Unstable	Plains	2.43	0.33	11.4	24.5	31.5
Unstable	Low Mount.	2.78	0.27	16.2	30.2	37.1
Unstable	High Mount.	2.76	0.35	15.9	35.7	46.6

TABLE 4.26

LOG-NORMAL DISTRIBUTION OF EXTREME VALUES, LATERAL COMPONENT

PHASES I AND II

Stability	Terrain	Mean α	Standard Deviation β	Median Extreme ft/sec e^{α}	1% Extreme Gust ft/sec $e^{\alpha+2.33\beta}$	0.1% Extreme Gust ft/sec $e^{\alpha+3.09\beta}$
Very Stable	Desert	1.79	0.42	6.0	15.9	21.9
Very Stable	Plains	1.92	0.47	6.8	20.4	29.1
Very Stable	Low Mount.	2.24	0.47	9.4	28.1	40.1
Very Stable	High Mount.	2.39	0.46	10.9	31.9	45.2
Stable	Desert	2.26	0.41	9.6	24.9	34.0
Stable	Plains	2.45	0.35	11.6	26.2	34.2
Stable	Low Mount.	2.64	0.37	14.0	33.2	43.9
Stable	High Mount.	2.71	0.39	15.0	37.3	50.2
Neutral	Desert	2.49	0.31	12.0	24.8	31.4
Neutral	Plains	2.60	0.34	13.5	29.7	38.5
Neutral	Low Mount.	2.83	0.36	17.0	39.2	51.5
Neutral	High Mount.	2.84	0.33	17.1	36.9	47.5
Unstable	Desert	2.72	0.30	15.2	30.5	38.4
Unstable	Plains	2.53	0.34	12.5	27.7	35.9
Unstable	Low Mount.	2.89	0.25	18.0	32.2	39.0
Unstable	High Mount.	2.92	0.33	18.6	40.0	51.4

TABLE 4.27

LOG-NORMAL DISTRIBUTION OF EXTREME VALUES, VERTICAL COMPONENT

PHASES I AND II

Stability	Terrain	Mean α	Standard Deviation β	Median Extreme ft/sec e^{α}	1% Extreme Gust ft/sec $e^{\alpha+2.33\beta}$	0.1% Extreme Gust ft/sec $e^{\alpha+3.09\beta}$
Very Stable	Desert	1.70	0.45	5.5	15.6	22.0
Very Stable	Plains	1.92	0.43	6.8	18.6	25.8
Very Stable	Low Mount.	2.14	0.43	8.5	23.1	32.1
Very Stable	High Mount.	2.34	0.44	10.4	28.9	40.4
Stable	Desert	2.29	0.39	9.9	24.5	33.0
Stable	Plains	2.37	0.36	10.7	24.9	32.5
Stable	Low Mount.	2.56	0.37	13.0	30.6	40.6
Stable	High Mount.	2.66	0.38	14.3	34.7	46.3
Neutral	Desert	2.42	0.30	11.3	22.6	28.4
Neutral	Plains	2.50	0.29	12.2	23.9	29.8
Neutral	Low Mount.	2.73	0.33	15.3	33.1	42.5
Neutral	High Mount.	2.81	0.39	16.6	41.2	55.4
Unstable	Desert	2.71	0.21	15.0	24.5	28.8
Unstable	Plains	2.48	0.35	11.9	27.0	35.2
Unstable	Low Mount.	2.83	0.33	16.9	36.6	47.0
Unstable	High Mount.	2.88	0.26	17.9	32.6	39.8

TABLE 4.28

EXPECTED EXTREME GUST VELOCITIES USING THE LOG-NORMAL DISTRIBUTION PHASES I AND II

Flight Hours	Number of Minutes	Number of Low-Level Legs of 5.5 Minutes	Number of Extremes	Probability	Standard Score Z
10	600	109.1	218.2	.004583	2.61
50	3000	545.5	1091.0	.000917	3.12
100	6000	1090.9	2181.8	.000458	3.32
200	12000	2181.8	4363.6	.000229	3.50
500	30000	5454.5	10909.0	.000092	3.74
1000	60000	10909.1	21818.2	.000046	3.89

Expected Extreme Gust $= e^{\alpha + \beta Z}$

61

behavior indicates more variability in the distribution of extremes under very stable air even though the median extreme is smaller under this condition. The implications of this behavior are given in Figure 4.4 which contains a plot of the extreme distribution under all stability conditions for the longitudinal component over desert terrain. This figure illustrates that even though more severe turbulence would be encountered with increased instability in the air, the ultimate loads under the various stability conditions would be similar. That is, atmospheric stability is not responsible for ultimate loads encountered by an aircraft even though atmospheric stability would seem to be important in the accumulation of damage to the structure of the aircraft. Similar trends as those reported in Figure 4.4 were observed in the other components and under the other terrain conditions.
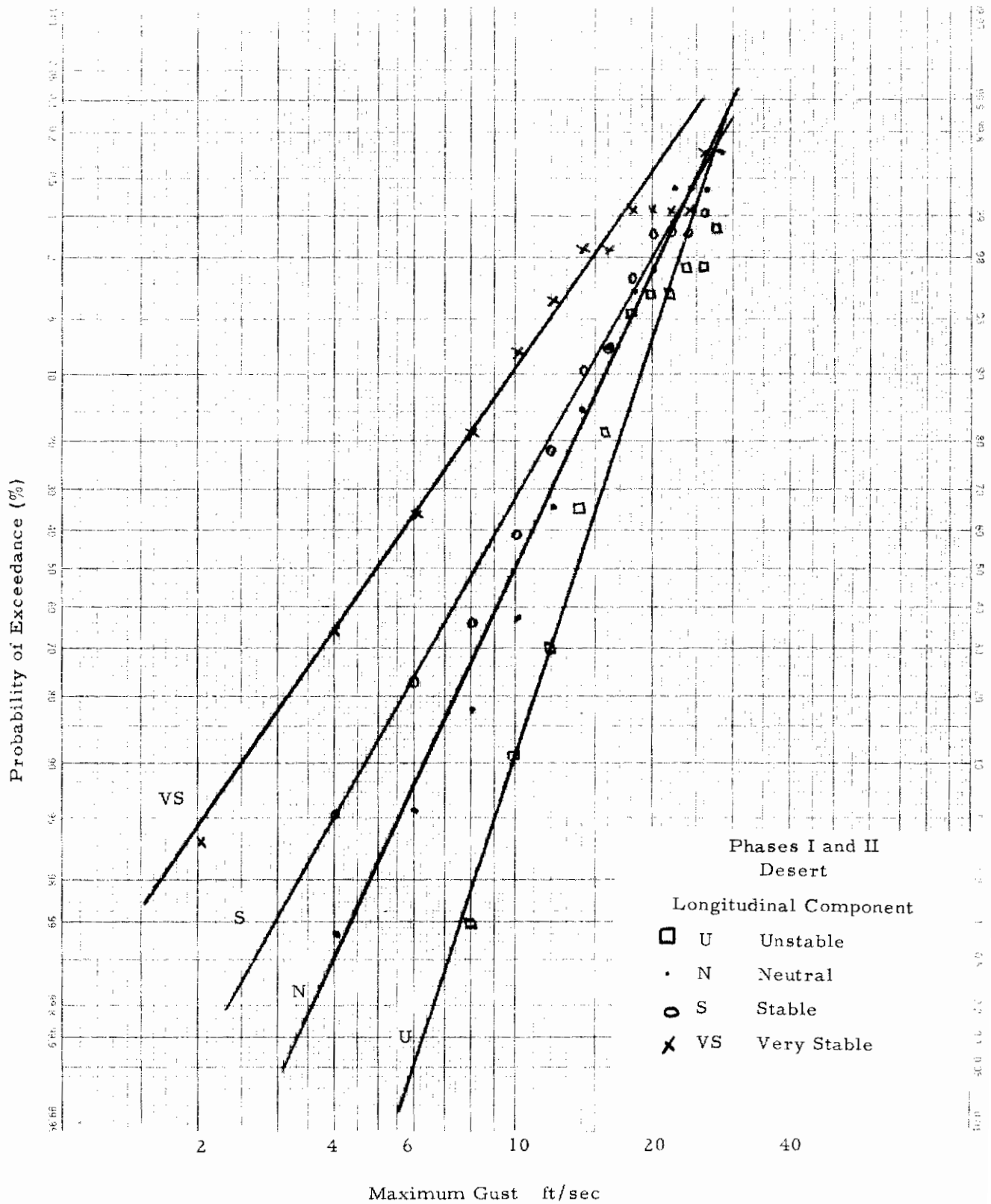
Figure 4.4 - Cumulative Distribtuion of Extreme Values
Longitudinal Component over Desert Terrain

63

SECTION V

ANALYSIS OF PEAK COUNT DATA BY CATEGORY

Cumulative probability exceedance curves have been determined for various categories from the peak counts of Phases I and II and Phase III data. The technique discussed in Section 3.2.3 has been used to determine the P's and b's from the analytic fit. This section of the report discusses the P's and b's calculated under various categories with respect to the influence each category has on the turbulence parameter σ. Comparisons are made between the results from Phases I and II data and those from Phase III. A final discussion is a comparison of LO-LOCAT data (Phases I and II and Phase III) with the results of other turbulence investigations

5.1   LO-LOCAT Data

Cumulative probability exceedance curves have been calculated on the basis of decomposition by the six categories - LOCATION, TERRAIN, ALTITUDE, STABILITY, SEASON, and TIME OF DAY. Prior to the discussion of these decompositions, it is worthwhile to observe the statistical balance of the data relative to each category. Table 5.1 shows the percentage of flights in the decomposition of each category for the Phases I and II and Phase III data. The total number of flight legs for Phases I and II (7632) and Phase III (1600) data is also given. Phases I and II data shows a good balance in the categories Location, Altitude, and Time of Day. In the category Terrain, only 6% of the data is over desert and 2% over water, both at Edwards. An overabundance of legs, 51%, were flown over plains. The category Stability shows only 10% of the legs in unstable air. Nevertheless, there is a large enough sample of unstable legs (716) to be statistically meaningful. The category Season shows somewhat fewer legs flown in spring and winter than in the other seasons. It is important to observe the percentage of legs for each condition of the Phase III data relative to the Phases I and II. For example, Griffiss Phases I and II data have been shown to have a larger mean sigma than the other bases. Since only 9% of Phase III data is from Griffiss, as compared to 20% of Phases I and II, one would expect this effect to result in a decrease of the mean sigma for all flight legs from Phase III data. This point is discussed further in Section 5.3, where the Phase III exceedance curves are compared to Phases I and II. In the Terrain and Season categories, Phase III data also shows a notable difference from Phases I and II. A majority (54%) of the Phase III legs were flown over high mountains, while only 17% were flown over plains. The corresponding figures for Phases I and II data are 20% and 51%, respectively. Phase III data consisted of a smaller percentage of summer flight legs (16%) and a larger percentage of spring and winter legs than Phases I and II.

5.2   Cumulative Exceedance Curves from Peak Counts

The peak counts from all Phases I and II flight legs were accumulated in two-feet-per-second bands and fitted to the analytic function (Equation 3.2) by

64

TABLE 5.1

PERCENTAGE OF FLIGHTS BY CATEGORY

PHASES I AND II VERSUS PHASE III DATA

Location

	Peterson	Edwards	McConnell	Griffiss	Total Legs
Phases I and II	27%	23%	30%	20%	7632
Phase III	48%	36%	7%	9%	1600

Terrain

	High Mts	Low Mts	Plains	Desert	Water
Phase I and II	20%	21%	51%	6%	2%
Phase III	54%	19%	17%	7%	3%

Altitude

	250 Ft	750 Ft	Non Contour
Phase I and II	45%	42%	13%
Phase III	56%	44%	-

Stability

	Very Stable	Stable	Neutral	Unstable
Phase I and II	29%	37%	24%	10%
Phase III	31%	29%	24%	16%

Season

	Spring	Summer	Fall	Winter
Phase I and II	19%	27%	40%	14%
Phase III	32%	6%	32%	30%

Time of Day

	Dawn	Mid-Morning	Mid-Afternoon
Phase I and II	31%	35%	34%
Phase III	28%	37%	35%

the techniques of Section 3.2.3. The number of peak counts in the 0-2 ft/sec band was modified to account for instrument noise by deleting this point from the least squares quadratic fit used to obtain P's and b's. The modified number of peak counts in the 0-2 ft/sec band is defined as the intercept of the quadratic fit. All of the Phase III flight legs were accumulated and P's and b's determined in a similar fashion. Figure 5.1 shows the cumulative exceedance curves for the Phases I and II and Phase III data.* Notice that the b_1 parameters are similar to the two curves even though the probability of exceeding a large gust velocity is much higher in the Phase III data. The difference in the two curves is due mainly to the decrease in P_1, or the corresponding increase in P_2, for the Phase III data. This behavior indicates that the light to moderate turbulence has the same intensity for all phases but that severe turbulence was encountered more often in Phase III. Possible explanations for the more frequent occurrence of severe turbulence in Phase III are as given below:

1) The Phase III program, with the faster T-33 aircraft, was designed to measure longer atmospheric wavelengths, up to 14,000 ft. Boeing has reported that there is some reason to suspect that the longer wavelengths are associated with the very high gust velocities and therefore account for the higher degree of turbulence experienced in the Phase III Program.

2) As shown in Table 5.1 the Phase III data is not statistically balanced among the location, terrain and season categories. In particular, there is an over abundance of data at Peterson over high mountains in Phase III where generally heavy turbulence was encountered and very little data at McConnell where generally light turbulence was encountered. Such an inbalance would tend to make the Phase III data look more severe than that of earlier phases.

3) In Phases I and II, it was found that more severe turbulence was encountered at Griffiss than at other bases under similar environmental conditions. Griffiss, being merely a geographical position, could not in itself cause turbulence but rather an unidentified meteorological cause could be strongly manifested at Griffiss. Such a situation could be occurring at Peterson in Phase III where unusually high turublence was encountered.

The regression analysis indicated that little difference was observed between the mean sigma for the 250 ft. altitude legs and that of the 750 ft. legs. To determine if the same is true for the peak count probabilities the cumulative exceedance curves were obtained for all Phases I and II flight legs at 250 ft. and for all legs at 750 ft. The results appear in Figure 5.2. Little departure is seen between the 250 ft. and 750 ft. curves. Very little effect on peak count gust velocities can be attributed to the difference between altitudes at 250 ft. and 750 ft.

---

*For Phases I and II a maximum gust of 66 ft/sec in the vertical component was observed at Peterson during a non-contour flight - Category No. 242343. During Phase II the maximum gust was 76 ft/sec over high mountains at Peterson.

Phases I and II
All Flight Legs
All Components Combined
(Includes Peterson Non-Contour)

P_1 = .99989 b_1 = 2.822

P_2 = .00011 b_2 = 10.309

Phase III
All Flight Legs

P_1 = .932 b_1 = 2.866

P_2 = .068 b_2 = 6.840

Phase III
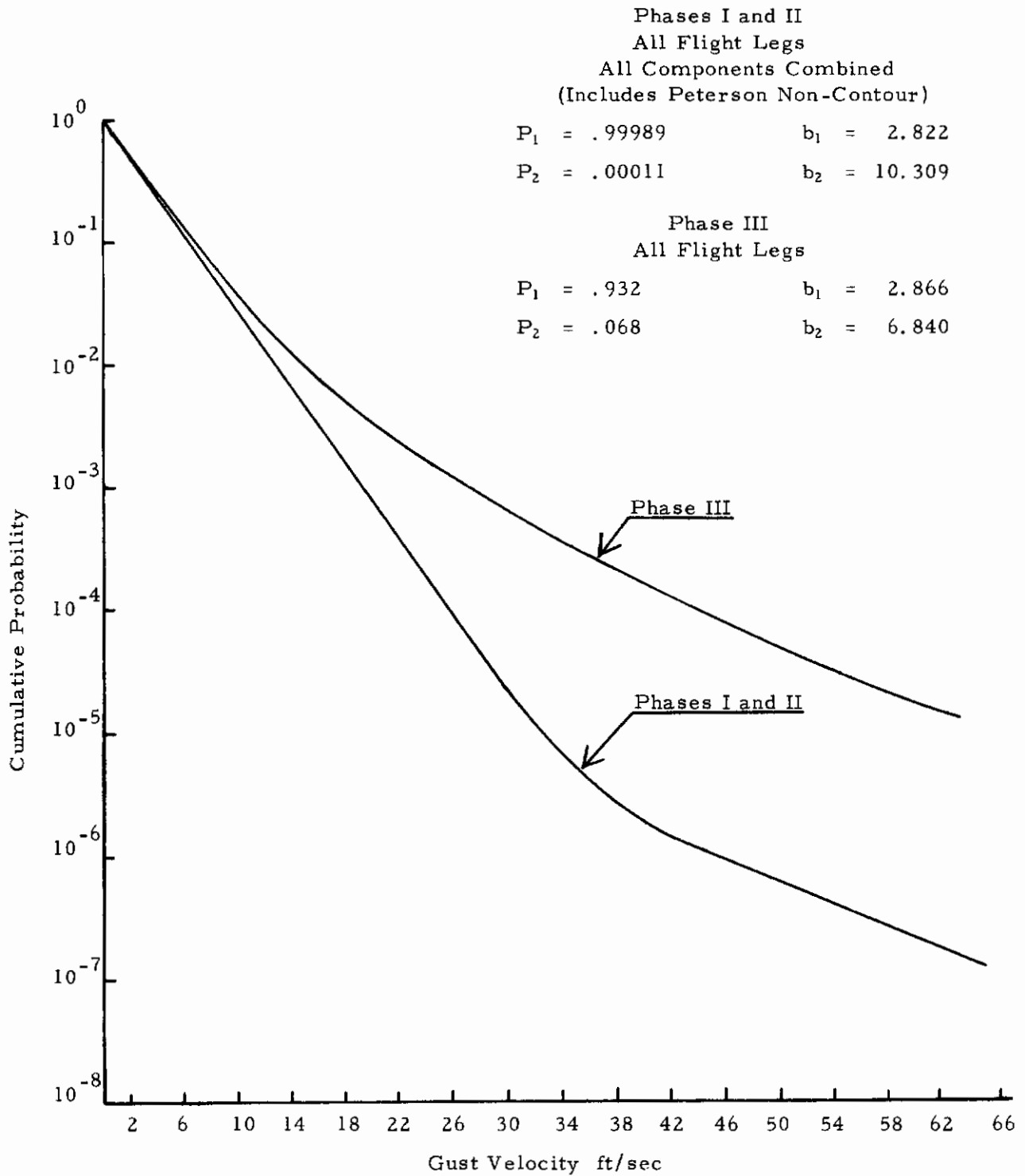
Phases I and II

Figure 5.1 Cumulative Probability of Exceedance, Phases I and II vs. Phase III.

67

Phases I and II
All Components Combined

All Legs at 250 ft. Altitude

$P_1 = .875 \qquad b_1 = 2.345$

$P_2 = .125 \qquad b_2 = 3.401$

All Legs at 750 ft. Altitude

$P_1 = .989 \qquad b_1 = 2.353$
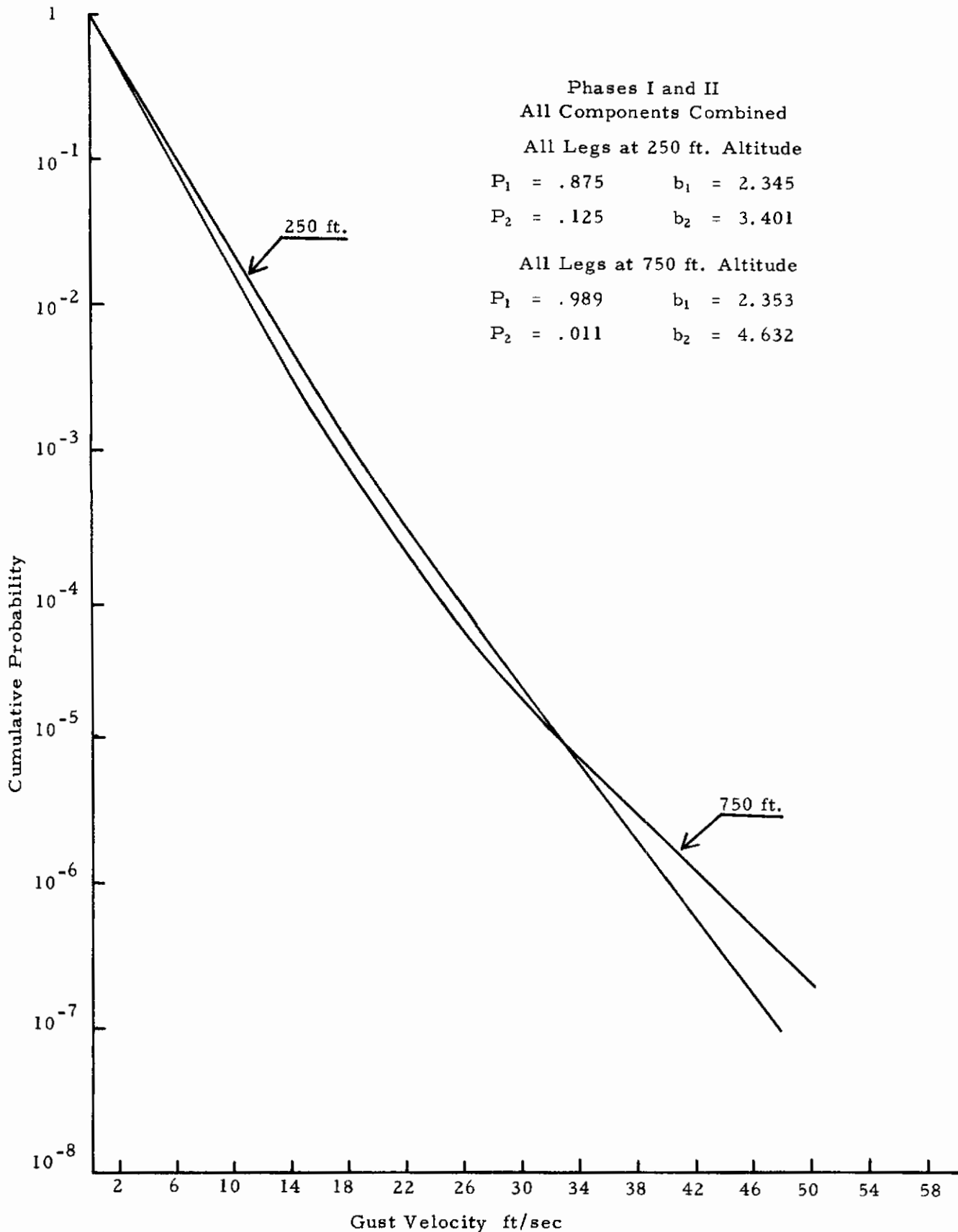
$P_2 = .011 \qquad b_2 = 4.632$

Figure 5.2 Cumulative Probability of Exceedance, 250 ft. and 750 ft. Altitude

The cumulative probability curves for each component of Phases I and II data is shown in Figure 5.3. Some difference is noticeable between the curves. In particular, the lateral component indicates a higher probability of a gust velocity than does the longitudinal or vertical component. Similar results are obtained for the Phase III data, as seen in Figure 5.4. Even though discernible differences are observed between components, they are small compared to the difference that will be shown to exist for other category parameters. It is worthwhile to recall at this time that in the regression on σ, a difference in σ attributable to a component was not observed until the eleventh step of the stepwise procedure as shown in Table 4.12.

5.3   F(x) for Categories Based on Sigma Decomposition

The σ regression for Phases I and II and Phase III data indicated the Stability, Geographic Location, Desert and Non-Desert Terrain at Edwards, and Dawn and Non-Dawn Time of Day have the highest correlation with the turbulence parameter sigma. Since σ is the standard deviation of the time history of a turbulence sample, one would antiticpate that the parameters that influence σ would also influence the cumulative peak gust velocity probabilities. Hence, initially the σ decomposition served as the basis for determining cumulative probability of exceedance curves.

Cumulative probability exceedance curves have been determined for each gust velocity component according to the decomposition by the variables;

1)   Four Bases
2)   Four Stability Conditions
3)   Desert and Non-Desert Terrain at Edwards
4)   Dawn and Non-Dawn

It was felt that this decomposition into 40 classes provided an upper limit on the number of parameters that could possibly influence turbulence from a practical standpoint of design criteria. P's and b's have been determined for each component of each class. Sample plots of the resulting curves are presented in Figures 5.5 and 5.6.

A comparison was then made to observe if the effect of, for example, stability on the sigmas was similar to its effect on the P's and b's. The parameter b_1, the negative reciprocal of the slope of the first exponential component, was anticipated to behave in a similar fashion to σ. b_2 reflects the effect of very large gust velocity and would appear to be less related to the standard deviation of the gust velocity σ than b_1. Tables 5.2 - 5.5 show the P's and b's for the lateral components, at each base, for each stability condition, and Dawn and Non-Dawn. The corresponding mean sigma is also presented.

Phases I and II

Longitudinal

$P_1 = .945 \qquad b_1 = 2.174$

$P_2 = .055 \qquad b_2 = 3.571$

Lateral

$P_1 = .974 \qquad b_1 = 2.387$

$P_2 = .026 \qquad b_2 = 4.348$

Vertical

$P_1 = .99972 \qquad b_1 = 2.463$
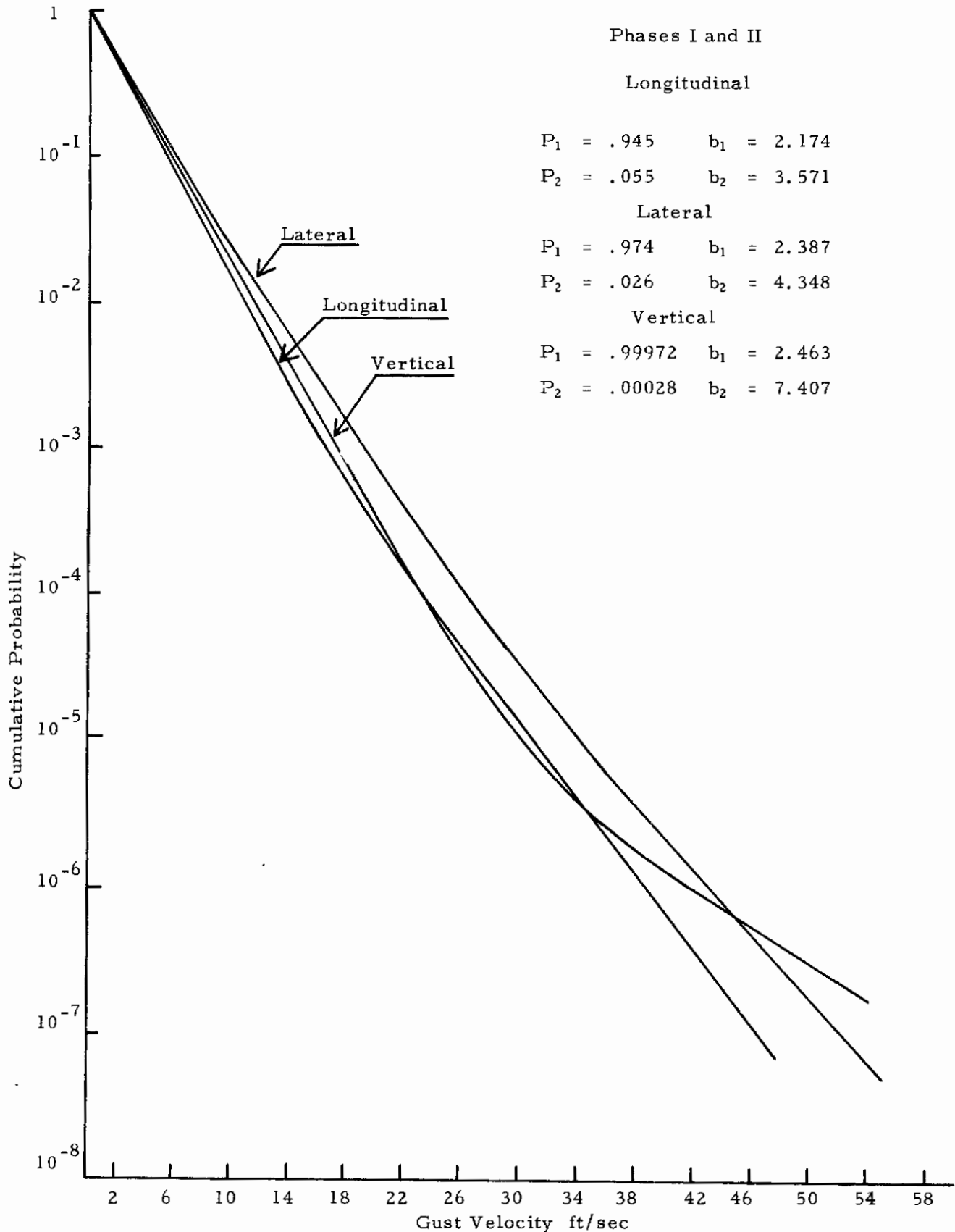
$P_2 = .00028 \qquad b_2 = 7.407$

Figure 5.3 Cumulative Probability of Exceedance, Phases I and II, Longitudinal, Lateral, and Vertical Components

70
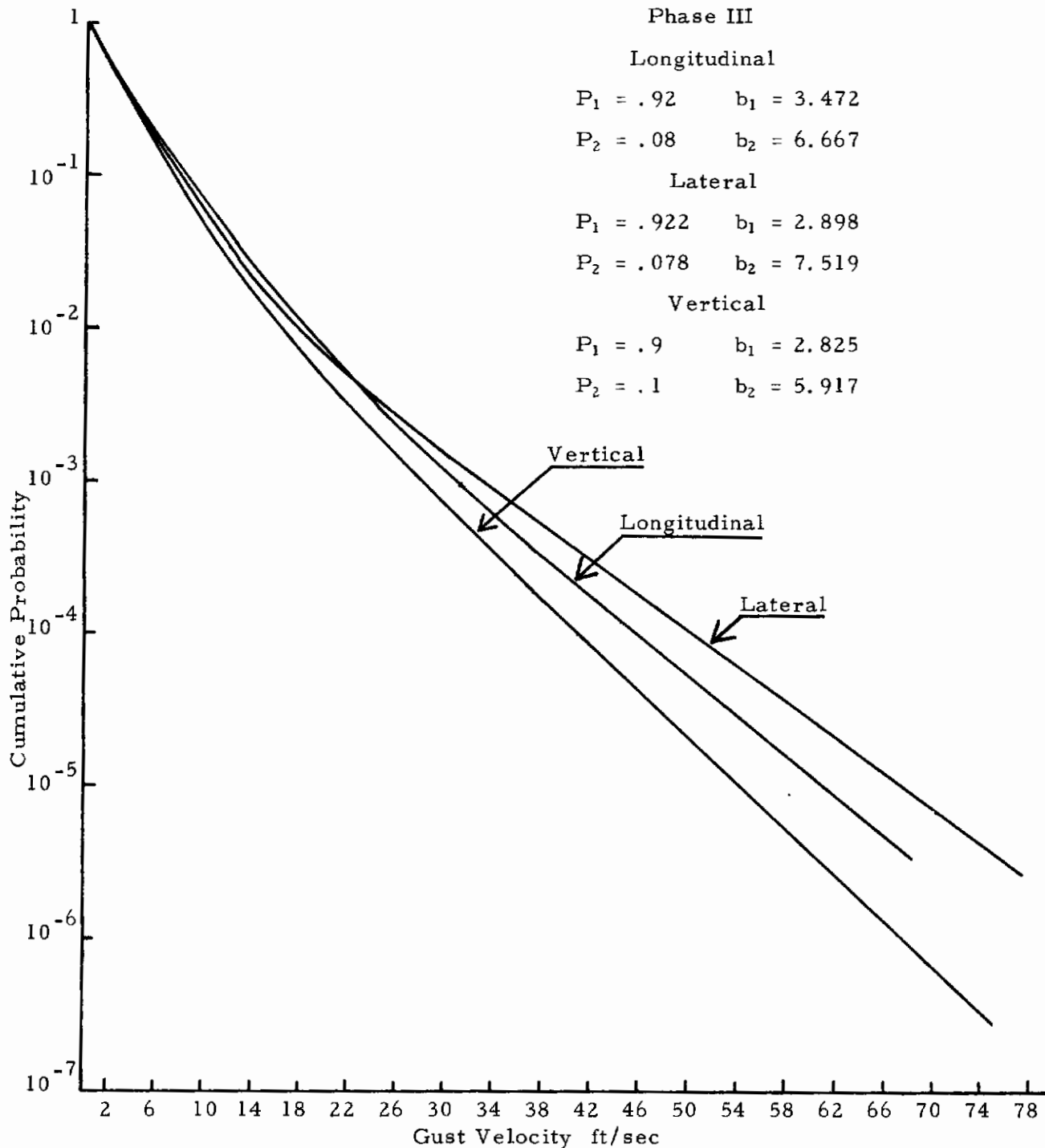
Figure 5.4 Cumulative Probability of Exceedance, Phase III, Longitudinal, Lateral, and Vertical Components

71

Edwards Desert
Dawn
Very Stable
Longitudinal

$P_1 = 0.92540$ $b_1 = 1.2111$

$P_2 = 0.07460$ $b_2 = 2.11434$

Edwards Desert
Non-Dawn
Very Stable
Longitudinal

$P_1 = 0.99754$ $b_1 = 1.82408$

$P_2 = 0.00246$ $b_2 = 7.42997$

Griffiss
Dawn
Stable
Vertical

$P_1 = 1$ $b_1 = 2.74876$

Griffiss
Non-Dawn
Stable
Vertical

$P_1 = 0.99453$ $b_1 = 2.34323$

$P_2 = 0.00547$ $b_2 = 4.77783$
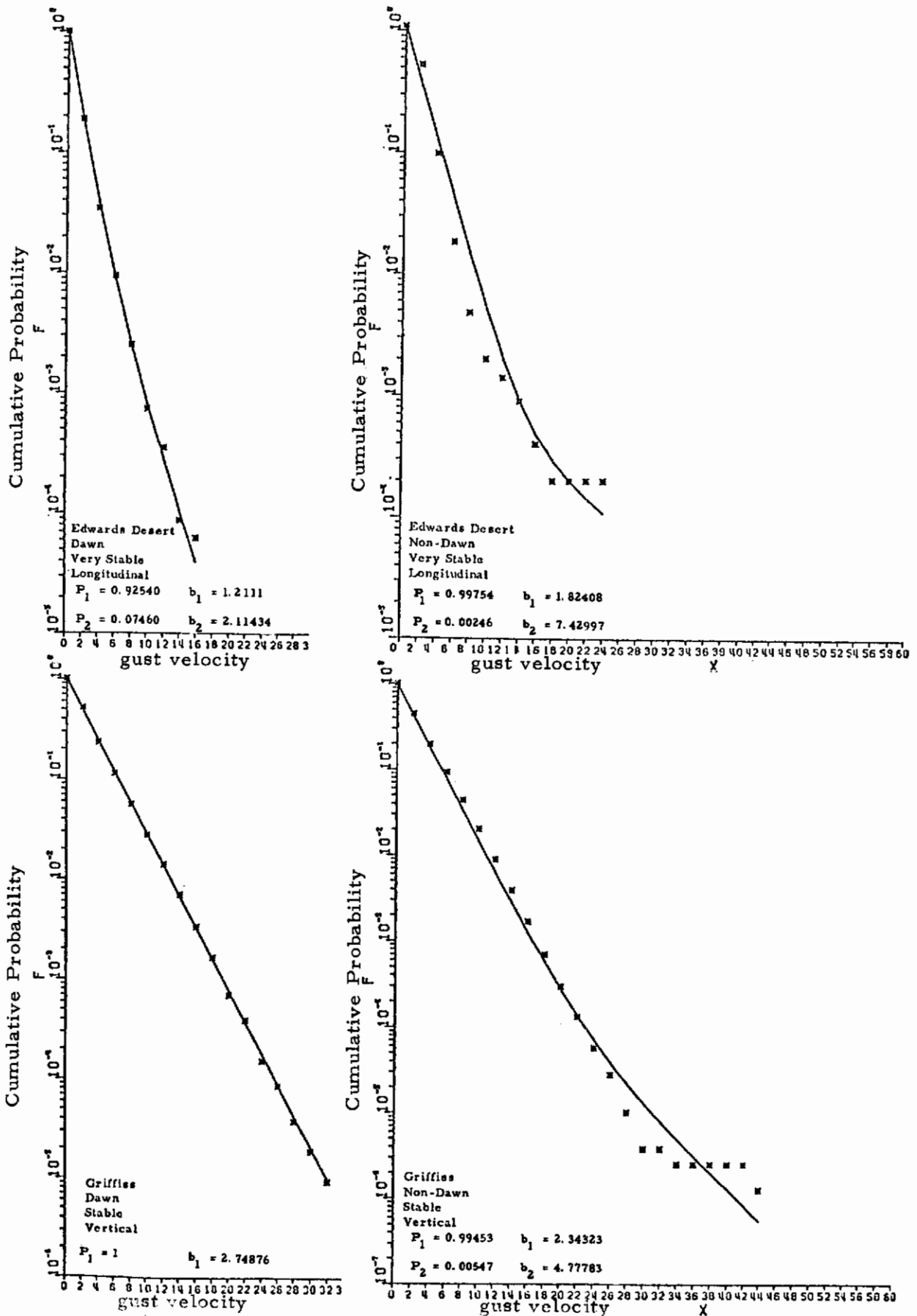
Figure 5.5 Cumulative Probability of Exceedance for Various Classes

72
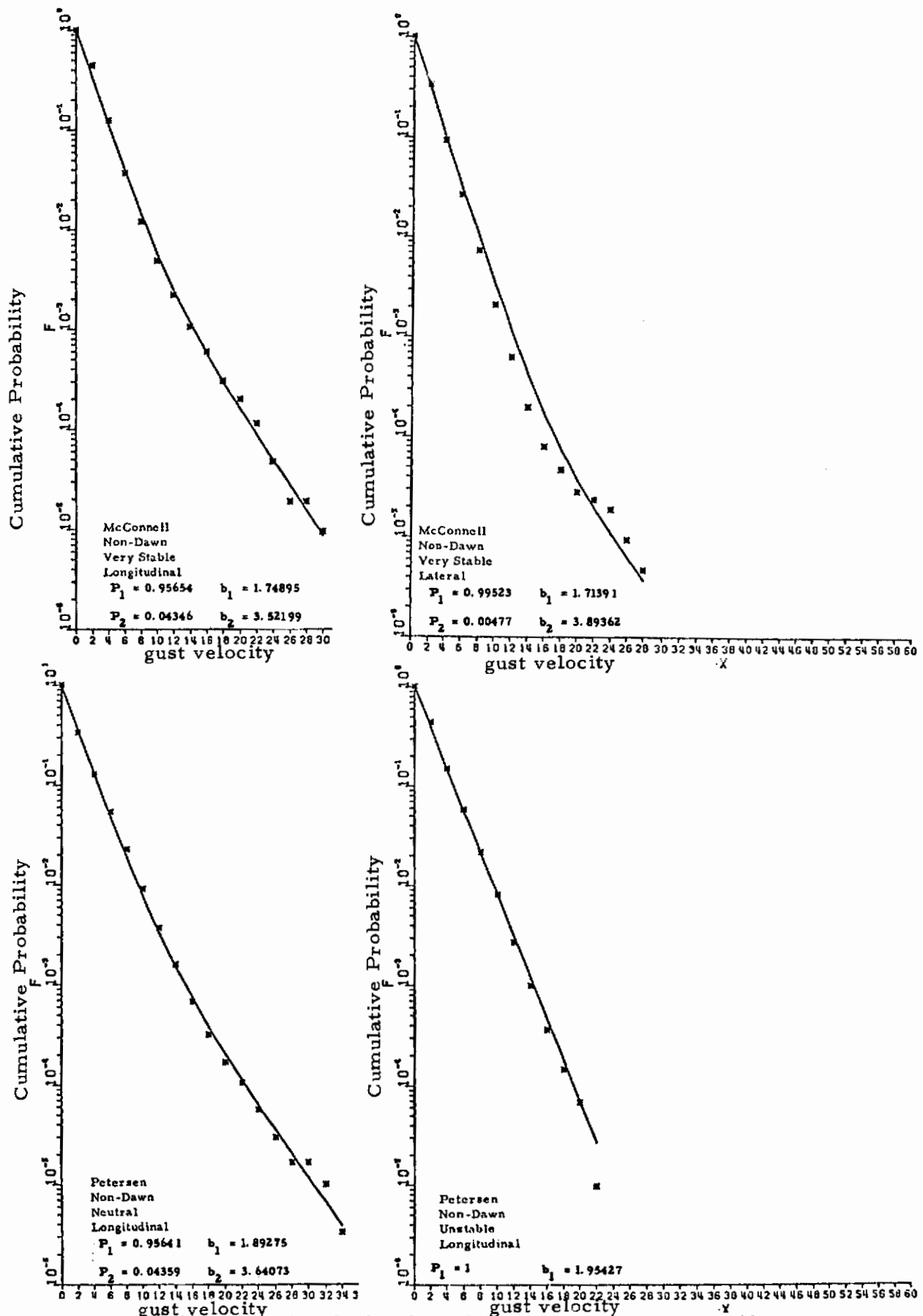
Figure 5.6 Cumulative Probability of Exceedance for Various Classes

73

TABLE 5.2

COMPARISON OF VARIATIONS IN b_1 AND σ BY STABILITY AND TIME OF DAY-GRIFFISS

LATERAL   GRIFFISS

	DAWN				NON-DAWN			
	P_1	P_2	b_1	b_2	P_1	P_2	b_1	b_2
VERY STABLE	.737	.263	2.262	2.532	.848	.152	2.217	3.205
STABLE	1.0	-	3.484	-	.719	.281	2.801	3.003
NEUTRAL	1.0	-	4.237	-	.936	.064	3.058	4.464
UNSTABLE	-	-	-	-	1.0	-	2.976	-

SIGMAS

	DAWN	NON-DAWN
VERY STABLE	2.133	2.903
STABLE	3.888	3.603
NEUTRAL	6.083	4.154
UNSTABLE	-	4.464

TABLE 5.3

COMPARISON OF VARIATIONS IN b_1 AND σ BY STABILITY
AND TIME OF DAY, PETERSON

LATERAL   PETERSON

	DAWN				NON-DAWN			
	P_1	P_2	b_1	b_2	P_1	P_2	b_1	b_2
VERY STABLE	.8579	.1421	1.965	2.705	.9688	.0312	1.868	3.789
STABLE	.9684	.0316	1.802	3.984	.9402	.0598	2.251	3.656
NEUTRAL	.7581	.2419	3.279	3.948	.9292	.0708	2.753	4.003
UNSTABLE	.8688	.1312	1.557	2.401	.9161	.0840	1.905	3.039

SIGMAS

	DAWN	NON-DAWN
VERY STABLE	1.628	2.094
STABLE	1.653	2.887
NEUTRAL	3.500	3.263
UNSTABLE	1.321	3.041

75

TABLE 5.4

COMPARISON OF VARIATIONS IN b_1 AND σ BY STABILITY AND TIME OF DAY, MCCONNELL

LATERAL   McCONNELL

| | DAWN | | | | NON-DAWN | | | |
	P_1	P_2	b_1	b_2	P_1	P_2	b_1	b_2
VERY STABLE	1.0	-	1.492	-	.9952	.0048	1.714	3.894
STABLE	1.0	-	2.010	-	.6700	.3300	2.096	2.105
NEUTRAL	1.0	-	1.998	-	.8936	.1065	1.946	2.737
UNSTABLE	1.0	-	2.039	-	1.0	-	2.370	-

SIGMAS

	DAWN	NON-DAWN
VERY STABLE	1.291	2.052
STABLE	2.951	2.899
NEUTRAL	3.435	3.177
UNSTABLE	3.292	3.405

TABLE 5.5

COMPARISON OF VARIATIONS IN b_1 AND σ BY STABILITY
AND TIME OF DAY, EDWARDS

LATERAL

EDWARDS
DESERT

	DAWN				NON-DAWN			
	P_1	P_2	b_1	b_2	P_1	P_2	b_1	b_2
VERY STABLE	1.0	-	1.480	-	.849	.515	.992	1.372
STABLE	.695	.305	1.916	2.028	.938	.062	1.508	2.632
NEUTRAL	-	-	-	-	.742	.258	1.934	2.183
UNSTABLE	-	-	-	-	.965	.035	2.188	3.906

EDWARDS
NON-DESERT

	DAWN				NON-DAWN			
	P_1	P_2	b_1	b_2	P_1	P_2	b_1	b_2
VERY STABLE	.961	.038	2.058	4.048	.991	.009	2.314	4.950
STABLE	.746	.253	3.571	4.149	.855	.144	2.557	3.623
NEUTRAL	.893	.107	3.699	6.173	.825	.175	2.512	3.268
UNSTABLE	-	-	-	-	.895	.105	2.695	4.237

SIGMAS

DESERT AND NON DESERT
INCLUDED

	DAWN	NON-DAWN
VERY STABLE	1.765	1.878
STABLE	2.420	2.817
NEUTRAL	3.675	3.230
UNSTABLE	4.250	3.811

77

b_1 is influenced by Stability and Time of Day in the same fashion as is sigma. In general, sigmas increase with decreased stability. b_1's behave likewise. When a sigma value is unusually large, the corresponding b_1 generally reflects the same phenomenon. For example, Peterson-Neutral-Dawn gives $\sigma = 3.5$ which is considerably larger than the sigma for Peterson-Unstable-Dawn. Similarly, the b_1 for Peterson-Neutral-Dawn is larger than for the other stability conditions. The same trends hold when comparing Dawn to Non-Dawn data. When the mean sigma for Non-Dawn increases over Dawn, the same effect is nearly always observed in b_1. The similarity between the influence of a parameter on σ and on b_1 has led the UDRI to use the results of the σ regression to estimate the relative effect the parameter has on the cumulative peak count distributions. The order in which the parameters were found to influence sigma is the order that has been used to decompose the cumulative peak count distributions.

The Regression Analysis on sigma of Phases I and II and Phase III data found Very Stable Air to be the most important predictor of sigma. Griffiss has been chosen as the second most important parameter because of the strong correlation found in Phases I and II data. Phase III data was not sufficiently balanced with respect to geographic location to determine the influence of each base. The third most important characteristic was taken as Stable Air because of its influence on Phases I and II and Phase III data. Cumulative probability of exceedance curves were determined for Phases I and II and Phase III data for each class in the decomposition sketched below.
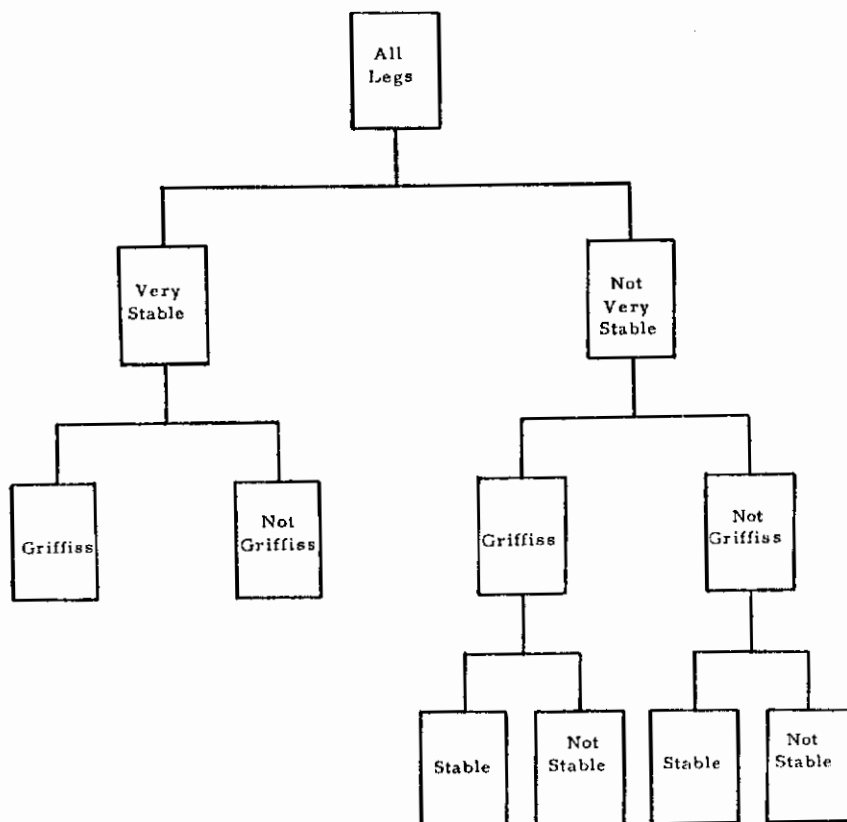
Figures 5.7 - 5.11 show the cumulative probability curves and give the P's and b's for each of the ten classes of Phases I and II and also Phase III data. Figure 5.7 shows that large differences exist between the stability conditions for Phases I and II and Phase III data. Even though the cumulative probability curves for the Phases I and II data are considerably different from those of Phase III, it is interesting to note the similarity between the b_1's and b_2's. For all flight legs, the b_1's and b_2's compare as follows: Phase III b_1 = 2.866, Phases I and II b_1 = 2.822. Phase III b_2= 6.840, Phase I and II b_2 = 10.309. Since each exponential component e^{-x/b_1} (e^{-x/b_2}) has similar slope for the Phases I and II and Phase III data, the intensity of turbulence experienced is about the same, but there is a much greater probability of being in turbulence of intensity b_2 with the Phase III data than with Phases I and II. This is further delineated in Figure 5.7 by observing the transition point between the influences of the first and second exponential components. For the Phase III data, the transition point occurs at a gust velocity of about 16 ft/sec. On the Phases I and II data, the transition occurs at 34 ft/sec.

For both Phases of data, the very stable flight legs showed markedly less turbulence than the other flight legs. For Phases I and II data a sharp drop in intensity (b_2) of the second component was observed. This would indicate that generally less severe turbulence was encountered in very stable air during Phases I and II. In Phase III however there was about the same intensity of turbulence b_2 for very stable legs as for non-very stable legs. This fact, plus a sharp decrease in P_2 for the very stable legs would imply that while severe turbulence occurred under both stability conditions, it occurred less frequently in very stable air.

Figure 5.8 shows the further decomposition of the Phases I and II data by the category Griffiss and Non-Griffiss. As anticipated from earlier studies on σ reported in Table 4.13, the exceedance curve shows stronger turbulence at Griffiss than at the other bases. However this decomposition does not yield as strong a separation in the cumulative probability curves as that produced by the very stable - not very stable decomposition because the Griffiss decomposition is only of secondary importance in relation to the initial stability decomposition. Figure 5.9 shows a similar breakdown by the base Griffiss for the Phase III data. This graph appears to contradict the results of Figure 5.8 by showing stronger turbulence for the Non-Griffiss legs. It will be shown later that the discrepancy between the two graphs can be explained by the presence of a large amount of high mountain data at Peterson and Edwards in Phase III where severe turbulence was frequently encountered.

A further decomposition of both Phases I and II and Phase III data by Stable Air adds little change to the cumulative probability curves (Figures 5.10 and 5.11) and is not considered significant to design criteria.

To further investigate the relationship between Phases I and II and Phase III data, the base Edwards was investigated. Edwards was chosen

79

PHASE III

All Components Combined

ALL FLIGHT LEGS

$P_1 = .932$ $b_1 = 2.866$

$P_2 = .068$ $b_2 = 6.840$

VERY STABLE

$P_1 = .9905$ $b_1 = 2.714$

$P_2 = .0095$ $b_2 = 7.163$

NON VERY STABLE

$P_1 = .919$ $b_1 = 3.149$

$P_2 = .081$ $b_2 = 6.734$

PHASES I AND II

All Components Combined

ALL FLIGHT LEGS

$P_1 = .99989$ $b_1 = 2.822$

$P_2 = .00011$ $b_2 = 10.309$

VERY STABLE

$P_1 = .9534$ $b_1 = 1.871$

$P_2 = .0463$ $b_2 = 3.195$

NON VERY STABLE

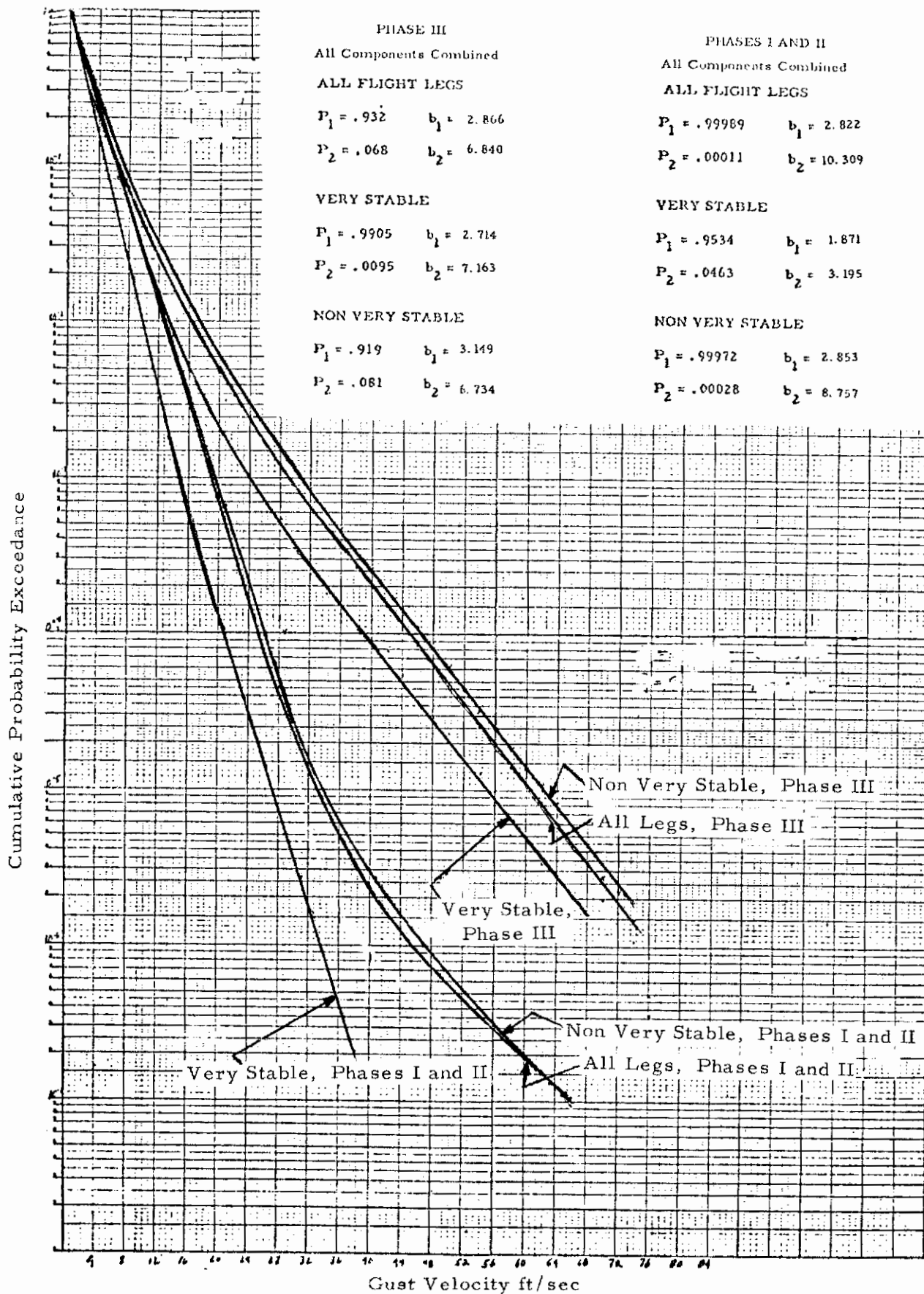$P_1 = .99972$ $b_1 = 2.853$

$P_2 = .00028$ $b_2 = 8.757$

Figure 5.7 Cumulative Probability of Exceedance, Very Stable and Not Very Stable, Phases I and II vs Phase III
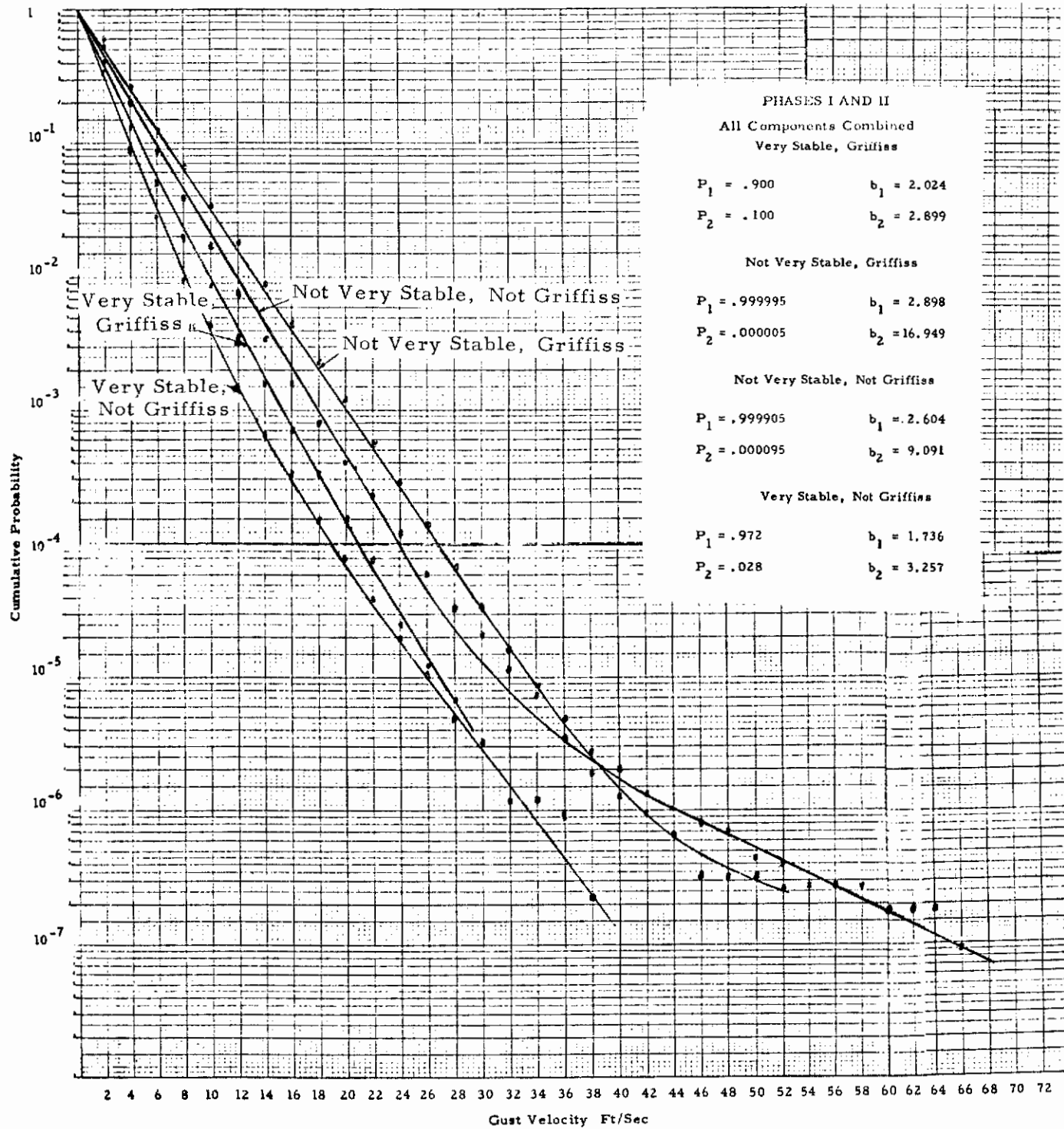
80

Figure 5.8 Cumulative Probability of Exceedance, Phases I and II,
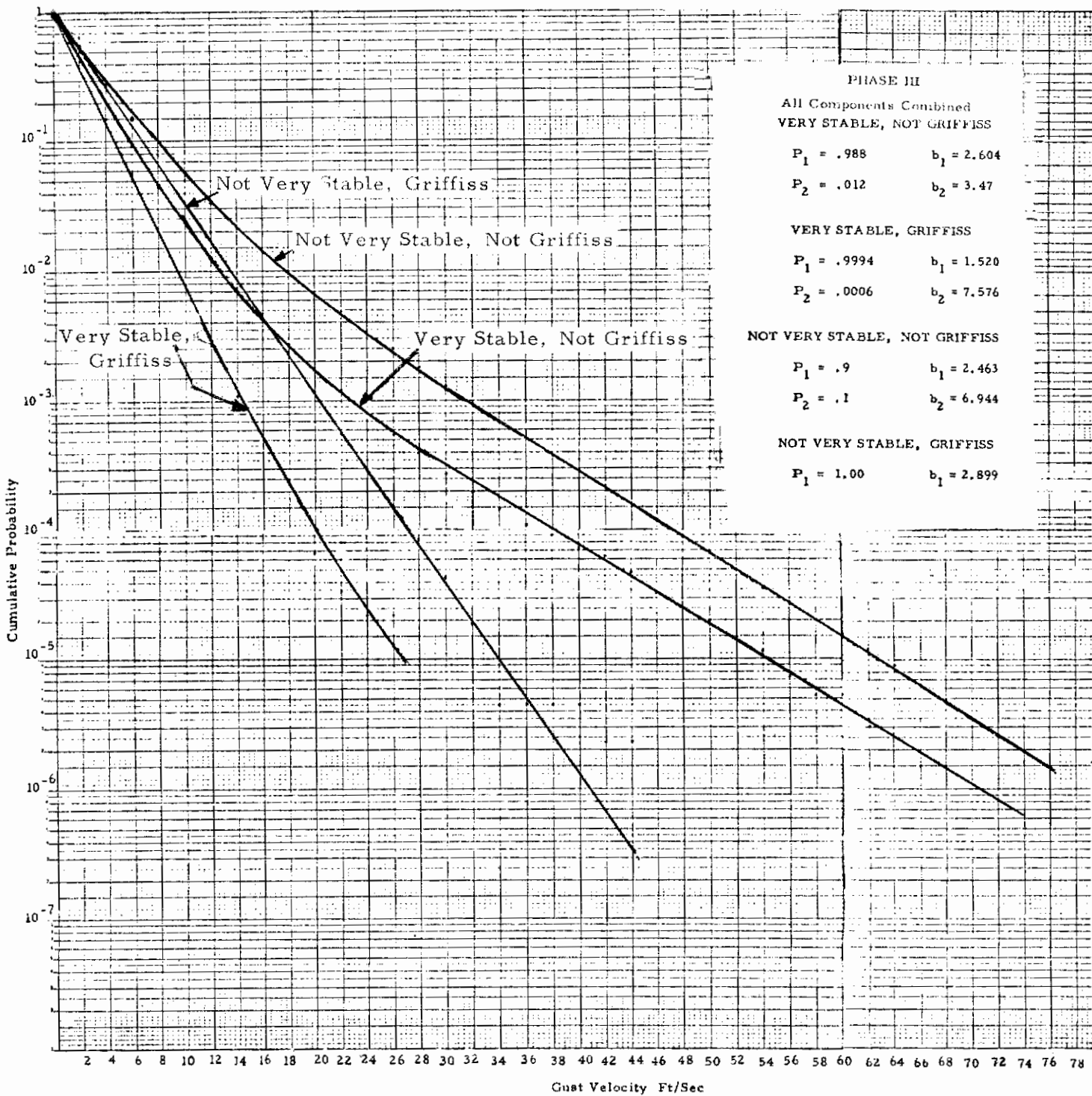Very Stable, Griffiss

81

Figure 5.9 Cumulative Probability of Exceedance, Phase III, Very Stable, Griffiss
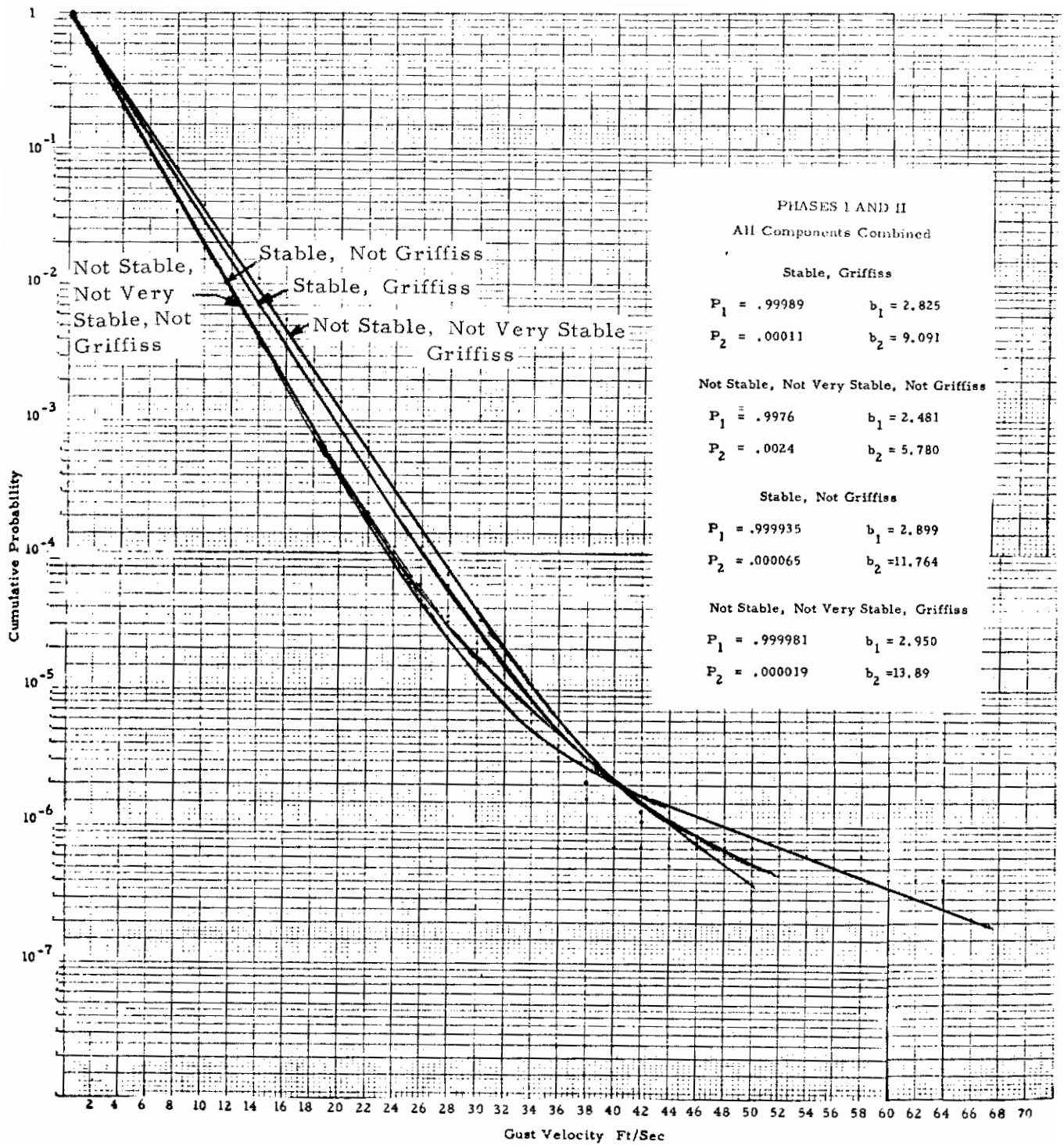
82

Figure 5.10 Cumulative Probability of Exceedance, Phases I and II, Griffiss, Stable

Labels within figure:

Not Stable, Not Very Stable, Not Griffiss

Stable, Not Griffiss

Stable, Griffiss

Not Stable, Not Very Stable Griffiss

Axis: Cumulative Probability (vertical), Gust Velocity Ft/Sec (horizontal)

PHASES I AND II
All Components Combined

Stable, Griffiss

$P_1 = .99989$ $b_1 = 2.825$

$P_2 = .00011$ $b_2 = 9.091$

Not Stable, Not Very Stable, Not Griffiss

$P_1 = .9976$ $b_1 = 2.481$

$P_2 = .0024$ $b_2 = 5.780$

Stable, Not Griffiss

$P_1 = .999935$ $b_1 = 2.899$

$P_2 = .000065$ $b_2 = 11.764$

Not Stable, Not Very Stable, Griffiss

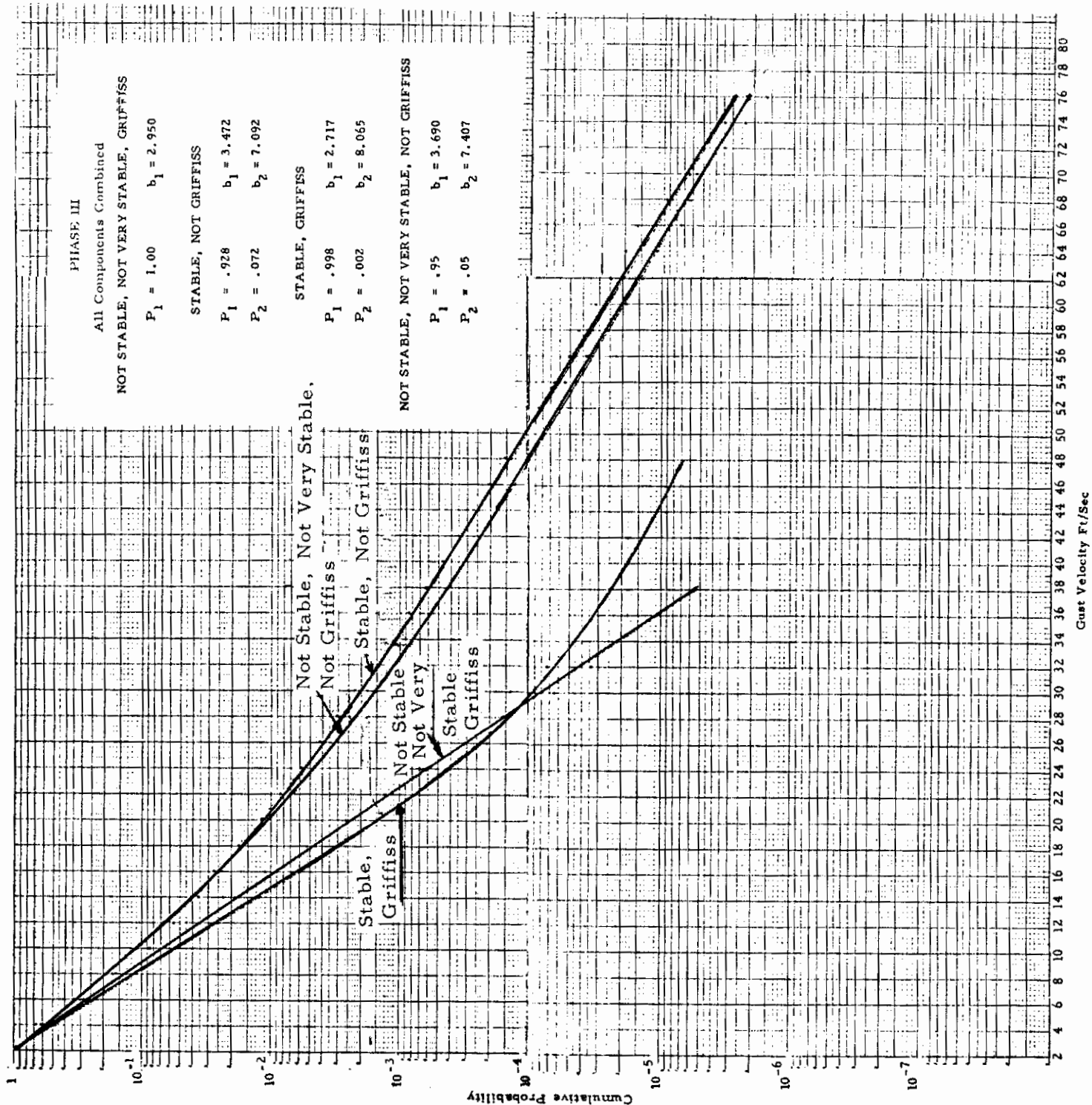$P_1 = .999981$ $b_1 = 2.950$

$P_2 = .000019$ $b_2 = 13.89$

83

Figure 5.11 Cumulative Probability of Exceedance, Phase III, Griffiss, Stable

84

because of the balanced distribution of each category of Phases I and II data relative to Phase III. Table 5.6 shows the category decomposition at Edwards for each of the Phases of data. The percentage of flights in each condition from Phase III agrees favorably with those of Phases I and II except with respect to season. A seasonal bias in Phase III data should not bias the results since Season has been shown to have very little correlation to σ. Figures 5.12 and 5.13 show at Edwards a) all flight legs, b) High Mountain Legs, and c) Not High Mountain Legs for Phases I and II and Phase III. The comparison of all flight legs from Phases I and II with Phase III shows poor agreement. Again, the probability curves are much higher from the Phase III legs than those of Phases I and II. However, when the High Mountain data is extracted from Edwards, an interesting result is apparent. The Not High Mountain data at Edwards from Phase III agrees exceedingly well with the Not High Mountain Edwards data from Phases I and II. To test whether this relationship is unique to Edwards, a comparison was made between Phase III data (from all bases) not flown over high mountains and the corresponding data from Phases I and II. The results are presented in Figure 5.14.

By ignoring the High Mountain Phase III data, the rest of the Phase III data shows cumulative probability curves that agree remarkably well with Phases I and II. The question is why is Phase III High Mountain data more turbulent than Phases I and II. One possible explanation is the following: All High Mountain data was flown at Peterson and Edwards. Phases I and II High Mountain data at Peterson was flown non-contour, that is, instead of attempting to maintain a treacherous 250 or 750 ft. above mountain terrain, a low altitude or high altitude course was followed. On Phase III legs, however, an adventurous pilot flew 250 and 750 ft. contour legs. The possibility exists that aircraft maneuvers associated with flying a contour profile over high mountains have not been eliminated from the gust velocity time histories. These large gust velocities associated with the High Mountain Phase III flights may not be true gust velocities, but fictitious results from aircraft maneuvering. This would also explain why the correlation from the regression analysis of Phase III data is smaller than for Phases I and II. If the large gust velocities are really maneuver-related, they will not correlate to stability or the other categories. This explanation however is not without difficulty. Both Phases I and II and Phase III High Mountain Edwards Legs were flown at 250 ft. and 750 ft. Table 5.7 shows the mean radar altitude of all the flight legs flown at Peterson and Edwards over High Mountains versus planned terrain altitude. From Table 5.7 it is observed that there is little difference between Phase III mean radar altitudes and those of Phases I and II at Edwards. Hence it appears the flight profile was essentially the same as that of Phases I and II. Why then is Phase III High Mountain Legs at Edwards more turbulent than Phases I and II. Another difficulty with the maneuver explanation is the similarity between the cumulative probability curves for three components. If the high gust velocities were maneuver induced one would anticipate the effect to appear primarily in the lateral and vertical components - not the longitudinal. This is not substantiated by Figure 5.4.

TABLE 5.6

PERCENTAGE OF FLIGHTS BY CATEGORY AT EDWARDS

EDWARDS

TERRAIN

	High Mnts.	Low Mnts.	Plains	Desert	Water	Total Legs
Phases I and II	28%	36%		29%	7%	1745
Phase III	34%	38%		20%	8%	582

ALTITUDE

	250 ft.	750 ft.
Phases I and II	46%	54%
Phase III	51%	49%

STABILITY

	Very Stable	Stable	Neutral	Unstable
Phases I and II	35%	24%	25%	16%
Phase III	48%	23%	16%	13%

SEASON

	Spring	Summer	Fall	Winter
Phases I and II	19%	34%	34%	13%
Phase III	--	--	81%	19%

TIME OF DAY

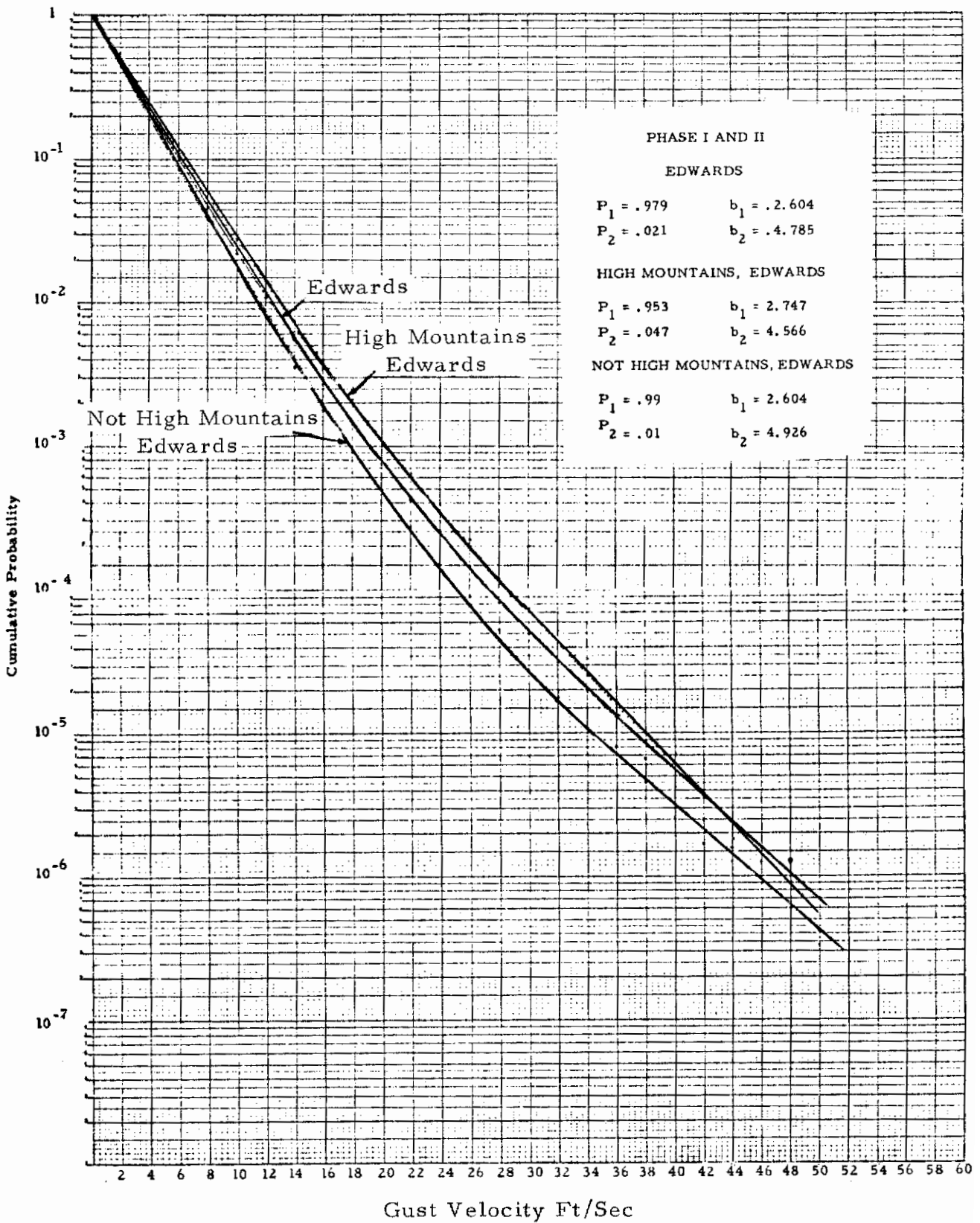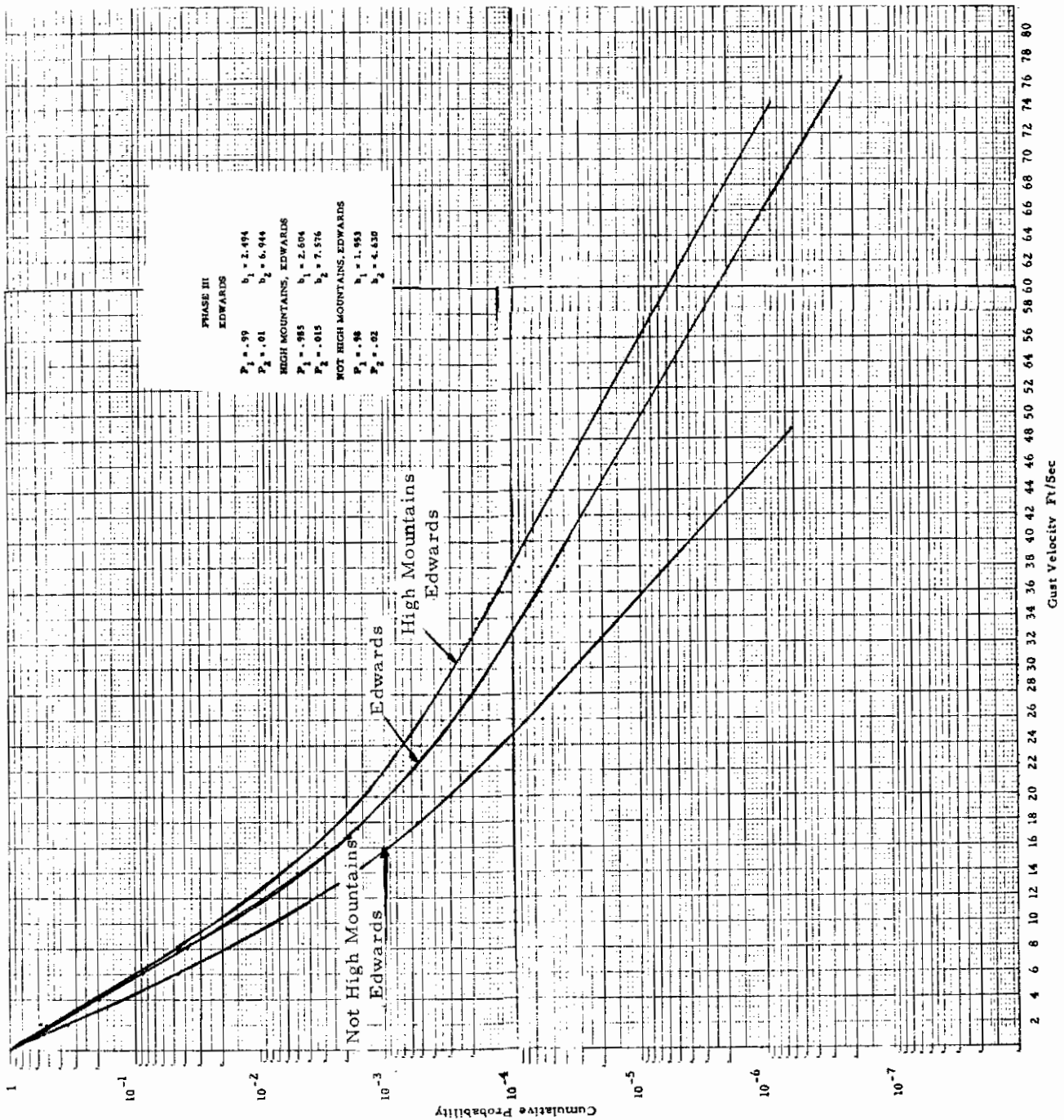|	Dawn	Mid morning	Mid afternoon
Phases I and II	35%	33%	32%
Phase III	31%	41%	38%

Figure 5.12 Cumulative Probability of Exceedance, Phases I and II, Edwards, High Mountains

87

Figure 5.13 Cumulative Probability of Exceedance, Phase III, Edwards, High Mountains

88

Phase III

$P_1 = .9968 \qquad b_1 = 2.463$

$P_2 = .0032 \qquad b_2 = 5.650$

Phases I and II

$P_1 = .9999 \qquad b_1 = 2.463$

$P_2 = .0001 \qquad b_2 = 9.091$

Phase III, Not High Mountains

Phases I and II, Not High Mountains
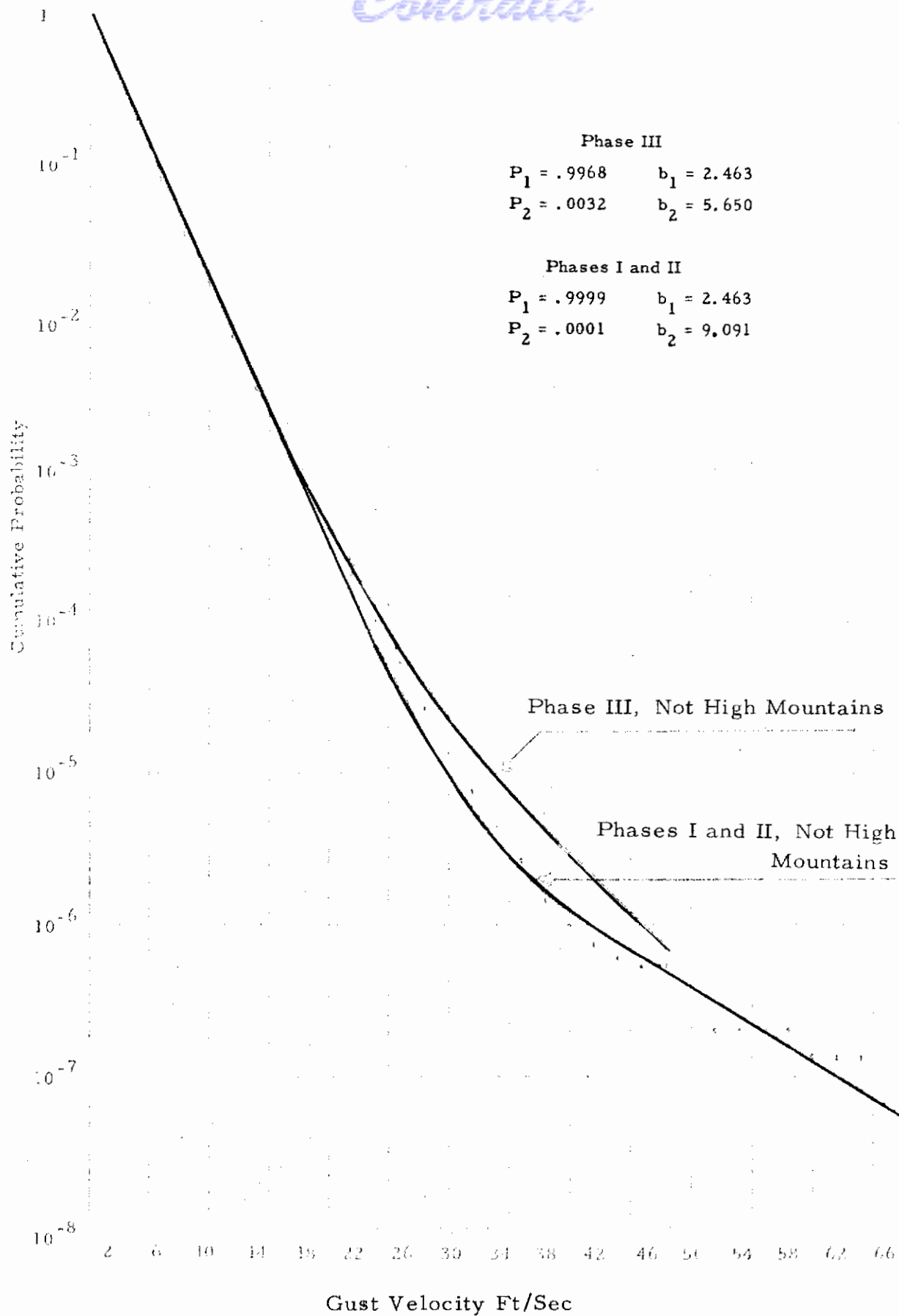
Gust Velocity Ft/Sec

Figure 5.14 Cumulative Probability of Exceedance, Not High Mountains,
Phases I and II versus Not High Mountains, Phase III

89

TABLE 5.7

MEAN RADAR ALTITUDE OF HIGH MOUNTAINS
AT PETERSON AND EDWARDS

PETERSON MEAN RADAR ALTITUDE

	Phases I and II	Phase III
250 ft. (Low Altitude)	1254 ft.	340 ft.
750 ft. (High Altitude)	1693 ft.	655 ft.

EDWARDS MEAN RADAR ALTITUDE

	Phases I and II	Phase III
250 ft.	367ft.	469 ft.
750 ft.	728 ft.	826 ft.

5.4 Conclusions

Cumulative probability exceedance curves (P's and b's) have been obtained for LO-LOCAT Phases I and II and Phase III by various category decompositions based upon the influence a parameter has on sigma. A comparison between b_1, a peak count exceedance parameter, and mean sigmas verified that parameters that influence σ also influence b_1 in the same way. This fact substantiates the use of the sigma regression decomposition for defining a cumulative peak count decomposition.

The following specific conclusions have been obtained from the analysis of Section 5.

1) There is a large separation between the cumulative probability curves for all of Phases I and II data and for Phase III data.

2) If the Phase III High Mountain data is not used in the analysis, the cumulative probability curve for the remainder of the Phase III data (Not High Mountains) agrees remarkably well with the corresponding Phases I and II data.

3) Phase III High Mountain data appears statistically to be from a different population. The cause has not been ascertained but several possibilities have been discussed.

4) The most important parameter correlating to turbulence is Very Stable Air. P's and b's have been obtained for the decomposition into Very Stable legs and Non Very Stable legs.

5) The second most important parameter for correlating to turbulence is associated with Griffiss. The geographic location Griffiss, however, is not the cause, but only reflects a correlation to certain meteorological conditions that exist at Griffiss.

6) A further decomposition of peak counts by the third parameter of influence, Stable Air, produced minor changes in the cumulative probability curves.

7) There is negligible difference between the cumulative probability curves for the flight legs at 250 ft. and those at 750 ft.

8) Small differences in the cumulative probability curves for the three components u, v, and w were observed. The lateral component shows somewhat higher peak velocity probabilities than the other two components. However, this difference was negligible compared with the effect produced by other environmental conditions.

5. 5   Comparison of LO-LOCAT Data to Results from
        Other Turbulence Investigations

In Section VIII of Reference 7, John C. Houbolt develops expressions
for load exceedance curves, and shows how various parameters of these curves
vary with altitude. The LO-LOCAT data is restricted to clear air turbulence
and to a small altitude segment of the atmosphere. Houbolt data refers to the
general atmospheric environment, including storm and cloud conditions. Never-
theless it was felt that it would be useful to express the results of the LO-LOCAT
data analysis in the Houbolt format. Comparison for various cases considered
in Reference 7 are as given below.

Case A - Houbolt develops the equation

$$\frac{N}{PN_o} = .993 \, ext(\frac{-a_1 \, x}{A \, \sigma_w}) + .007 \, \exp (\frac{-a_2 \, x}{A \, \sigma_w})$$

where

$$a_1 = [.993 + .007a^2]^{1/2}$$

$$a_2 = \frac{a_1}{\alpha}$$

P = Proportion of time in an intensity σ_w

Since UDRI uses the form for exceedance curves of

$$\frac{N}{N_o} = P_1 \, \exp (\frac{-x}{b_1}) + P_2 \, \exp (\frac{-x}{b_2})$$

it is observed that P_1 can be compared to $.993$, P_2 to $.007$, $\frac{1}{b_1}$ to $\frac{a_1}{\sigma_w}$ and
$\frac{1}{b_2}$ to $\frac{a_2}{\sigma_w}$ algebraically it can be shown that $\frac{b_2}{b_1} = \alpha$ and $\sigma_w = a_1 b_1$.

The following table   compares UDRI's Phase I and II values to
Houbolt's Case A.

	Houbolt	UDRI
P_1	.993	.9999
P_2	.007	.0001
α	1.2	3.65
σ_w	3.00	2.94

	Houbolt	UDRI
$\frac{1}{b_1}$	.333	.406
$\frac{1}{b_2}$	.278	.110

For Case B, Houbolt developed the equation

$$\frac{N}{N_o} = P_1 \ \exp \ (\frac{-x}{A\sigma_1}) + P_2 \ \exp \ (\frac{-x}{A\sigma_2})$$

Curves for $P = P_1 + P_2$ are given as are σ_i values. The following Table compares UDRI's Phases I and II values to Houbolt's Case B.

	Houbolt	UDRI
P_1	.7	.9999
P_2	.0005	.0001
σ_1	3	2.822
σ_2	6	10.309

Results of other low level turbulence programs are given in Reference 9 and the results summarized in Table 5.8. While these earlier turbulence programs do not cover the wide range of environmental conditions included in the LO-LOCAT Program, they none-the-less provide valuable information about particular segments of the atmosphere. Further details about these low level programs are given in Reference 9.

TABLE 5.8

SOURCES FOR LOW-LEVEL TURBULENCE DATA

DATA SOURCE AND TYPE OF DATA	P_1	b_1	P_2	b_2	L (feet)
NACA TN 4332 0-2000 ft	0.34	4.6	0.00025	9.4	1000
MIL-A-8866 0-1000 ft	1.0	3.9	0	-	500
ASD-TR-61-235 0-1000 ft	1.0	2.72	0.01	5.44	500
SEG-TDR 64-24 low level contour	0.9974	3.62	0.0026	7.62	1000
B-66, vertical peak count	1.0	2.7	-	-	500
B-66, lateral peak count	1.0	3.1	-	-	500
F-106, vertical peak count	-	-	0.068	10.65	500
F-106, lateral peak count	-	-	0.068	14.06	500

SECTION VI

ANALYSIS OF PEAK COUNT DATA BY LEG

Peak count data for the low level legs in Phases I and II have been provided by ETAC at the request of UDRI. This data contains the number of gust velocity peaks encountered for each leg by component in histogram form in gust velocity increments of 2 ft/sec. A turbulence parameter, b, has been determined from these data for each leg by component and this parameter used as the dependent variable in a regression analysis. The purpose of this section is to show that the turbulence parameter b relates to the environmental conditions in roughly the same way as does σ, the standard deviation of the gust velocity time history. That is, the parameters b and σ contain much the same information about the turbulence, thus adding creditability to the results of the regression on both parameters. The parameter b is not used in determining the gust load exceedance equation but b does provide a measure of the intensity of the turbulence encountered on each leg.

6.1 Determination of the Turbulence Parameter b by Leg

A plot of $N(x)$, the number of gust velocity peaks greater than gust velocity x, versus x on semi-log paper revealed that for most legs the relationship was approximately linear. Figures 6.1 - 6.3 give typical examples of such plots under various environmental conditions. It was therefore decided that $N(x)$ could be adequately represented by a relationship of the form

$$N(x) = N_o \ e^{-x/b}$$

Taking logarithms of both sides, gives

$$\ln \ N(x) = \ln \ N_o - \frac{x}{b} \ .$$

A linear least squares fit is then made to $\ln \ N(x)$ versus x to obtain values for $\ln \ N_o$ and b, using the peak count distribution in increments of 2 ft/sec. The data in the 0-2 ft/sec interval is ignored in the least squares fit because the peak count in this interval is often contaminated due to the presence of noise.

6.2 Regression Analysis by Leg

The b turbulence parameters for each leg of Phases I and II data are used as the dependent variables in a regression analysis with the environmental conditions (1) - (6) and the three components used as the independent variables. The results of this analysis together with the previously obtained results on σ are given in Table 6.1. A comparison between the regression results on the two turbulence parameters shows general consistency with a few notable differences as listed below:
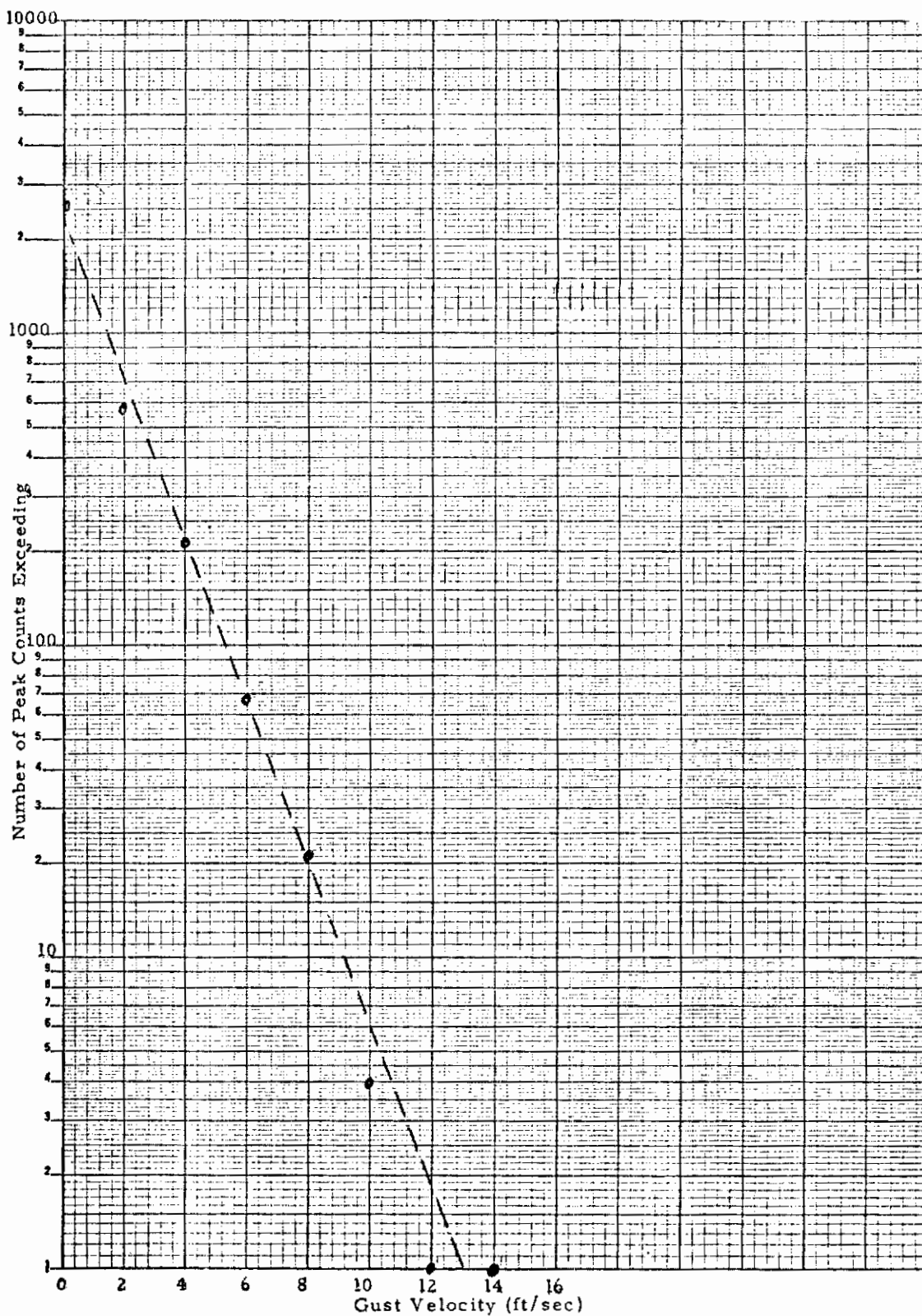
95

Figure 6.1: Peak Count Exceedance, Test No. 1050,
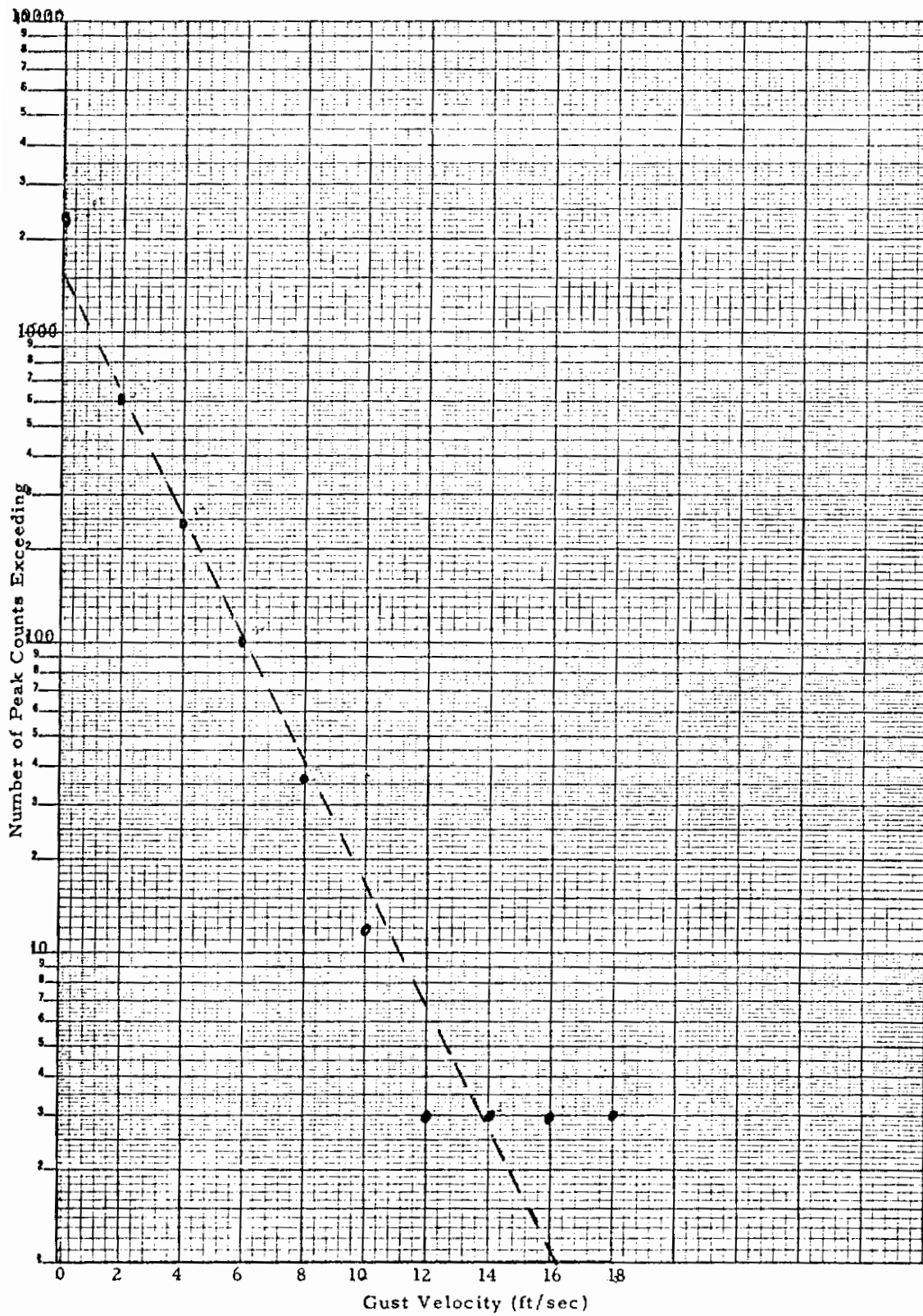Longitudinal, Category No. 413332

96

Figure 6.2: Peak Count Exceedance, Test No. 5087,
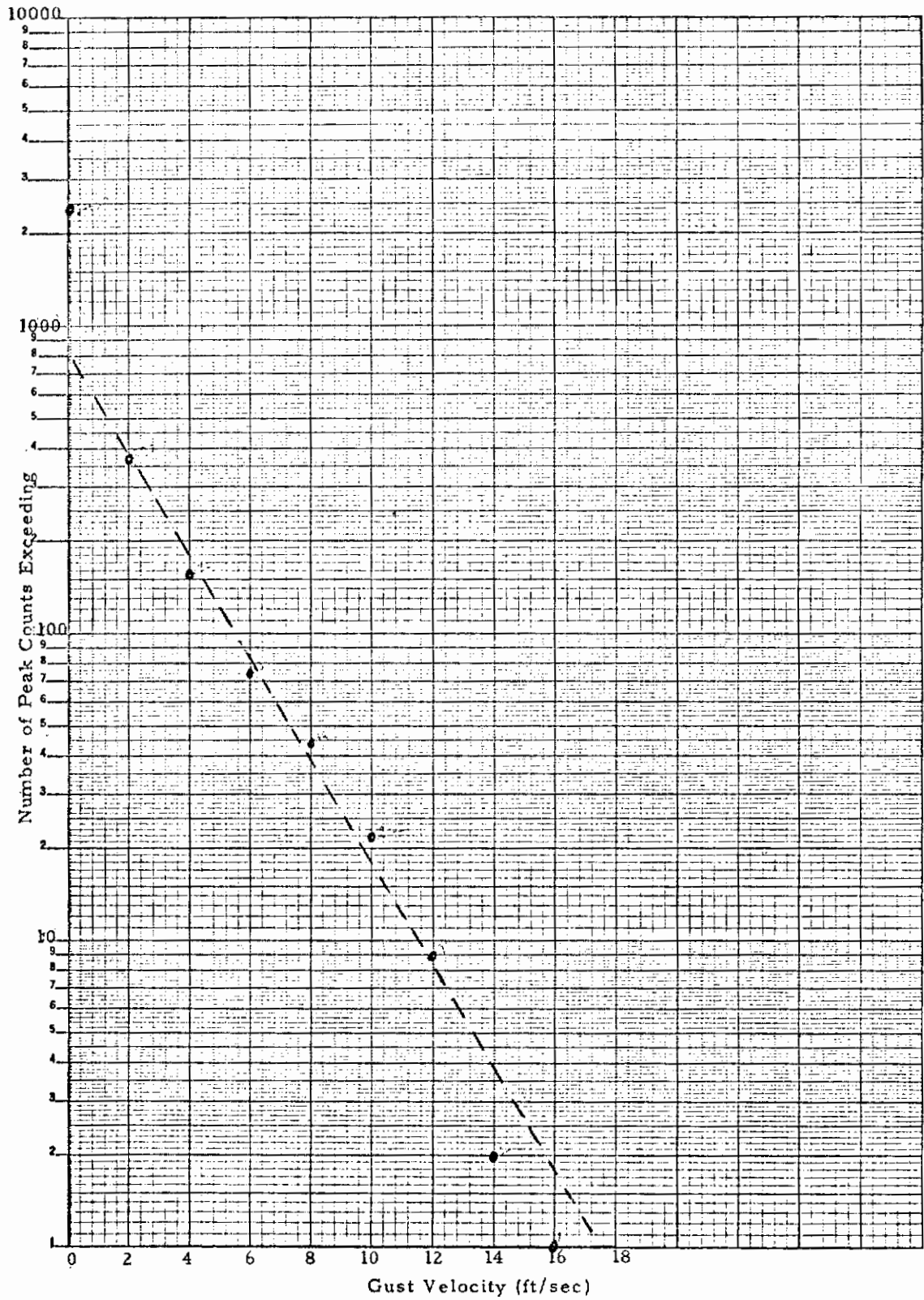Lateral, Category No. 412144

97

Figure 6.3: Peak Count Exceedance, Test No. 2222, Vertical, Category No. 322321

98

TABLE 6.1

COMPARISON OF SIGMA REGRESSION TO b REGRESSION

Step	Constant	Altitude 750	Stability: Very Stable	Stability: Stable	Time of Day: Dawn	Season: Spring	Season: Winter	Base: Griffiss	Base: Edwards	Component: Lateral	Terrain: Desert	Terrain: Plains	Terrain: High Mts.	Terrain: Low Mts.	Correlation Coefficient	Standard Deviation
σ Regression																
0	2.685														.51	1.047
1	3.078		-1.30												.56	1.006
2	2.922		-1.34					+.73							.60	.974
3	3.187		-1.62	-.60				+.81							.62	.957
4	3.220		-1.27	-.53	-.50			+.78							.64	.940
5	3.145		-1.25	-.50	-.52			+.84					+.68		.65	.924
6	3.043		-1.17	-.45	-.58	+.43		+.80					+.66		.66	.910
7	3.182	-.32	-1.18	-.43	-.57	+.44		+.78					+.68		.68	.899
8	3.313	-.33	-1.18	-.43	-.57	+.44		+.58					+.74	+.40	.68	.893
9	3.071	-.33	-1.18	-.43	-.57	+.43		+.58		+.22			+.74	+.40	.68	.890
10	3.028	-.33	-1.17	-.42	-.57	+.48	+.19	+.55		+.22			+.75	+.40	.68	.890
b Regression																
0	1.916														.27	1.014
1	2.086		-.64												.34	.990
2	2.356		-.66									-.45			.37	.980
3	2.462		-.65								-.56	-.56			.38	.972
4	2.593		-.78	-.28							-.59	-.55			.39	.966
5	2.519		-.75	-.26		+.26					-.58	-.54			.40	.964
6	2.526		-.61	-.23	-.21	+.29					-.58	-.54			.41	.962
7	2.490		-.62	-.23	-.21	+.29				+.11	-.58	-.55			.41	.961
8	2.446		-.62	-.25	-.20	+.28		+.11		+.11	-.53	-.51			.41	.959
9	2.168		-.63	-.24	-.21	+.28		+.35		+.11	-.61	-.26			.42	.958
10	2.200	-.08	-.62	-.24	-.21	+.28		+.36		+.11	-.61	-.26			.42	.957
11	2.180	-.08	-.63	-.23	-.21	+.30	+.11	+.37	+.30	+.11	-.61	-.26			.42	.957

The following categories were omitted from the above because they were not significant: 250 ft. Altitude, Neutral and Unstable Stability conditions, Mid-morning and Mid-afternoon Times of Day, Summer and Fall Seasons, Peterson and McConnell Bases, and the Longitudinal and Vertical Components.

1)   The quantity b was generally smaller than σ for a given leg.
In fact, using the mean values at step 0 in the regression analysis shows that

$$\frac{\bar{b}}{\bar{\sigma}} = 0.713.$$ A plot of the relationship $b = 0.713\ \sigma$ for a representative

cross section of legs is given in Figure 6.4.

2)   The terrain features Desert and Plains enter into the b
regression with negative coefficients while High Mountains and Low Mountains
enter into the σ regression with positive coefficients. While the two regressions
indicate essentially the same relationship to terrain the dependence is expressed
in a different way. This difference indicates why some dichotomous variables
were omitted in earlier runs to give a standard frame of reference for the
results.

3)   The regression coefficients in the b regression are generally
smaller than those in the σ regression. This is due to the generally smaller
values of b obtained for each leg but can also be attributed to the fact that
the correlation coefficients in the b regression are smaller.   Smaller
correlations indicate a weaker dependence of the b parameter upon the environ-
mental conditions which in turn produces less of a separation in the distributions
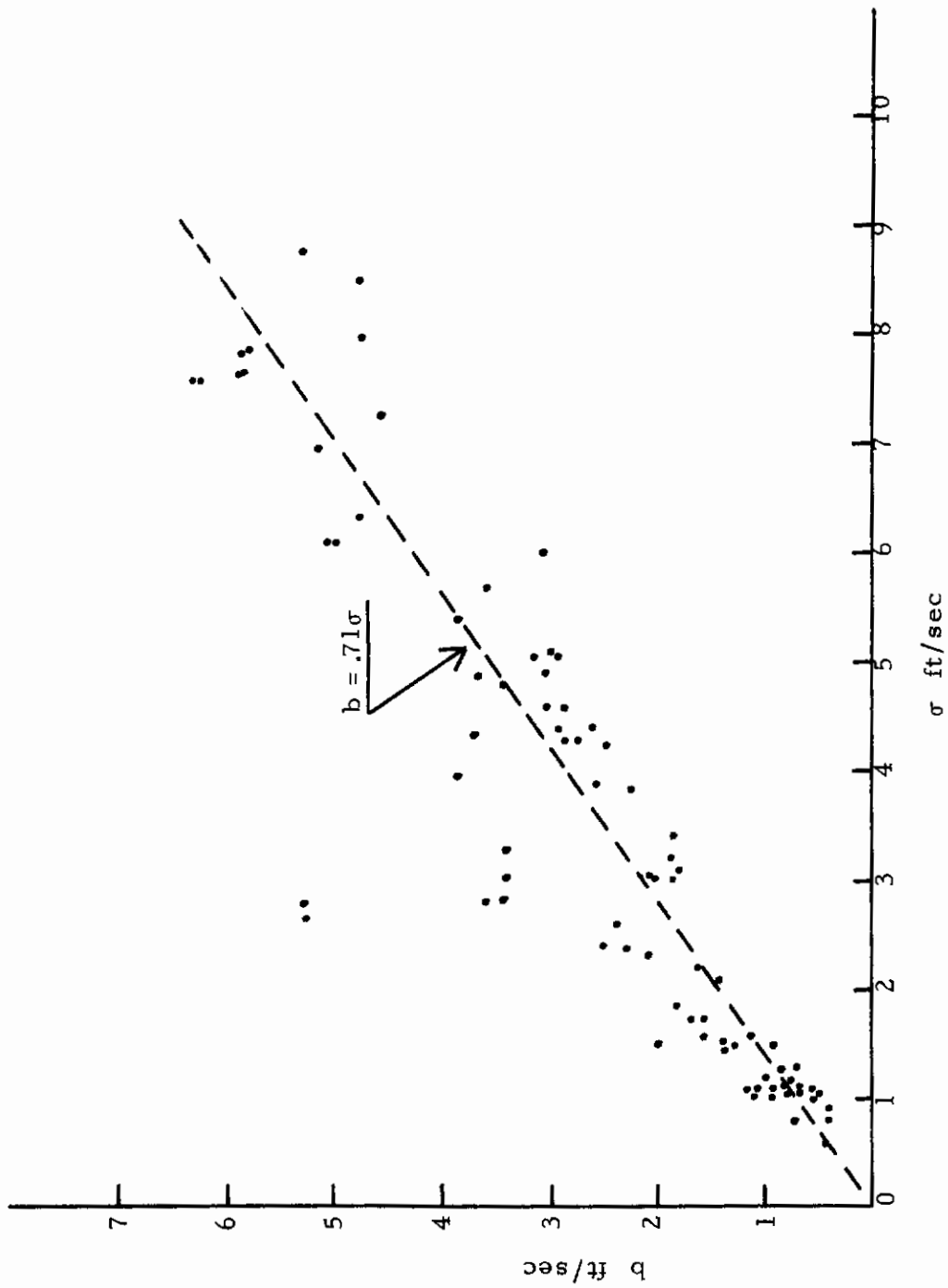of the b values under various environmental conditions.

Figure 6.4 σ Versus b for Representative Legs

b = .71σ

σ ft/sec

b ft/sec

SECTION VII

APPLICATION OF LO-LOCAT DATA TO DESIGN CRITERIA

In order to properly design an aircraft, the manufacturer must have a representative statistical mathematical model of the gust velocity environment. Use of power spectral methods allows this to be done, as both the continuous nature of atmospheric turbulence and the variation in turbulence intensity with wavelength are considered. Modelling of the atmospheric turbulence environment is made in terms of (a) a spectrum shape (the Von Karman model with specified scale of turbulence L), (b) an RMS gust intensity variable σ, (c) scale parameters, b_1 and b_2, indicative of probable intensities of turbulence, and (d) parameters, P_1 and P_2, depicting the portion of flight time spent in turbulence. These relationships have been discussed in Section III. The generalized prediction equation for any load parameter (acceleration, bending moment, stress, etc.) can be expressed by:

$$\frac{N(y)}{N_o} = P_1 \exp\left(\frac{-y/\overline{A}}{b_1}\right) + P_2 \exp\left(\frac{-y/\overline{A}}{b_2}\right)$$

where

$N(y)$ = average number of response peaks of the aircraft per foot exceeding the value y

N_o = average number of response peaks per foot in turbulence (characteristic response frequency)

y = response parameter (acceleration, bending moment or stress)

$\overline{A}$ = gust response factor for a particular location on the aircraft relating gust velocity to the response parameter y.

P_1, P_2, b_1, and b_2 are the parameters that define the cumulative probability of gust velocity exceedance by Equation 3.2. In order to determine the gust response factor ($\overline{A}$) and the characteristic response frequency (N_o) it is essential to have a PSD model which represents the spectrum shape. Reference 1 shows that the Von Karman spectra provided the best fit to the calculated PSD data for all gust velocity components. The Von Karman spectra is given by:

$$\varphi(\Omega) = \frac{\sigma^2}{\pi} L \frac{1 + 8/3 (1.339 L\Omega)^2}{[1 + (1.339 L\Omega)^2]^{11/6}}$$

It is noted that

$$\sigma^2 = \int_0^\infty \varphi(\Omega) \, d\Omega.$$

The response y can be related to the input by a linear transformation

$$\varphi_y(\Omega) = |H_y(\Omega)|^2 \varphi(\Omega)$$

which relates the output spectra of the response variable y to the input spectra of the gust velocity through the frequency response function H_y. This response function H_y is defined as the response y resulting from a sinusoidal gust encounter of unit amplitude at each frequency Ω over the required frequency range. The aircraft manufacturer must determine these values using equations of motion and model or lumped-mass approach for the response value involved. The frequency response function is not only determined for a specific parameter and a specific location on the aircraft but is also a function of the aircraft configuration including wing area, gross weight and associated weight distribution, airspeed and altitude.

The expression for $\overline{A}$ is

$$\overline{A} = \frac{\sigma_y}{\sigma}$$

and since

$$\sigma_y^2 = \int_o^\infty \varphi(\Omega) |H_y(\Omega)|^2 \, d\Omega$$

then

$$\overline{A} = \left[\int_o^\infty \frac{\varphi(\Omega)}{\sigma^2} |H_y(\Omega)|^2 \, d\Omega \right]^{1/2}$$

The characteristic response frequency, N_o, is a function of the RMS of the second moment of the response PSD divided by the RMS of the area under the response PSD curve and therfore:

$$N_o = \frac{1}{2\pi} \left[\frac{\int_o^\infty \Omega^2 |H_y(\Omega)|^2 \varphi(\Omega) \, d\Omega}{\int_o^\infty |H_y(\Omega)|^2 \varphi(\Omega) \, d\Omega} \right]^{1/2}$$

The LO-LOCAT data consists exclusively of clear air data. No storm flights are included. Hence, one is cautioned against applying the results indiscriminantly to aircraft design without regard to percentage of time flown in storm and non-storm conditions. The LO-LOCAT program consisted of flying specific routes on a scheduled basis without regard to the degree of

103

turbulence anticipated except that if a storm was encountered the flight was aborted. The data sample can be considered a random sample of the gust environment of the atmosphere during non-storm conditions. The LO-LOCAT data is also, of course, limited to design criteria applications in the 0-1000 ft. terrain altitude region.

The following section gives the authors' recommendations for the P_1, P_2, b_1, b_2 and the Von Karman L for the 0-1000 ft. altitude region in non-storm flight conditions.

7.1 Gust Environment Parameters

The cumulative probability exceedance curves for all Phase III flight legs have been shown to be considerably larger than those of Phases I and II. However, if one considers only those Phase III legs NOT flown over high mountains, there is good agreement with Phases I and II. All of Griffiss data as well as Edwards legs not over high mountains have been shown to produce similar cumulative exceedance curves as their Phases I and II counterparts. The cause of this phenomenon in Phase III high mountain legs has not been deduced. Several possibilities have been considered:

(a)　Due to a faster aircraft the Phase III data contain wavelengths to 14,000 ft., or twice as long as those measured in Phases I and II. The presence of larger amplitudes in these wavelengths could result in the higher cumulative probability curves. If it is true that the large gust velocities are associated with the longer wavelength, then one should anticipate the effect to appear over all terrain conditions. This has not been observed. As stated previously, only the Phase III High Mountains terrain shows higher cumulative probability curves.

(b)　The Phase III high mountain data may be biased with aircraft maneuvers induced by contour flying over rugged high mountain terrain. This explanation is plausible for Peterson data. The Phases I and II high mountain data at Peterson were non-contour flown and presumably required little aircraft maneuver. The resulting data did not significantly differ from the rest of Phases I and II data. On the other hand, Peterson high mountain Phase III data were flown contour at 250 ft. and 750 ft. altitudes. These data show the extreme gust velocities not encountered in Phases I and II. Since altitude has been shown to have only minor effect on turbulence, there is little reason to suspect that 250 ft. or 750 ft. contour flights would experience considerably more turbulence than non-contour flights. On the other hand, both Edwards high mountain Phases I and II and Phase III legs were flown contour at 250 ft. and 750 ft. The Phase III high mountain legs experienced the same extreme gust as at Peterson, while the Phases I and II high mountains Edwards legs did not differ significantly from the rest of the Phases I and II data.

(c)   The high mountain Phase III extreme gust velocities are caused by some unknown meteorological condition prevalent in the Phase III legs, but not present in Phases I and II. Had this condition been known and considered in the regression procedure, it could have explained the differences between the two phases of data.

The possible causes mentioned are not exhaustive. Further investigation is necessary to determine the representativeness of Phase III high mountain data.

Since no direct cause of the high mountain Phase III data could be determined, and since the rest of Phase III data is compatible with Phases I and II, it was decided to combine the Phase III not high mountain data with all of Phases I and II. Cumulative probability exceedance curves are calculated for this grouping of data and are recommended for use in design criteria for the 0-1000 ft. altitude region in non-storm conditions. In addition, the cumulative probability curve is also presented for Phase III high mountain legs.

7.1.1   Cumulative Probability Curves

Figure 7.1 shows the cumulative probability curve for all of Phases I and II and not high mountains Phase III data. The corresponding P's and b's are also listed. Phase III high mountain data is also shown. Of the parameters investigated, very stable air has been shown to have the greatest influence on turbulence. A decomposition of the data of Figure 7.1 into legs flown in very stable air and those not flown in very stable air is given in Figure 7.2. It is recommended that this decomposition be used for aircraft design by estimating the percentage of time an aircraft flies in very stable and non-very stable air. If this type estimate is not feasible from presently available knowledge, Table 7.1 can be used to correlate very stable air with other parameters. From Table 7.1 it is seen that dawn is highly correlated with very stable air. Over 71% of all legs flown at dawn were flown in very stable air. Mid-morning shows fewer very stable air flights and mid-afternoon only 5.4%.

A further decomposition of Figure 7.2 by the second highest correlation parameter to turbulence, Griffiss, is not recommended. Griffiss is not the cause of higher intensity turbulence but only reflects the effects of certain meteorological conditions which produce the results. Since the results for Griffiss are not applicable to other geographic locations, a further decomposition to include flight legs at Griffiss and not at Griffiss is not useful to design criteria. A further decomposition by the third highest correlated parameter, stable air, produces only minor changes in the cumulative probability curves and is not recommended for use in design critera. Table 7.2 summarizes the recommended P's and b's for the 0-1000 ft. altitude range.

Phases I and II All Legs
Phase III Not High Mountains
All Components Combined

$P_1 = .99986$ $b_1 = 2.605$

$P_2 = .00014$ $b_2 = 8.684$

Phase III High Mountains

$P_1 = .85$ $b_1 = 3.365$

$P_2 = .15$ $b_2 = 6.947$

Phase III
High Mountains

All Phases I and II
and Phase III Not
High Mountains
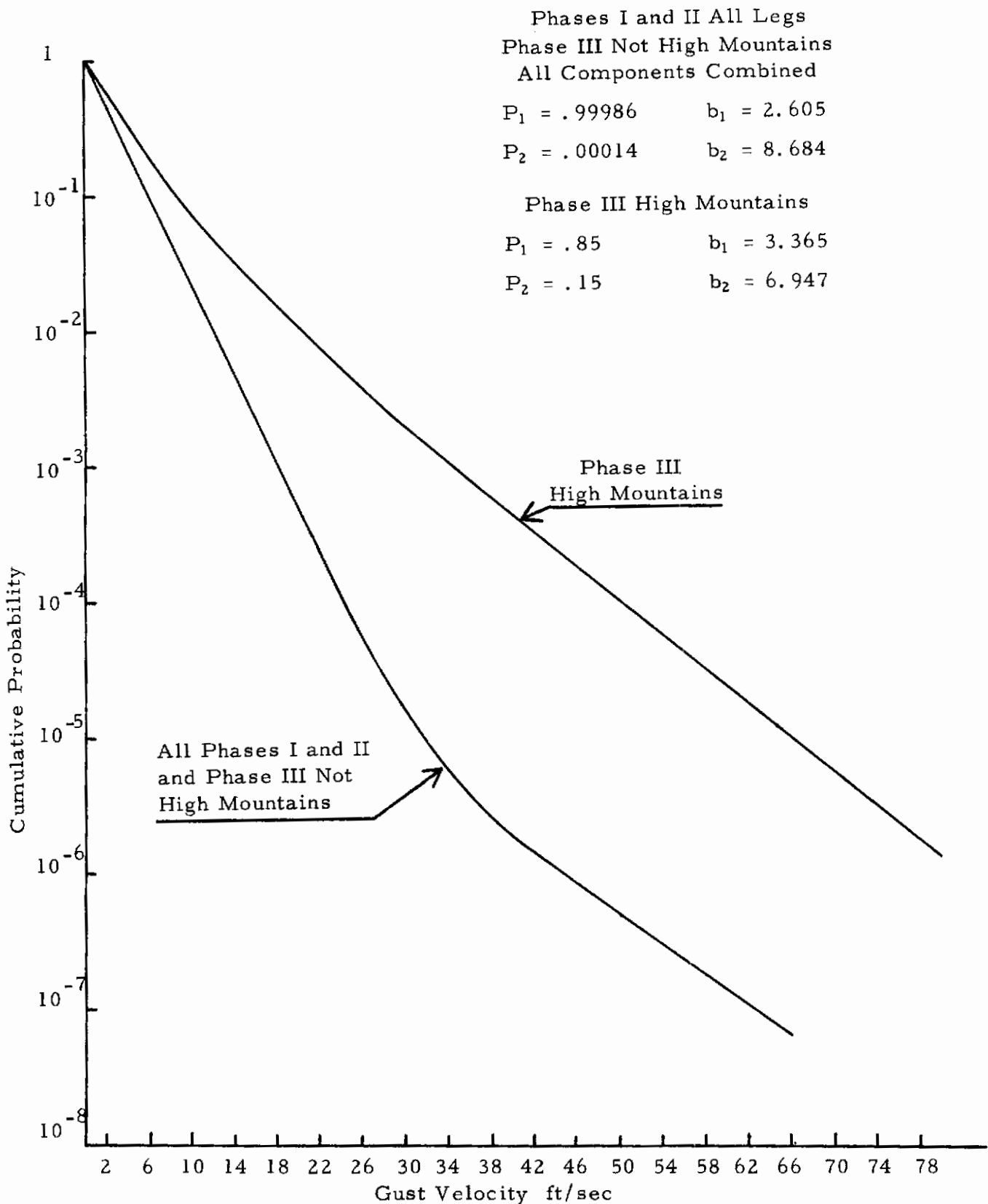
Figure 7.1 Cumulative Probability of Exceedance for Phases I and II and Not
High Mountains Phase III Legs; Phase III High Mountains Legs

TABLE 7.1

PHASES I AND II FREQUENCY AND PERCENTAGE
VERY STABLE AIR

		Edwards	Griffiss	Peterson	McConnell	Total
Dawn	Frequency	421	307	215	529	1472
	Percentage	76.0%	76.8%	59.0%	72.1%	71.7%
Mid-Morning	Frequency	63	55	109	140	367
	Percentage	11.4%	10.2%	27.0%	19.4%	16.5%
Mid-Afternoon	Frequency	60	18	26	16	120
	Percentage	11.7%	3.3%	8.2%	1.8%	5.4%

All Components Combined
Phases I and II and Phase III Not High
Mountains, Not Very Stable

$P_1 = .99978$ $b_1 = 2.678$

$P_2 = .00022$ $b_2 = 8.033$

Phases I and II and Phase III Not High
Mountains, Very Stable

$P_1 = .9975$ $b_1 = 2.099$

$P_2 = .0025$ $b_2 = 5.211$

High Mountains, Not Very Stable

$P_1 = .88$ $b_1 = 3.387$

$P_2 = .12$ $b_2 = 7.165$

High Mountains, Very Stable

$P_1 = .983$ $b_1 = 2.931$

$P_2 = .017$ $b_2 = 8.033$

Phase III, High
Mountains, Not Very
Stable

Phases I
and II and
Phase III Not
High Mountains,
Very Stable

Phase III
High Mountains
Very Stable

Phases I and I and
Phase III Not High
Mountains, Not Very Stable
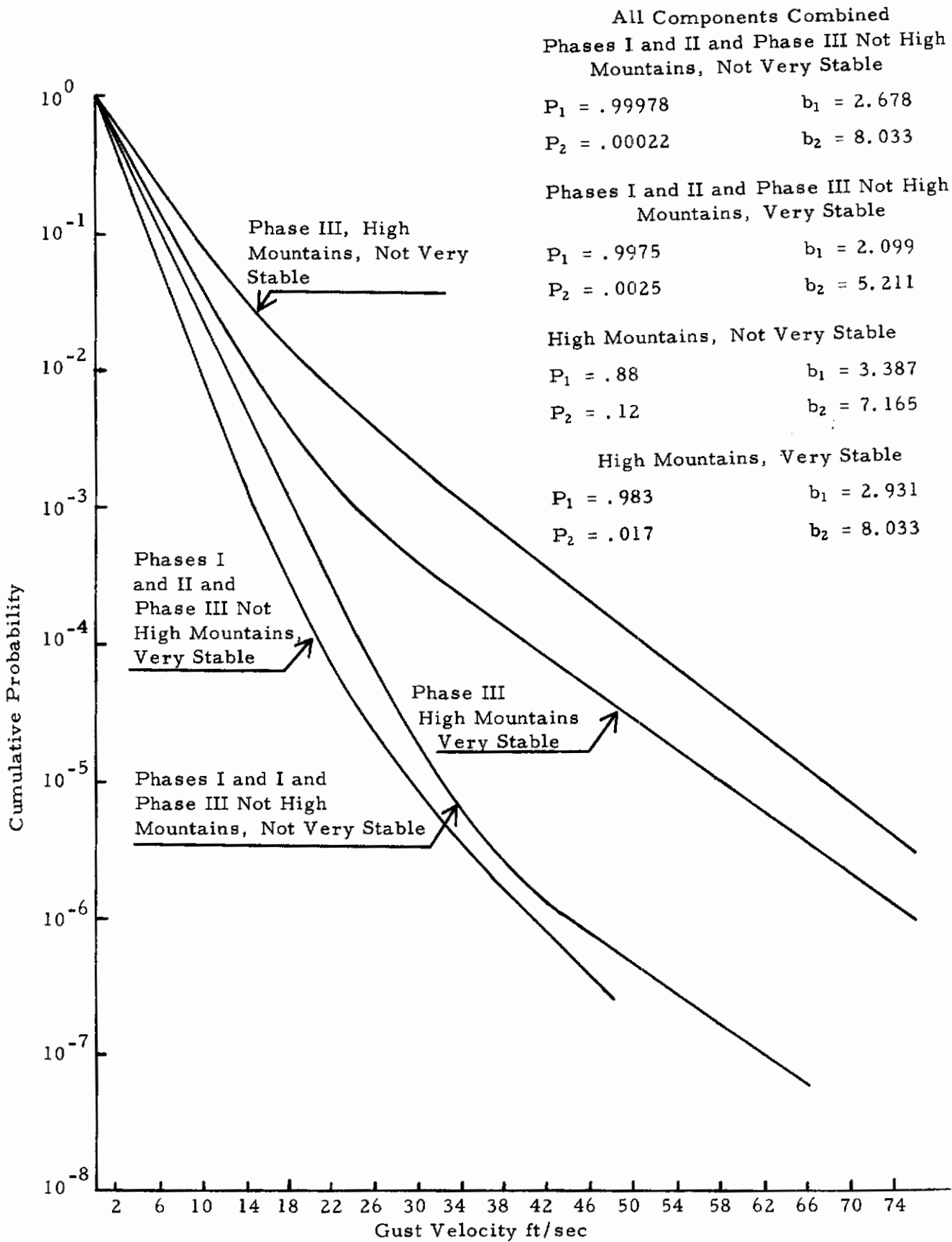
Gust Velocity ft/sec

Figure 7.2 Cumulative Probability of Exceedance, Very Stable -vs- Not
Very Stable Legs

108

TABLE 7.2

RECOMMENDED P's AND b's FOR 0-1000 FOOT ALTITUDE
NON-STORM CONDITION

Data Includes All Phases I and II Legs
and Phase III Legs Not Over High Mountains

All Components Combined

	P_1	P_2	b_1	b_2
All Legs	.99986	.00014	2.605	8.684
Very Stable	.99750	.00250	2.099	5.211
Not Very Stable	.99978	.00022	2.678	8.033

Data Includes Phase III High Mountain Legs Only
All Components Combined

	P_1	P_2	b_1	b_2
High Mountains	.85	.15	3.365	6.947
High Mountains Very Stable	.983	.017	2.931	8.033
High Mountains Not Very Stable	.88	.12	3.387	7.165

The stepwise regression procedure has shown in Table 4.12 that there is very little difference in the gust velocity time histories by component since none of the component variables enter the regression scheme until the eleventh step. A breakdown of the data therefore by component is not recommended since this decomposition provides a relatively small separation in the data. However, since it has been customary to separate data by its longitudinal, lateral, and vertical compoents, the two curves in Figure 7.1 have been decomposed by component in Figures 7.3 and 7.4 for comparison with earlier results.

7.1.2   Von Karman L's

The regression analysis on L indicated that the order in which parameters influence the scale of turbulence L is different from their order of influence on σ or the cumulative probability curves.

For example very stable air has the highest correlation to sigma, but is not highly correlated to L. Altitude, on the other hand, showed the highest correlation with L for Phases I and II legs. The comparison of Phase III Von Karman L's to those of Phases I and II also showed contrasting difference. Furthermore, these differences cannot be explained by eliminating the high mountain Phase III data. The mean of the Phase III L's is considerably larger than that of Phases I and II even if the high mountain data is excluded. The Phase III legs also showed considerably more scatter in the L value. The standard deviation of all Phase III L's is 349 feet compared to 152 feet for all of Phases I and II. Reference 2 indicates difficulty in obtaining a random sample of L's for Phase III data. Many legs flown in light turbulence did not satisfy the necessary test to run a PSD. Consequently, it is possible that the mean of the L's has been biased.

In spite of this difficulty with the scale length data, mean L's were determined for Phases I and II for the group of (a) all flight legs, (b) legs at 250 feet, and (c) legs at 750 feet. The decomposition by high mountains and not high mountains served to define L's for the Phase III data. The decomposition of the Von Karman L's was also obtained by component for each of the groups mentioned above. The results of these calculations are given in Table 7.3.

7.2   Example

To illustrate the use of Tables 7.2 and 7.3 in design criteria, the following example is presented:

Determine $\dfrac{N(y)}{N_o}$, the estimated probability of exceeding the response

Phases I and II **All** Legs
Phase III Not High Mountains

Longitudinal

P_1 = .954	b_1 = 2.258
P_2 = .046	b_2 = 3.691

Lateral

P_1 = .935	b_1 = 2.258
P_2 = .065	b_2 = 3.184

Vertical

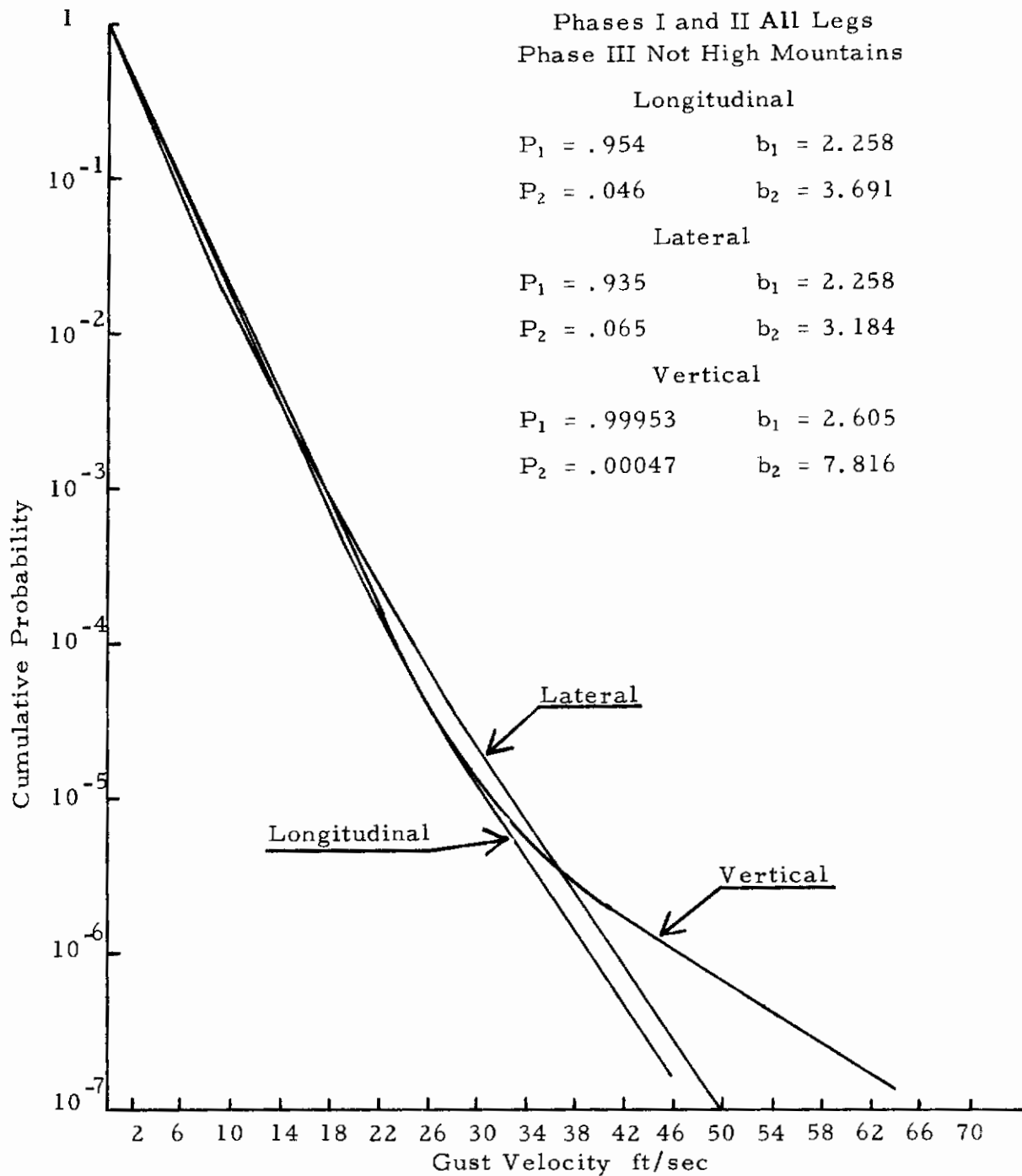|	
P_1 = .99953	b_1 = 2.605
P_2 = .00047	b_2 = 7.816

Figure 7.3 Cumulative Probability of Exceedance for Phases I and II
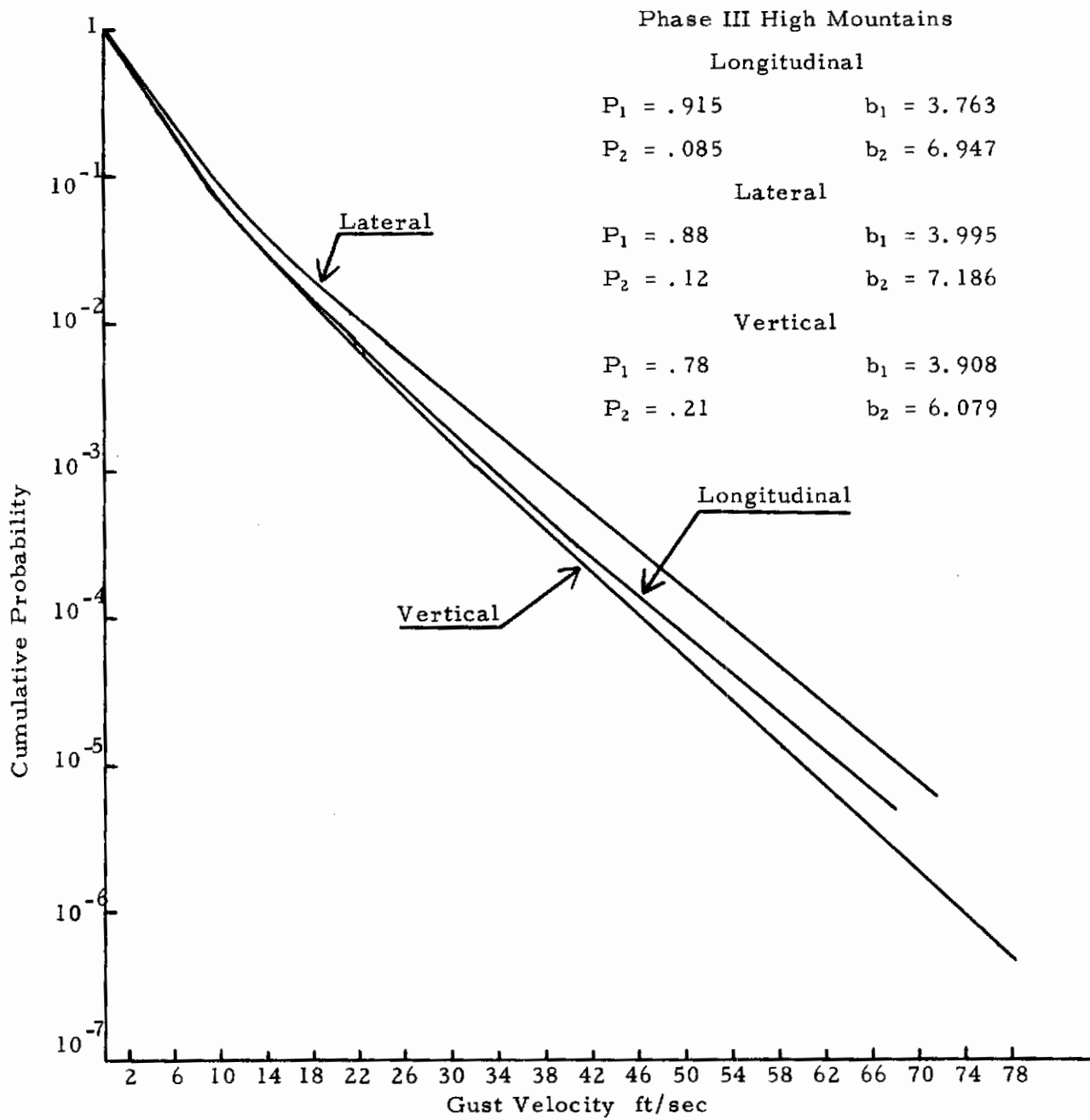and Not High Mountains Phase III Legs by Component

111

Figure 7.4 Cumulative Probability of Exceedance for Phase III High Mountains Legs by Component

TABLE 7.3

MEAN VON KARMAN L's

Phases I and II

Component	Altitude	
	250 ft.	750 ft.
All Components	342	442
Longitudinal Component	368	411
Lateral Component	361	465
Vertical Component	302	449

Phase III

Component	Terrain	
	High Mountains	Not High Mountains
All Components	704	564
Longitudinal Component	813	687
Lateral Component	704	555
Vertical Component	579	430

parameter y (acceleration, bending moment, stress, etc.) for an aircraft flying a) 40% of its missions at dawn and 60% at non-dawn, b) 75% of its missions at 250 feet altitude and the remaining 25% at 750 feet, and c) all of its missions under clear air (non-storm weather conditions).

Since the flight time is not defined by stability, the time of day correlation to very stable air (Table 7.1) is used. A 40% mission time at dawn and a 71.7% probability of being in very stable air at dawn gives .40 x .717 = 28.7% in very stable air and 11.3% in non very stable air. The remaining 60% of the missions are at non dawn. With no further information given, one assumes equal mission time at mid-morning and mid-afternoon. The percentable of non-dawn flights in very stable air is therefore (from Table 7.1) 1/2(16.5% + 5.4%) = 11.5%. The 60% non-dawn flights decomposes into 6.9% in very stable air and 53.1% in non very stable air. Summing the 40% dawn and 60% non-dawn flights gives:

$$28.7\% + 6.9\% = 35.6\% \text{ in very stable air}$$

$$11.3\% + 53.1\% = 64.4\% \text{ in non very stable air.}$$

The associated P's and b's from Table 7.2 are:

	P_1	P_2	b_1	b_2
Very Stable	.9975	.0025	2.099	5.211
Not Very Stable	.99978	.00022	2.678	8.033

Using these values of the P's and b's in the generalized load equation and weighting by the percentage of time in very stable and non very stable air, gives the probability P(y) of exceeding the response parameter y as:

$$P(y) = \frac{N(y)}{N_o} = .356 \left[.9975 \exp\left(\frac{-y/\overline{A}}{2.099}\right) + .0025 \exp\left(\frac{-y/\overline{A}}{5.211}\right) \right]$$

$$+ .644 \left[.99978 \exp\left(\frac{-y/\overline{A}}{2.678}\right) + .00022 \exp\left(\frac{-y/\overline{A}}{8.033}\right) \right] .$$

The calculation of $\overline{A}$ requires the response function H_y, which is determined by the manufacturer, and an L value which defines the Von Karman Spectra. (A value of σ for the Von Karman Spectra is not required to calculate $\overline{A}$ since its appearance in both numerator and denominator of the expression for $\overline{A}$ cancels.) For the 75% of the mission time at 250 feet, the corresponding L for Phases I and II data is obtained from Table 7.3 as 342 feet. For the

25% at 750 feet, the value of L is given as 442 feet. Weighting the values of L by the proper percentages and employing the previous equation for P(y), gives the final expression for the probability P(y) of exceeding y as:

$$P(y) = \frac{N(y)}{N_o} = .75 \left\{ .356 \left[.9975 \exp \left(\frac{-y/\overline{A}(342)}{2.099} \right) + .0025 \exp \left(\frac{-y/\overline{A}(342)}{5.211} \right) \right] \right.$$

$$+ .644 \left[.99978 \exp \left(\frac{-y/\overline{A}(342)}{2.678} \right) + .00022 \exp \left(\frac{-y/\overline{A}(342)}{8.033} \right) \right] \right\}$$

$$+ .25 \left\{ .356 \left[.9975 \exp \left(\frac{-y/\overline{A}(442)}{2.099} \right) + .0025 \exp \left(\frac{-y/\overline{A}(442)}{5.211} \right) \right] \right.$$

$$+ .644 \left[.99978 \exp \left(\frac{-y/\overline{A}(442)}{2.678} \right) + .00022 \exp \left(\frac{-y/\overline{A}(442)}{8.033} \right) \right] \right\}$$

where the expression $\overline{A}(342)$ denotes the value of $\overline{A}$ obtained from an L = 342. Similarly $\overline{A}(442)$ is the value of $\overline{A}$ obtained from an L = 442.

SECTION VIII

CONCLUSIONS

The analysis of the LO-LOCAT data by UDRI essentially involved a stepwise regression scheme whereby various turbulence parameters were related to environmental conditions experienced by the aircraft. Having identified the environmental conditions with the strongest influence upon the turbulence parameters, gust velocity exceedance curves were obtained under the various conditions using peak count data obtained from ETAC. A summary of the results obtained from this investigation is given below.

(1)   In Section III it was reported that the gust velocity exceedance curve could not be obtained satisfactorily from the distribution of σ's of the gust velocity time histories. It was therefore necessary to obtain the exceedance curve directly from the peak count data supplied by ETAC. An analytical procedure was therefore developed to adequately fit the peak count data to an expression of the form

$$F(x) = P_1 e^{-x}/b_1 + P_2 e^{-x}/b_2$$

under various environmental conditions. The Cal-comp plotter was then utilized to graphically represent the relationship established.

(2)   Of all the environmental conditions considered it was found that very stable air had the strongest influence in reducing the turbulence encountered by the aircraft as reflected through the turbulence parameter σ. It was therefore recommended that data on atmospheric stability be used in the future as a major factor in the prediction of turbulence.

(3)   Stronger turbulence was encountered at Griffiss than under comparable conditions at other bases. No environmental conditions considered could explain the excessive turbulence.

(4)   Except for the high mountain Phase III data, the gust exceedance curves for Phases I and II data agreed with the curves for the Phase III data. The cause of the differences has not been determined, but several possible explanations have been proposed. Further investigation is warranted.

(5)   Generally longer scale lengths L were observed in Phase III and generally smaller N_0 values were observed in Phase III.

(6)   The regression analysis on the turbulence parameters σ, N_0, and L provides a detailed outline of how the turbulence is related to the environmental conditions as well as providing information about the relationships

between environmental conditions. The information obtained from the regression analysis has also been used as a guide for fruitful avenues of investigation. That is, relationships uncovered by the regression scheme have been pursued analytically and frequently illustrated graphically.

(7)   Some difference in the cumulative probability curves for the three components u, v, and w was observed. In particular, the lateral component shows somewhat higher peak gust probabilities than the other two components. However, the differences in the cumulative probability curves produced by the three components is small when compared with differences produced by such environmental conditions as atmospheric stability, wind velocity, terrain type, and location.

SECTION IX

REFERENCES

1. D.E. Gunter, G.W. Jones, J.W. Jones, K.R. Monson, "Low Altitude Atmospheric Turbulence, LO-LOCAT Phases I and II", The Boeing Company, ASD-TR-69-12.

2. J.W. Jones, R.H. Mielke, G.W. Jones, et al., "Low Altitude Atmospheric Turbulence, LO-LOCAT Phase III", The Boeing Company, AFFDL-TR-70-10, Volumes I, II; Parts I, II.

3. H. Press, M.T. Meadows, I. Hadlock, "A Reevaluation of Data on Atmospheric Turbulence and Airplane Gust Loads for Application in Spectral Calculations", NASA Report 1272, 1956.

4. H. Press, R. Steiner, "An Approach to the Problem of Estimating Severe and Repeated Gust Loads for Missile Operations", NACA-TN-4332, September 1958.

5. S.O. Rice, "Mathematical Analysis of Random Noise", Bell System Technical Journal, 23, 282-332 and 24, 46-156, 1944 and 1945.

6. F. Hoblit, N. Paul, J. Shelton, F. Ashford, "Development of a Power Spectral Gust Design Procedure for Civil Aircraft", FAA-ADS-53, January 1966.

7. J.C. Houbolt, "Design Manual for Vertical Gusts Based on Power Spectral Techniques", AFFDL-TR-70-106, December 1970.

8. J.C. Houbolt, et al., "Dynamic Response of Airplanes to Atmospheric Turbulence Including Flight Data on Input and Response", NACA Report TR R-199, Langley Research Center, Langley Station, Virginia, June 1964.

9. W.H. Austin, "Environmental Conditions to be Considered in the Structural Design of Aircraft Required to Operate at Low Levels", SEG-TR-65-4, Research and Technology Division, Wright-Patterson Air Force Base, Ohio, January 1965.

APPENDIX A

PHASE I AND II MASTER TAPE DATA CONTENT

This appendix describes the content of the Phases I and II master tapes. The parameters contained on the master tapes are grouped according to 15 card types. With each flight leg is associated one of each of the card types. The flight legs are given signatures as follows:

1) Six digit category number

2) Test number

3) Condition number

4) Leg number

5) Date of test

6) Run number

These signatures precede the data on each card. The parameters contained on each card have been defined by an equation and/or a referenced document where additional information is available. One can see from page 120 that, for example, the first card image (01) gives values for seven parameters with lapse rate being the last entry.

SUBSCRIPTS

1	Pre Leg 100 ft. Observation Run (10 sec)
10	Pre Leg 1000 ft. Observation Run (10 sec)
2	Data for First 5 sec of Leg or Condition
3	Data for Last 5 sec of Leg or Condition

REF. 1   D3-7797-6 SECT. 2, Boeing "LO-LOCAT Phase III R and D Status - Monthly Report", 1 September through 30 September 1968.

REF. 2   D3-7797-7 SECT. 2, Boeing "LO-LOCAT Phase III R and D Status - Monthly Report", 1 October through 31 October 1968.

REF. 3   LO-LOCAT Report ASD-TR-69-12, Reference 1 of text.

REF. 4   D3-7797-10 SECT. 2, Boeing "LO-LOCAT Phase III R and D Status - Monthly Report", 1 December through 31 December 1968.

Parameter	Units	How Determined	Remarks	
(01) True Airspeed~V_T	ft/sec	average value $\dfrac{\sum V_{T1}}{33,000}$	Page 11, REF. 3 V_T on Pg. 184, REF. 3	Leg
Ground Speed~G_S	ft/sec	average for 33,000 values (Doppler)	Page 190, REF. 3	Leg
Wind Velocity~$\bar{W}$	ft/sec	$\bar{W}=f(V_T, G_S, h, \delta)$ Earth Referenced	page 185, REF. 3, page 24, 25, REF. 1	Leg
Wind Direction~WD	deg.	$WD=f(\bar{W}N, \bar{W}E)$ earth referenced	page 185, 186, REF. 3 page 24, 25, REF. 1	Leg
Richardson No. ~R_i	none	$[g\,10^{-3}(\Gamma_d-\Gamma)/T_{10}]/(\Delta W_V/\Delta H)^2$ $\Gamma_d=5.5°F/1000'$~adiabatic lapse rate	page 69, REF. 3, page 26, 27, REF. 1	Pre Leg
Std. Dev. Terrain	ft		pages 2-6, REF. 4	Leg
Lapse Rate~Γ	deg F/1000 ft	$\Gamma=1000\dfrac{\Delta T}{\Delta H}$	page 27, REF. 1 see equ. vert. temp. grad.	Pre Leg
(02) Ground Surf. Temp. ~T_{AR}	deg. F	value from Barnes radiometer pre leg pass corrected for emissivity	pages 190,219, REF. 3, pages 5-8, REF. 2	Pre Leg
Air Temp.~$\bar{t}_a$	deg. F	$T_a=f(T_I, M)$ $\bar{t}_a=\bar{T}_a-459.6$	page 190, REF. 3, page 11, REF. 1	Leg
Static Pres.~$\bar{P}_S$	in. hg.	$P_S=P_{S_1}-\Delta P_S$ $\bar{P}_S$ is mean value	page 11, REF. 1	Leg
Distance~S	miles	$S=G_S\dfrac{(t\,min)(60)}{5280}$	page 28, REF. 1	Leg
Radar Alt~RA	ft.	average for 33,000 values	page 8, REF. 2	Leg
Wind Angle~WA	deg.	$WA=f(V_T, G_S, \delta, \bar{W})$	flight path referenced page 25, REF. 1	Leg
Viscosity~μ	lb. sec./ft^2	$\mu=.317(10)^{-10}(\bar{T}_a)^{3/2}\left(\dfrac{734.7}{\bar{T}_a+216}\right)$	page 29, REF. 1	Leg
(03) Density~ρ	lb. sec.^{2}/ft^4	$\bar{\rho}=.041187(\bar{P}_S/\bar{T}_a)$	Page 29, REF. 1	Leg
Vert. Wind Grad. EW~$\dfrac{\Delta WE_V}{\Delta H}$	(ft/sec)/ft	$\dfrac{\Delta WE_V}{\Delta H}=(\bar{W}E_1-\bar{W}E_{10})/(\bar{H}_{10}-\bar{H}_1)$	page 26, REF. 1	Pre Le
Vert. Wind Grad. NS~$\dfrac{\Delta WN_V}{\Delta H}$	(ft/sec)/ft	$\dfrac{\Delta WN_V}{\Delta H}=(\bar{W}N_1-\bar{W}N_{10})/(\bar{H}_{10}-\bar{H}_1)$	page 26, REF. 1	Pre Le
Vert. Delta Wind Angle ~$\dfrac{\Delta WD_V}{\Delta H}$	deg/ft	$\dfrac{\Delta WD_V}{\Delta H}=(WD_1-WD_{10})/(\bar{H}_{10}-\bar{H}_1)$	Ground referenced page 26, REF. 1	Pre Le
(04) Vert. Temp. Grad~$\dfrac{\Delta T}{\Delta H}$	deg F/ft	$\dfrac{\Delta T}{\Delta H}=(\bar{T}_1-\bar{T}_{10})/(\bar{H}_{10}-\bar{H}_1)$	page 26, REF. 1	Pre Le
Vert. Wind Grad~$\dfrac{\Delta W_V}{\Delta H}$	(ft/sec)/ft	$\dfrac{\Delta W_V}{\Delta H}=\left[\left(\dfrac{\Delta WE_V}{\Delta H}\right)^2+\left(\dfrac{\Delta WH_V}{\Delta H}\right)^2\right]^{1/2}$	page 26, REF. 1	Pre Le
Horiz. Wind EW Grad ~$\dfrac{\Delta WE_H}{S}$	(ft/sec)/ft	$\dfrac{\Delta WE_H}{S}=(\bar{W}E_3-\bar{W}E_2)/S$	page 29, REF. 1	Leg
Horiz. Wind NS Grad ~$\dfrac{\Delta WN_H}{S}$	(ft/sec)/ft	$\dfrac{\Delta WN_H}{S}=(\bar{W}N_3-\bar{W}N_2)/S$	page 29, REF. 1	Leg
Horiz. Delta Wind Angle ~$\dfrac{\Delta WD_H}{S}$	deg/mile	$\dfrac{\Delta WD_H}{S}=(WD_3-WD_2)/S$	page 29, REF. 1	Leg

Parameter	Units	How Determined	Remarks
(05)			
Horiz. Temp Grad.~ΔT_H	deg F/mi.	$\Delta T_H=(T_{a_3}+\Delta H_{32}\Gamma^*-T_{a_2})/S$ $\Delta H_{32}=(H_{t_3}-H_{t_2})+RA_3-RA_2$	$\Gamma^*=.00356$ Page 28, REF. 1
Horiz. Wind Grad.~$\dfrac{\Delta W_H}{S}$	(ft/sec)/mi	$\dfrac{\Delta W_H}{S}=\left[\left(\dfrac{\Delta WE_H}{S}\right)^2+\left(\dfrac{\Delta WN_H}{S}\right)^2\right]^{1/2}$	page 29, REF. 1
Horiz. Press Grad~ΔP_H	in hg./mi	$\Delta P_H=f(H_{P_3},H_{P_2},\Delta H_{32})/S$	page 28, REF. 1
Heading~h	deg.	ave. for 33,000 counts; $h=h_m+\Delta h$	page 24, REF. 1, Page 185, REF. 3
(06)			
Charact. Frequ. Long	cyc/ft	$N_0=\sigma_1/\sigma\sim$ truncated spectrum (.04-10 cps)	page 8, REF. 3, page 17,18, REF.
Charact. Frequ. Lat.	cyc/ft	$\sigma_1=\left[\displaystyle\int_{k_1}^{k_3}\phi(k)\,dk\right]^{1/2}$	page 8, REF. 3, page 17,18, REF.
Charact. Frequ. Vert.	cyc/ft	$\sigma=\left[\displaystyle\int_{k_1}^{k_3}\phi(k)\,dk\right]^{1/2}$	page 17, 18, REF. 1
σ_T(.04-10 cps) Long.	ft/sec	integral of the truncated spectrum (.04-10 cps)	pages 71,72, REF. 3
σ_T(.04-10 cps) Lat.	ft/sec		pages 71,72, REF. 3
σ_T(.04-10 cps) Vert.	ft/sec		pages 71,72, REF. 3
(07)			
σ_T(.33-10 cps) Long.	ft/sec	integral of the truncated spectrum (.33-10 cps) Equ. 4.12	page 72, REF. 3
σ_T(.33-10 cps) Lat.	ft/sec		page 72, REF. 3
σ_T(.33-10 cps) Vert.	ft/sec		page 72, REF. 3
L_{K_U} Von Karman (Long.)	ft	$L_{K_V}=.110\left(\dfrac{\sigma_L}{\sigma_{T.33}}\right)^3 V\left(\dfrac{1}{k_{.33}^{2/3}}-\dfrac{1}{k_{10}^{2/3}}\right)^{3/2}$	pages 74-78, 15-17, REF. 3 pages 18, 19, REF. 1
L_{K_V} Von Karman (Lat.)	ft	$L_{K_U}=.0717\left(\dfrac{\sigma_L}{\sigma_{T.33}}\right)^3 U\left(\dfrac{1}{k_{.33}^{2/3}}-\dfrac{1}{k_{10}^{2/3}}\right)^{3/2}$	pages 74-78, 15-17, REF. 3 pages 18, 19, REF. 1
L_{K_W} Von Karman (Vert.)	ft	Same as L_{K_V} using vert. σ's	pages 74-78, 15-17, REF. 3 pages 18, 19, REF. 1
L other model ? Long.	ft	Equa. (4.15-4.18)	pages 74-78, 15-17, REF. 3 pages 18, 19, REF. 1
L other model ? Lat.	ft	Equa. (4.15-4.18)	pages 74-78, 15-17, REF. 3 pages 18, 19, REF. 1
L other model ? Vert.	ft	Equa. (4.15-4.18)	pages 74-78, 15-17, REF. 3 pages 18, 19, REF. 1
(08)			
Max Gust Vel Long	ft/sec	from peak count dist. vs lower band limit see page 317	page 60-61, REF. 3
Max Gust Vel Lat	ft/sec	from peak count dist. vs lower band limit see page 317	page 60-61, REF. 3
Max Gust Vel Vert	ft/sec	from peak count dist. vs lower band limit see page 317	page 60-61, REF. 3
Min Gust Vel Long	ft/sec	from peak count dist. vs lower band limit see page 317	page 60-61, REF. 3
Min Gust Vel Lat	ft/sec	from peak count dist. vs lower band limit see page 317	page 60-61, REF. 3
Min Gust Vel Vert	ft/sec	from peak count dist. vs lower band limit	page 60-61, REF. 3

Parameter	Units	How Determined	Remarks
(09)			
σ_t Longitudinal	ft/sec	} standard deviation of amplitude count distribution (time histories)	page 61, REF. 3, Page 15, REF. 1
σ_t Latitudinal	ft/sec		page 61
σ_t Vertical	ft/sec		page 61
.10.			
No. of Runs Long	none	} based on amplitude observations see page 312 of Sept. 1967 Canadian Aeronautics and Space Journal	page 21-23, REF. 1
No. of Runs Lat	none		
No. of Runs Vert	none		
Run Test Level Long	none	} max. level of significance at which a stationarity hypothesis may be made is determined from a table of run statistics	page 21-23, REF. 1
Run Test Level Lat	none		
Run Test Level Vert	none		
(10)			
Slope of Cum. Prob. Density Long	none	} Least squares solution to determine slope of $\log e [F'(x)]$ vs $(xb)^2$	pages 59, 60, 66, REF. 3 page 33, REF. 1
Slope of Cum. Prob. Density Lat	none		
Slope of Cum. Prob. Density Vert	none		
(11)			
Normal Slope, Long	$(ft/sec)^2$	} Normal probability density fct	pages 6-7, also NASA 1272, page 33, REF. 1
$\dfrac{1}{2\sigma_t^2}$ Lat	$(ft/sec)^2$	slope $= 1/2\sigma^2$	
Vert	$(ft/sec)^2$	$\sigma_p F(x)$ vs x^2/σ_p^2 OR $\sigma_t F(x)$ vs x^2/σ_t^2	page 105, REF. 3
(12)			
CHI Square Long	none	} $\chi^2 = \dfrac{N_T}{N} \displaystyle\sum_{b=1}^{Nb} f_b^2 - N$	amplitude data page 60. REF. 3 also pg. 312, Sept. 1967 Canadian ASJ
Lat	none		
Vert	none		
CHI Square Long	none	} fct of χ^2 and number of degrees of freedom $= m = N_b - 1$ and CHI square tables	page 60, REF. 3
Level of Lat	none		
Sig. Vert	none		
(13)			
Viscous Dissipation Rate			
E_1	ft^2/sec^3		
E_2	ft^2/sec^3		
E_3	ft^2/sec^3		
E_4	ft^2/sec^3		
E_5	ft^2/sec^3		
E_6	ft^2/sec^3		
(14)			
E_7	ft^2/sec^3		
E_8	ft^2/sec^3		
E_9	ft^2/sec^3	Derivation From Page 78-81, REF. 3	Page 78-81, REF. 3
E_{10}	ft^2/sec^3		
E_{11}	ft^2/sec^3		
E_{12}	ft^2/sec^3		
(15)			
E_{13}	ft^2/sec^3		
E_{14}	ft^2/sec^3		
E_{15}	ft^2/sec^3		
E_{16}	ft^2/sec^3		
Taylor Microscale	ft.	$\lambda = \left[\dfrac{15 u \sigma_{tu}^2}{\sigma E} \right]^{1/2}$	page 78, REF. 3

APPENDIX B
ADDITIONS AND CHANGES TO MASTER TAPE CONTENT FOR PHASE III DATA

Parameter	Units	How Determined	Remarks
(09)			
σ_t Longitudinal	ft./sec.	$\sigma_t = \left[\dfrac{1}{N} \sum_{i=1}^{N} (x_i - \bar{x})^2\right]^{1/2}$	pg. 95, 100 ref. 3, pg. 15, ref. 1
σ_t Latitudinal	ft./sec.		
σ_t Vertical	ft./sec.	$\bar{x}$ is mean gust velocity value	
No. mean runs, Long.	none		
No. mean runs, Lat.	none		
No. mean runs, Vert.	none	See card image type (09) in Phases I and II	
"Y" or "N" mean runs acceptance, Long.	none		
"Y" or "N" mean runs acceptance, Lat.	none		
"Y" or "N" mean runs acceptance, Vert.	none		
No. of mean square runs, Long.	none		
No. of mean square runs, Lat.	none	Exact definition for calculation of these values are not presently available	
No. of mean square runs, Vert.	none		
"Y" or "N" mean square runs acceptance, Long.	none		
"Y" or "N" mean square runs acceptance, Lat.	none	Exact definition for calculation of these values are not presently available	
"Y" or "N" mean square runs acceptance, Vert.	none		
(15)			
E_{13}	ft^2/sec^3		
E_{14}	ft^2/sec^3	Derivation from pg. 78-81, Ref. 3	pg. 78-81, Ref. 3
E_{15}	ft^2/sec^3		
E_{16}	ft^2/sec^3		
Taylor Microscale	ft.	$\lambda = \left[\dfrac{15_\mu \sigma_{tu}^2}{\rho\epsilon}\right]^{1/2}$	pg. 30, Ref. 1
Kolmogoron Microscale (η)	ft.	$\eta = \left(\dfrac{\nu^3}{\epsilon}\right)^{1/4}; \nu = \dfrac{\mu}{\rho}$	pg. 30, Ref. 1
(16)			
σ_p, Longitudinal	ft/sec		
σ_p, Lateral	ft/sec	$\sigma_p = \left[\sum_{b=1}^{N} \dfrac{f_b (x_b)^2}{N}\right]^{1/2}$	pg. 20, 21, Ref. 1
σ_p, Vertical	ft/sec	N is total number of peaks f_b is number of peaks in the b-th band x_b is the mid-value of the	
(16)			
N_p, Longitudinal	none		
N_p, Lateral	none	N is total number of peaks N is found by extrapolation of the cumulative distribution curves	pg. 21, Ref. 1
N_p, Vertical	none		
(17)			
σ_L, Longitudinal	ft/sec		
σ_L, Lateral	ft/sec	$\sigma_L = \left[\sum_{i=1}^{N} \dfrac{F_\alpha X_\alpha^2}{N_\alpha L}\right]^{1/2}$	pg. 95, Ref. 3
σ_L, Vertical	ft/sec		
N_L, Longitudinal	none		
N_L, Lateral	none	$N_\alpha = \dfrac{E_\alpha}{d}$ The number of level crossings per mile of the level $x(t) = \alpha$ is computed for each level	pg. 95, Ref. 3
N_L, Vertical	none		
(18)			
N_v			
N_h			
Q_v		Lapse Rate Parameters (not used)	Exact definition for calculation of these values are not presently available
Q_h			
B		$B = \dfrac{g}{T_a}\left(\dfrac{RA}{W}\right)^2\left(T_d - \dfrac{\delta T}{\delta H}\right)$ Stability Ratio	pg. 27, Ref. 1

DOCUMENT CONTROL DATA - R & D

(Security classification of title, body of abstract and indexing annotation must be entered when the overall report is classified)

1. ORIGINATING ACTIVITY (Corporate author)	2a. REPORT SECURITY CLASSIFICATION
University of Dayton Research Institute Dayton, Ohio 45409	Unclassified
	2b. GROUP

3. REPORT TITLE

STATISTICAL ANALYSIS OF LO-LOCAT TURBULENCE DATA FOR USED IN THE DEVELOPMENT OF REVISED GUST CRITERIA

4. DESCRIPTIVE NOTES (Type of report and inclusive dates)
Scientific   March 1969 through February 1971

5. AUTHOR(S) (First name, middle initial, last name)

John W. McCloskey, James K. Luers, John P. Ryan, Nicholas A. Engler

6. REPORT DATE	7a. TOTAL NO. OF PAGES	7b. NO. OF REFS
April 1971	140	9

8a. CONTRACT OR GRANT NO.	9a. ORIGINATOR'S REPORT NUMBER(S)
F33615-69-C-1477	
b. PROJECT NO.	
c.	9b. OTHER REPORT NO(S) (Any other numbers that may be assigned this report)
d.	AFFDL-TR-71-29

10. DISTRIBUTION STATEMENT

This document has been approved for public release; distribution is unlimited.

11. SUPPLEMENTARY NOTES	12. SPONSORING MILITARY ACTIVITY
TECH, OTHER	Air Force Flight Dynamics Laboratory Aeronautical Systems Division Wright-Patterson AFB, Ohio 45433

13. ABSTRACT

   LO-LOCAT is an extensive low level turbulence program utilizing statistically representative samples of turbulence data obtained over a wide range of meteorological, topographical, seasonal, and time of day conditions. UDRI has attempted to identify which of the various meteorological and environmental conditions affect the turbulence as reflected through a number of turbulence parameters. The turbulence parameters considered were: σ, the standard deviation of the gust velocity; b, the turbulence intensity; L, the scale of turbulence; and N_O, the characteristic frequency.

   The basic method of mathematical analysis was a stepwise regression scheme which related the environmental conditions to the various turbulence parameters based upon statistical priority. It is felt that the regression scheme provides a detailed outline of statistical relationships which can be used as a guide for further investigation.

14. KEY WORDS	LINK A		LINK B		LINK C	
	ROLE	WT	ROLE	WT	ROLE	WT
LO-LOCAT						
Clear Air Turbulence						
Design Criteria						
Gust Velocity						
Scale of Turbulence						